# Investigations of Measles virus regulation on activation and function of antigen presenting cells

Thesis submitted to

the Julius-Maximilians-University

Würzburg, Germany

towards fulfillment of the requirements for the degree of

Dr. rer. nat.

Yoana Shishkova

Bulgaria, Kazanlak

Würzburg, Germany

18.04.2008

Eingereicht am:

18.04.2008.....

Mitglieder der Promotionskommission:

.....

Vorsitzender: Prof. Dr. G. Krohne (vom Dekan beauftragt)

.....

Gutachter : Prof. Dr. S. Schneider-Schaulies

.....

Gutachter: Prof. Dr. T. Raabe

.....

Tag des Promotionskolloquiums: 02.07.2008

.....

Doktorurkunde ausgehändigt am:

.....

## Declaration

I declare that the submitted dissertation was completed by myself and none other, and I have not used any sources or materials other than those enclosed. Moreover, I declare that the dissertation has not been submitted further in this form and has not been used for obtaining any other equivalent qualification in any other organization. Additionally, other than this degree I have not applied or will not attempt to apply for any other degree, title or qualification in relation to this work.

Würzburg 18.04.2008 *Shishkova Y.*

Yoana Shishkova

Die vorliegende Arbeit wurde in der Zeit vom 01.Oktober 2003 bis 31. Januar 2007 am Institut für Virologie und Immunbiologie der Bayerischen Julius-Maximilians-Universität Würzburg unter der Anleitung von Professor Sibylle Schneider-Schaulies und Herr Prof. Dr. Thomas Raabe gemacht.

## Acknowledgement

Here, I thank my tutor,

professor Sibylle Schneider-Schaulies, for directing my research project and helpful suggestions on my manuscript

professor Georg Krohne, Dr. Elita Avota for scientific discussion,

Dr. Harms for his help with cell imaging,

Elisabeth Meier-Natus for the technical help

and Steffen Schwab for his german translation of the summary,

and our entire group members for their kind help in both lab work and daily life.

Thank you !

# Contents


**1. Introduction ..... 1**

1.1. Measles virus ..... 1

1.1.1. Pathogenesis ..... 1

1.1.2. MV organization ..... 3

1.2. Dendritic cells ..... 5

1.2.1. Dendritic cell biology: differentiation, migration and functions ..... 5

1.2.2. MV and DCs ..... 7

1.2.2.1. Infection of dendritic cells by MV ..... 7

1.2.2.2. Activation of DCs by MV ..... 8

1.2.2.3. Impairment of DC function by MV ..... 9

1.2.2.4. MV induced immunosuppression ..... 10

1.3. DC/T Cell interaction ..... 11

1.3.1. Adhesion, signaling and integrins ..... 11

1.3.2. Cytoskeletal rearrangements in DCs and T cells ..... 14

1.3.3. Immunological synapse (IS) ..... 15

1.3.3.1. Organisation of IS ..... 15

1.3.3.2. Different types of IS ..... 16

1.4. Aim of the work ..... 18

**2. Materials ..... 19**

2.1. Cell lines ..... 19

2.3. Viruses ..... 19

2.4. Cell culture media ..... 20

2.5. Solutions and buffers used for cell separation ..... 22

2.6. Antibodies for purity determination of the isolated cell populations ..... 23

2.7. Immunofluorescence ..... 24
2.7.1. Antibodies for immunofluorescence ..... 24
2.7.2. FACS buffers ..... 27
2.8. In situ-immunlocalisation ..... 27
2.8.1. Buffers for in situ-immunolocalisation ..... 27
2.8.2. Reagents for in situ-immunolocalisation ..... 28
2.9. FN/ICAM-1 adhesion assays ..... 28
2.9.1. Buffers for adhesion assays ..... 28
2.9.2. Reagents for adhesion assays ..... 28
2.10. Kit for fast activated cell ELISA-based adhesion assay ..... 28
2.11. Cell lysis ..... 29
2.12. Determination of protein concentration ..... 29
2.13. Western Immunoblotting of proteins ..... 29
2.13.1. Buffers for WB ..... 29
2.13.2. Antibodies for WB ..... 30
2.13.3. SDS-polyacrylamide gel electrophoresis (SDS-PAGE) ..... 31
2.14. Kinase assay ..... 32
2.14.1. Kinase buffer ..... 32
2.14.2. Washing solutions ..... 33
2.15. Plasmids ..... 33
2.15.1. Human MHCII-GFP plasmid ..... 33
2.15.2. Human GTP-ases –GFP Plasmids ..... 34
2.16. Transfection ..... 35
2.17. Materials ..... 35
2.18. Devices ..... 35

**3. Methods ..... 37**

3.1. Cell culture ..... 37

3.1.1. Adherent cells ..... 37

3.1.2. Passaging cells in suspension culture ..... 37

3.1.3. Freezing and cryo-storage of cells ..... 37

3.2. Isolation of primary human mononuclear cells ..... 38

3.2.1. Elutriation ..... 38

3.2.2. Density-gradient separation ..... 39

3.2.2.1. Isolation of primary human mononuclear cells ..... 39

3.2.2.2. Isolation of primary T cells via rosetting ..... 39

3.2.2.3. Isolation and purification of monocytes ..... 40

3.3. Cultivation of primary human cells ..... 41

3.3.1. Dendritic cells ..... 41

3.3.2. T cells ..... 41

3.4. Viruses ..... 41

3.4.1. Wild type virus ..... 41

3.4.2. Vaccine strain Edmonston ..... 42

3.4.3. Infection of Monocyte derived Dendritic Cells ..... 44

3.5. Molecular biological methods ..... 44

3.5.1. Amplification of Plasmids ..... 44

3.5.1.1. Transformation ..... 44

3.5.1.2. Mini- culture and maxi- culture ..... 45

3.5.1.3. Transfection ..... 45

3.6. Biochemical methods ..... 45

3.6.1. Preparation of cell lysates ..... 45

3.6.2. Determination of protein concentration ..... 46

3.6.3. Western Blot ..... 46

3.6.4. Immunoprecipitation /Co- Immunoprecipitation ..... 47

3.7. Cell biological methods ..... 47

3.7.1. Scanning electron microscopy ..... 47

3.7.2. Cell adhesion assay ..... 48

3.7.3. FACE method by using FAK Kit ..... 48

3.7.4. Immunofluorescence ..... 49

3.7.5. Extra- and intra- cellular FACS staining ..... 50

3.7.6. Conjugate formation between DC and T cells ..... 50

3.7.7. Deconvolution /XY/analyses; 3-D confocal images ..... 50

3.7.8. Fluo-4 loading of T cells ..... 51

3.7.9. Live-cell imaging ..... 51

3.7.10. Cell tracking ..... 52

**4. Results ..... 53**

4.1. DCs morphology and adhesion ..... 53

4.1.1. Morphology and adhesion of WTF- DCs on Poly-L-Lysin (PLL) ..... 53

4.1.2. Morphology and adhesion of WTF-infection DCs on FN and ICAM-1 ..... 54

4.2. Integrin β-1 in DCs ..... 57

4.2.1. β-1 and activated form of β1-integrin expression levels on DCs were not affected by attachment on FN ..... 58

4.2.2. Activated β1-integrin distribution in WTF-DCs ..... 60

4.3. Signalling pathway and regulation of integrins in DCs ..... 61

4.3.1. Focal adhesion kinase activity in infected DCs ..... 63

4.3.2. Fascin expression in MV-infected DCs ..... 65

4.3.3. In FN stimulated WTF-DCs fascin interacted with PKCα ..... 67

4.4. Role of Rac1-GTPase in adhesion and movement of DCs ..... 69

4.5. DC/T cell immunological synapse (IS) ..... 71

4.5.1. MTOC orientation in WTF-DC/T cell conjugates ..... 71
4.5.2. Analyses of the IS architecture ..... 73
4.5.2.1. LFA-1/talin distribution in DC-T cell conjugates ..... 73
4.5.2.2. CD3/talin distribution in DC-T cell conjugates ..... 75
4.5.2.3. MHCII / CD3 distribution in DC-T cell conjugates ..... 77
4.5.3.1. WTF infection up-regulated surface expression of HLA-DR, but not FN1-reactive MHC-II ..... 79
4.5.3.2. The distribution of tetraspannin associated MHC-II in WTF-infected DC/T cell synapses ..... 80
4.5.3.3. Surface accumulation of clustered MHCII occurred inefficiently in WTF-DCs ..... 81
4.5.3. Most of the WTF-infected DCs failed to promote sustained T cell activation ..... 83
4.5.4. Localisation of MV-H and MV-N proteins in the IS ..... 87
4.5.5. MGV infection up-regulated surface expression of HLA-DR, but not FN-1 ..... 89
4.5.6. MGV-infected DC/T cell conjugation pattern differed from WTF-DC/T cell ..... 90

**5. Discussion ..... 92**

**6. Summary ..... 104**

**7. Zusammenfassung: ..... 106**

**8. Abbreviation ..... 108**

**9. Reference ..... 112**

**10. Publication ..... 127**

**11. Curriculum Vitae ..... 128**

# 1. Introduction

## 1.1. Measles virus

### 1.1.1. Pathogenesis

Measles is a highly contagious disease characterized by induction of lifelong immunity but associated with profound and transient immune suppression and ranks amongst the major causes of children's death in developing countries (Kerdiles et al., 2005). Immune suppression during measles starts at the onset of the rash, may last for weeks to months after recovery, and leads to increased susceptibility to secondary infections and reactivation of persistent infections. Paradoxically, MV-induced immune suppression occurs in the context of substantial immune activation (Griffin et al., 1989), which is associated with induction of a specific immune response allowing both virus clearance and induction of long-term immunity.

MV is airborne and initially replicates within tracheal and bronchial epithelia. The virus is subsequently transported through mononuclear cells to the draining lymph nodes, leading to the formation of giant multinucleated lymphoid or reticuloendothelial cells (Warthin et al., 1931). The syncytia identified in the submucosal areas of tonsils are thought to be a major source of virus spread to other organs. MV-specific RNA and proteins can be detected in a minor proportion of lymphocytes and monocytes during, and for a few days after, the rash (Esolen et al., 1993; Schneider-Schaulies et al., 1991). The rash clearly marks the onset of immune responses as determined by the appearance of virus-specific T cells and antiviral antibodies. A marked infiltration of mononuclear cells into local areas of viral replication is seen and virus-specific T cells appear in the blood. Plasma levels of the soluble T cell surface molecules CD4, CD8, IL-2R and β2 - microglobulin are elevated, as are IL-2, IL-4 and INFγ. During measles, a switch from an initial T helper1(Th1) to a long-lasting Th2

response is observed (Griffin et al., 1995). Whether generation of Th1 responses is less efficient after vaccination than after natural infection has not been clearly resolved (Schnorr et al., 2001; Ward et al., 1993).

Complications of acute measles are frequent and are especially severe in children under two years of age (Katz et al., 1995). Complications are common in the first four to six weeks after infection by MV. They affect mainly the respiratory and intestinal tract. In industrialised countries, more than 10% of MV cases present with otitis, pneumonia, diarrhoea or encephalitis. Central nervous system (CNS) complications can occur early (post-infectious measles encephalitis, which is thought to be a virus-induced autoimmune disease) or very infrequently, months to years after the acute disease, late complications - subacute sclerosing panencephalitis (SSPE) and measles inclusion body encephalitis (MIBE) develop as a result of a persistent MV infection of neuronal and macroglial cells.

### 1.1.2. MV organization

MV belongs to the Morbillivirus genus of the Paramyxoviridae family. It is an enveloped virus containing a non segmented negative stranded RNA genome encoding six structural

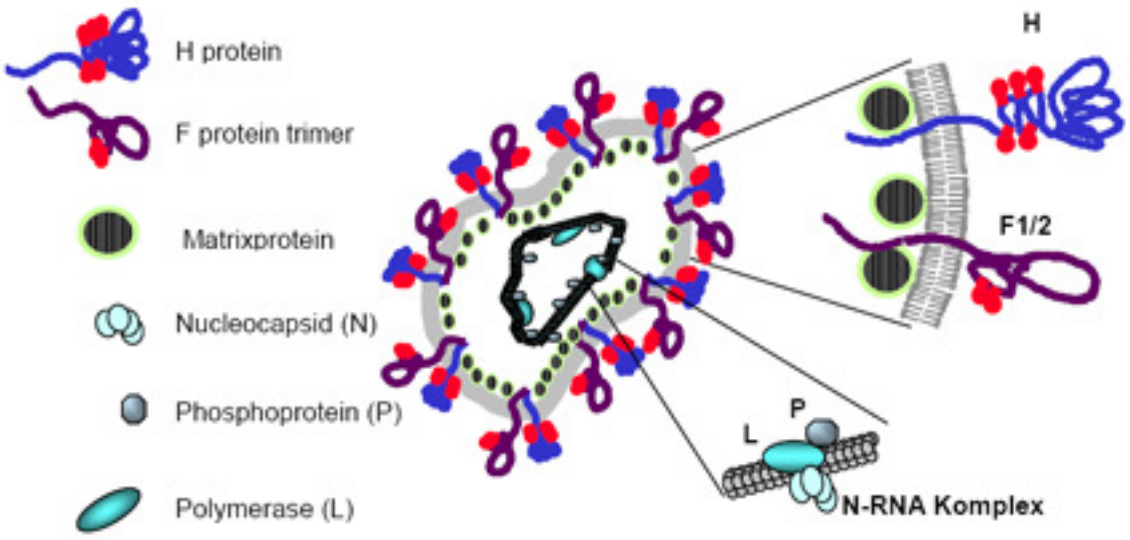


Fig.1 Schematic representation of measles virus organisation
(Abt et al., 2005)

and three non-structural proteins. The virus envelope consists of a lipid bilayer, derived from the cellular plasma membrane, with two inserted virus-encoded glycoproteins: hemagglutinin (H) protein and fusion (F) protein. The H protein is a type 2 glycoprotein (80 kD) which mediates virus attachment to susceptible cells, and is responsible together with the F protein for fusion with the cell membrane (Wild et al., 1995) Fig.1. The F protein is a type I glycoprotein, synthesised as a precursor protein (Fo) and activated after proteolytic cleavage by furin in the trans-Goldgi compartment into a disulphide-linked heterodimer, consisting of the F1 (40 kD) and F2 (20 kD) subunits. The matrix protein (M, 37 kD) links the RNP to the lipid envelop. M is thought to interact with the cytoplasmic tails of the

envelope glycoproteins. Virion RNA is packaged into a helical nucleocapsid by the nucleoprotein (N, 60 kD). The association between RNA and N is very stable and the function of N protein appears to be protection of the viral genomic nucleic acid and participation in the formation of a replication complex. The second component of the replication complex is a virus-encoded RNA-dependent RNA polymerase, which consists of two subunits: the phosphoprotein (P, 70 kD) and the large protein (L, 250 kD) (Horikami et al., 1995). L is the catalytic component of the viral polymerase. The P gene of MV encodes, in addition to P, three other accessory non-structural proteins: C (21 kD), V (46 kD) and R (40 kD). The C protein (186 aa) is encoded by an open reading frame that begins 22 nucleotides downstream of the P gene start codon. MV V protein is expressed from an edited mRNA. MV R protein is produced by ribosomal frameshifting (Liston et al., 1995; Bellini et al., 1994).

Two different cellular receptors have been identified to date: CD46, a complement regulatory glycoprotein expressed on all human nucleated cells (Naniche et al., 1993) and CD150, a glycoprotein belonging to the immunoglobulin superfamily, expressed on haematopoietic cells (Tatsuo et al., 2000). While vaccine MV strains can use CD46 and CD150, the wild type MV strains, preferentially use CD150, although low affinity binding to CD46 has been observed (Manchester et al., 2000; Masse et al., 2002).

## 1.2. Dendritic cells

### 1.2.1. Dendritic cell biology: differentiation, migration and functions

of binding to major histocompatibility complex (MHC). In response to danger signals like tissue damage, pathogen derived products or inflammatory products from neighbouring

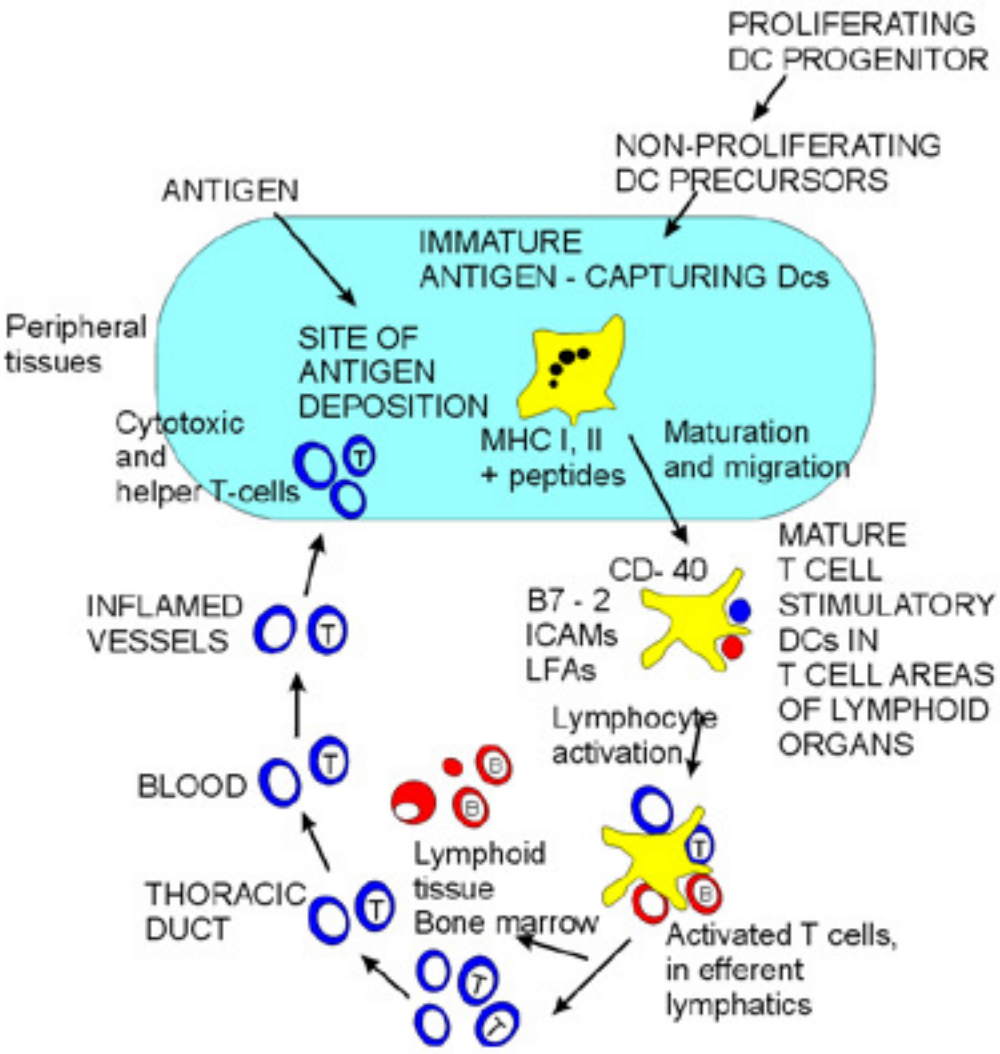


Fig.2 Schematic representation of immune reaction (in vivo). Dendritic cells in the periphery capture and process antigens, express lymphocyte co-stimulatory molecules, migrate to lymphoid organs and secrete cytokines to initiate immune responses. They not only activate lymphocytes, they also tolerize T cells to self-antigens.
(Banchereau and Steinman, 1998)

tissue cells, DCs cease their endocytic activity (Salluso et al., 1995), increase their surface expression of MHC class II molecules (Cella et al., 1997) and produce high levels of cytokines such as IL-12, TNF-α, IL-6 and IL-1α/β (Salluso et al., 1999). These changes called maturation occur while DCs migrate to lymphoid organs where they interact with B cells and antigen-specific CD4 T cells to initiate immune responses (Fig.2).

T cell scanning is facilited by extensive morphing of the maturing DCs which provide large contact planes. As they are the only APC subset licensed to activate naive T cells, DCs not only initiate clonal selection, they also shape the quality of the ensuing response by regulated expression of co-stimulatory molecules and directed release of cytokines. Mature DCs do not leave but rather die in lymphoid tissues thereafter and are not found in the efferent lymph (Pohl et al., 2007).

DCs can be generated in vitro from different precursors (Inaba et al., 1992; Caux et al., 1992; Szabolcs et al., 1995; Romani et al., 1996; Sallusto et al., 1995; Reddy et al., 1997). Their immature phenotype is characterised by low to intermediate expression levels of MHC class II and costimulatory molecules such as CD80 and CD86. These cells have a low capacity to stimulate allogenic T-cell proliferation in mixed lymphocyte reaction (MLR) in vitro. The major criteria for DC maturation are high expression levels of costimulatory molecules, which mediate adhesion and signalling to T cells and a high MLR stimulatory activity. DCs stimulate T-cell responses by displaying MHC-peptide complexes, together with costimulatory molecules, to naive and resting antigen-specific T cells. Activated T cells induce terminal DC maturation by CD40 ligation.

### 1.2.2. MV and DCs

#### 1.2.2.1. Infection of dendritic cells by MV

Uptake of MV by DCs and subsequent transport into the local lymphatics probably occurs after infection of the respiratory tract epithelium. The interaction of MV with DCs has been studied in tissue culture with Langerhans cells, DCs isolated from blood or generated in vitro from monocytes or CD34+ precursor cells. Immature and mature DCs are readily infected with MV and extensive formation of syncytia both in pure DCs and mixed DC-Tcell cultures is seen (Grosjean et al., 1997; Klagge et al., 2000; Schnorr et al., 1997; Servet-Delprat et al., 2000). In addition to cellular fusion, apoptosis of both DCs and T cells has been noted in mixed cultures (Fugier-Vivier et al.1997) and there is evidence that expression of tumour necrosis factor (TNF)-related apoptosis-inducing ligand (TRAL) by DCs and expression of Fas ligand (FasL) by T cells might play a role in this process (Servet-Delprat et al., 2000). Production of infectious virus from DC cultures is usually low, but can be enhanced by CD40 ligation (Servet-Delprat et al., 2000). MV glycoproteins are important for DC tropism (Kardiles et al., 2006).

### 1.2.2.2. Activation of DCs by MV

MV infection induces phenotypic maturation of immature DCs since expression levels of MHC classII and CD40 are enhanced and costimulatory molecules such as CD80, CD86, CD83 and CD25 are induced (Klagge et al., 2000; Schnorr et al., 1997; Servet-Delprat et al., 2000) (Fig.3).

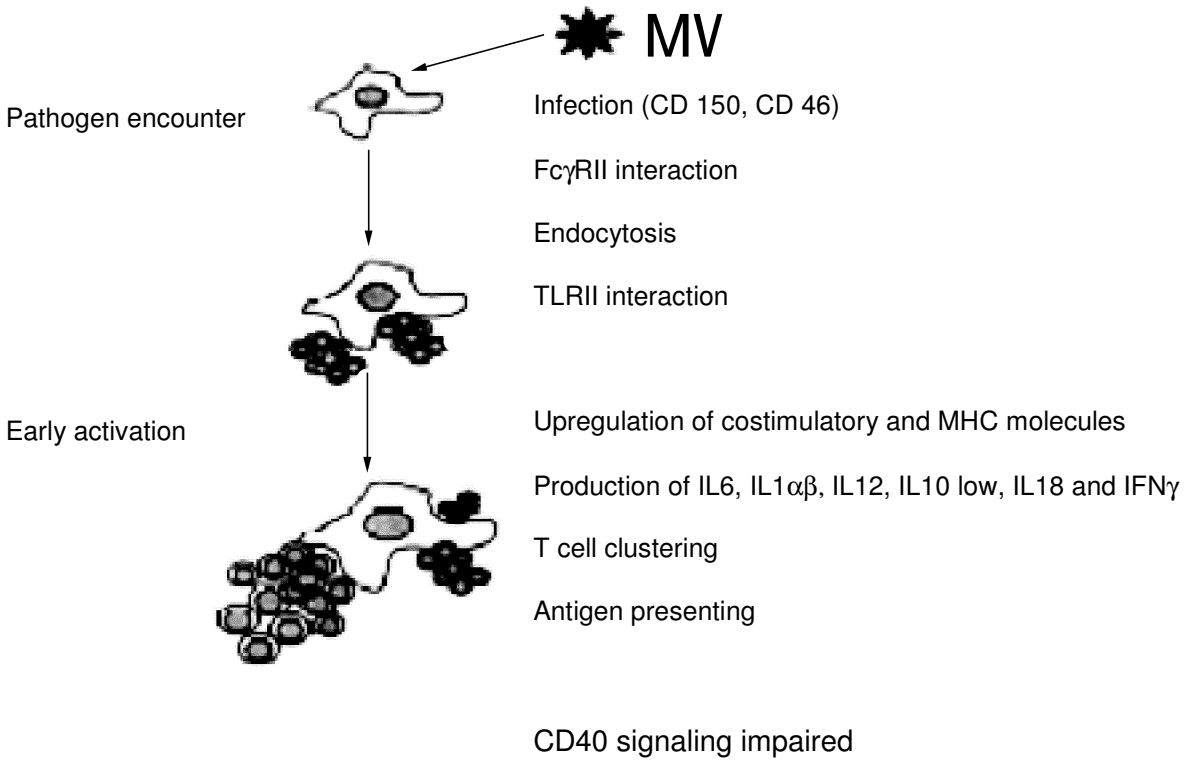


Fig.3 Schematic representation of measles virus interaction with DC
(Abt et al., 2005)

Although DC maturation was induced by all MV strains (Schnorr et al., 1997). MV infection triggers the release of type I IFN from monocyte-derived DCs, which contributes to DC maturation (Klagge et al., 2000). Consistent with DC activation, induction of low levels of transcripts for IL-12p40, IL-12p35, IL-1α/βIL-1 receptor antagonist and IL-6 were detected in MV-infected DCs (Servet-Delprat et al., 2000). Induction of these transcripts depends on

activation of NF-kB, which has been shown to occur after MV infection in a variety of cell types (Dhib-Jalbut et al., 1999; Helin et al., 2001).

#### 1.2.2.3. Impairment of DC function by MV

Despite their mature phenotype, MV-infected DCs fail to stimulate and even actively suppress, allogenic, T cell proliferation stimulated in vitro (Grosjean et al., 1997; Klagge et al., 2000; Schnorr et al., 1997; Servet-Delprat et al., 2000). Although MV infection of T cells causes proliferative arrest (Naniche et al. 1999; Yanagi et al., 1992), this might not play a major role in these systems, since transmission of infectious MV to T cells by DCs is very inefficient (Grosjean et al., 1997). Fusion and/or apoptosis observed in DC-Tcell cultures will certainly reduce the number of T cells, but is not likely to contribute to Tcell unresponsiveness (Vidalain et al., 2000). Similarly, although inhibitory soluble mediators have been suggested to be released by MV infected T or B cells (Sun et al., 1998; Fujinami et al., 1998), these have not been detected in supernatants of MV infected DC cultures (Klagge et al., 2000). It is more likely that the MV glycoproteins expressed at high levels on the surface of infected DCs account to a longer extent for the inhibition of T cell proliferation. Thus, DCs infected with a recombinant MV that contains the G protein of vesicular stomatitis virus (VSV) instead of the MV glycoproteins reveal a high allostimulatory activity and do not inhibit mitogen-driven T cell proliferation (Klagge et al., 2000). Furthermore, studies with CD46-transgenic mice have demonstrated a direct effect on DC functions by the MV N protein, as well as the glycoproteins of CD46-adapted MV strains (Marie et al., 2001)

### 1.2.2.4. MV induced immunosupprassion

MV glycoproteins expressed on the surface of infected cells and /or virus particles have been shown to inhibit mitogen-induced proliferation of uninfected peripheral blood lymphocytes (PBL) (Schlender et al., 1996). Direct involvement of MV envelope glycoproteins was confirmed by the inhibitory activity of fibroblasts transfected to express the MV F-H complex in vitro. This inhibition occurred independently of soluble mediators, complex glycosylation and the fusogenic activity of the effector F-H complex, but required proteolytic processing of the F protein (Weidmann et al., 2000). Neither CD46 nor CD150 appeared to be required for the induction of T-cell proliferative arrest (Erlenhoefer et al., 2001). Membrane contact of the F-H complex did not induce apoptosis but rather an accumulation of cells at the G1-S-phase restriction point (Schnorr et al., 1997). Although the F-H complex did not interfere with IL-2- dependent activation of the JAK1/3-STAT3/5 pathway, IL-2-dependent activation of Akt kinase was shown to be disrupted after F-H contact. MV directly interacts with T-cell lipid rafts, thereby causing profound alterations in their ability to recruit and segregate proteins central to TCR activation, such as the activated Akt kinase and Vav. As another MV-induced early event, CD28-dependent proteosomal degradation of Cbl-b is prevented (Avota et al., 2004). The binding of MV interferes with CD3/CD28 coligation induced GTP-loading of the Rho GTPases, Cdc42 and Rac1. GTP-loading of RhoA was not impaired after MV treatment (Müller et al., 2006). Rather, RhoA was slightly activated by MV alone and this was enhanced upon CD3/CD28 ligation. Consisting with the failure of CD3/CD28 ligation to induce GTP-loading of Cdc42 and Rac1, polymerization of F-actin and morphological changes such relaxation, flattening required for the formation of a contact plane did not occur in MV treated T cells. MV treatment also efficiently interfered with the ability of T cells to adhere to ECM components

(Müller et al., 2006) and the majority of MV exposed T cells failed to aquire a polar front-rear organization. Thus, MV induced signaling efficiently impairs stimulation dependent reorganisation of the F-actin cytoskeleton and adhesion in T cells. Scanning electron microscopy data show that exposure of T cells to MV induced an almost complete breakdown of microvillar structures associated with reduced phosphorylation levels of cofilin and ERM proteins (Müller et al., 2006). The ability of MV exposed T cells to interact with DCs and form DC/T-cells conjugates is not affected. MV signaling to T cells interfered with clustering and recruitment of CD3 into the central supramolecular activation cluster of the IS. MV also prevents their redistribution of the MTOC in T cells towards the synapse (Müller et al., 2006).

## 1.3. DC/T Cell interaction

### 1.3.1. Adhesion, signaling and integrins

Adhesion appears to involve active cellular processes involving the plasma membrane and the cytoskeleton. Cytoskeletal strengthening of adhesions can produce enormous increases in attachment strength and is related to the formation of multimolecular complexes in adhesion structures containing a variety of cytoskeletal and signal transduction proteins (Burridge et al., 1997; Yamada and Geiger, 1997). There are more than 20 distinct integrin subunits, which form heterodimers that consist of one $\alpha$and one $\beta$ subunit (Fig.4).

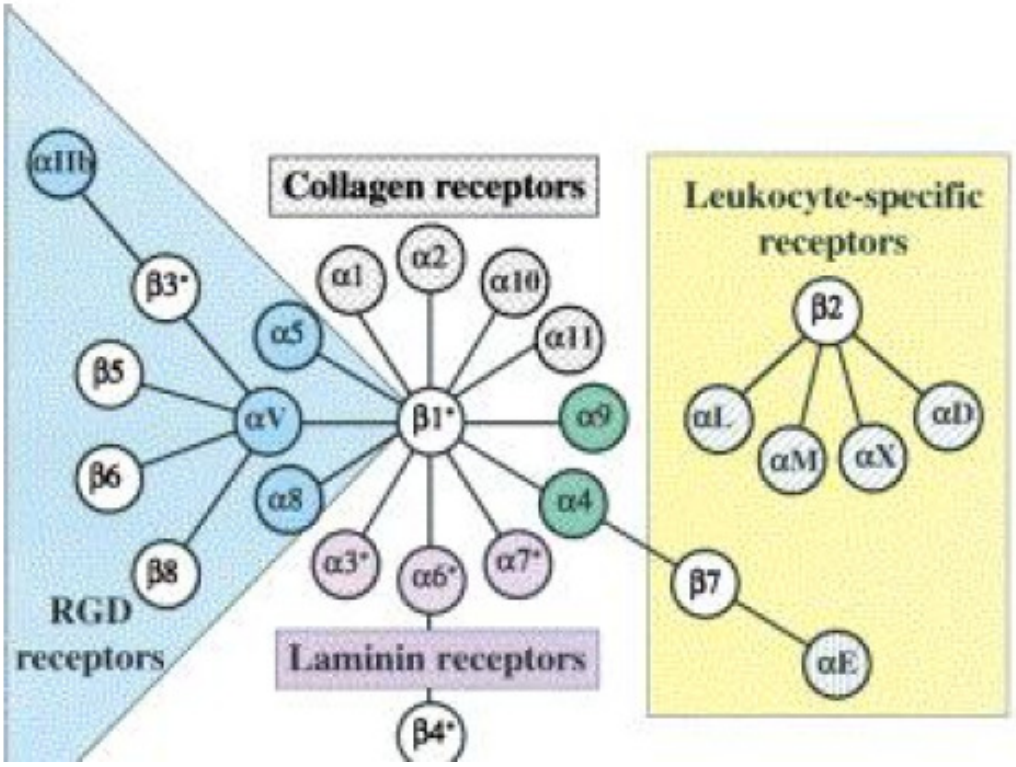


Fig.4 Integrins-Receptor-Family:
RGD receptors (in blue); Collagen receptors (in gray); Leukocyte-specific receptors (in yellow) and Laminin receptors (in violet).

(Hynes, 2002)

Humans have at least 24 integrins, and several bind to components of the extracellular matrix (ECM), often to the same component. Integrin molecules have a head domain containing a ligand-binding site, two spindly legs, and usually short cytoplasmic domains. Despite surface expression of both β1 and β2 integrin families, DC plated on fibronectin (a ligand for both families) selectively recruit CD18, CD11b, and CD11c to podosomes. For CD18 and CD11c (Burns et al., 2004) was demonstrated that recruitment was localized to rings around the F-actin podosome core, maintained on surfaces coated with serum, laminin, collagen 1, VCAM-1 and ICAM-1, suggesting that the integrin components of DC podosomes were conserved irrespective of the binding ligand. In part, this observation reflected the wide range of extracellular matrix proteins and intracellular adhesion molecules to which β2 integrins could bind (Plow et al., 2000). Cross-talk arised from activation of alternative integrins – β1 family could result in recruitment of β2 family

members (van Berg et al., 2001) and suggested an important role in the rapid attachment and detachment of DC protrusions during migration.

The functions of cell adhesion molecules and their receptors are important for attachment to other cells or extracellular matrix molecules and traction during cell migration. Adhesion proteins can mediate outside-in transfers of signalling information, such as cellular responses after binding to specific extracellular matrix proteins, but they can also mediate inside-out information in which intracellular signals modulate the activity of integrins (Yamada and Miyamoto, 1995).

The adhesion of T cells to their cellular partners is a tightly regulated and dynamic process. At various time, the T cell must adhere firmly to endothelial cells within the vasculature and to antigen-presenting cells in the lymph nodes. For each of these interactions, the primary adhesion molecule pair consists of T cell $\alpha_L\beta_2$ integrin (CD11a-CD18), known as leukocyte function-associated antigen-1 (LFA-1), and its ligand intracellular adhesion molecule-1 (ICAM-1) (Cairo et al., 2006). Changes in receptor conformation are known to be responsible for changes in receptor affinity (Shimaoka et al., 2003). The high-affinity forms of the integrins are necessary for adhesion (Lu et al., 2001b), both receptor and ligand must become engaged and aligned at the site of adhesion (Dustin et al., 1997).

Recognition of MHC-peptide complexes on DCs by Ag-specific TCRs is a first important signal in DC/ Tcell interaction (Banchereau et al., 2000). DC/Tcell clustering is mediated by several adhesion molecules (Hart et al., 1997). The crucial factor, that constitutes the second important signal, required to sustain T cell activation, is the interaction between co-stimulatory molecules expressed by DCs and their ligands expressed by T cells. CD86 on

DCs is so far the most critical molecule for amplification of T cell responses (Caux et al., 1994; Inaba et al., 1994)

### 1.3.2. Cytoskeletal rearrangements in DCs and T cells

patients with Wiskott-Aldrich Syndrome (WAS), where there is a genetic defect in the actin-binding protein WASp, which is normally regulated by the activity of Cdc42 (Binks et al., 1998 Morphological changes accompanying DC maturation include a loss of adhesive structures, cytoskeletal reorganization and acquisition of high cellular motility (Winzler et al., 1997). An important controller of cytoskeletal remodeling may be the actin-bundling protein Fascin, expressed at high level in blood DCs and in interdigitating DCs located in T cell areas of lymph nodes (Mosialos et al., 1996). The formation and retraction of membrane processes in DCs is driven by reorganization of the actin cytoskeleton, and is controlled by the Rho family of GTPases, including RhoA, Rac1 and Cdc42. This reorganization has been shown to be important in cell motility, phagocytosis and cell division (Ridley et al.1992; Carlier et al. 1998). RhoA regulates the release of adhesions to the substratum and associated cellular contraction. A recent study reported that down regulation of Cdc42 activity provided a master switch for suppression of DC endocytosis, which is an important feature of maturation (Garrett et al., 2000). It was allso previously shown that podosome assembly can not by restored by microinjection of mature DC with constitutively active V12Cdc42 or V12Rac1, or a combination of two, suggesting that temporal regulation of podosome distribution is more complex (Burns et al., 2001). RhoA-GTPase is low at the leading edge and higher at the rear and sides of the DC. RhoA-GTPase activation can be modulated by local activation of Cdc42 and Rac.

A specific illustration of the importance of Rho GTPases in regulating the cytoskeleton of DC is that morphology and dendrite formation is abnormal when the DC are derived from

patients with Wiskott-Aldrich Syndrome (WAS), where there is a genetic defect in the actin-binding protein WASp, which is normally regulated by the activity of Cdc42 (Aspenström et al., 1996). The Cdc42/Rac binding of WASp can control cytoskeleton rearrangement and may be of importance during DC capture of pathogens and establishment of DC-T cell contacts. The process of T cell-DC conjugation was first observed in vitro using dynamic imaging techniques (Stoll et al., 1994), which showed that on contact with a cell surface bearing appropriate antigen receptor ligands, naive T lymphocytes rapidly extend lamellipodia that spread along the surface membrane of the opposite cell (Negulescu et al., 1996). The modified shape of the T cell is then maintained as long as the T cell-DC conjugate exists (Delon et al., 1998). These T cell morphological alterations visualized after antigen-driven interactions with DCs involve substantial cytoskeletal changes. The most typical of these alterations is an increase in the cell's content of filamentous actin, especially in the region of cell-cell contact. A family of cytoskeletal proteins called the ezrin-radexin-moesin (ERM) proteins are involved in T cell activation (Allenspach et al., 2001; Roumier et al., 2001)

### 1.3.3. Immunological synapse (IS)

#### 1.3.3.1. Organisation of IS

The immunological synapse (IS) between T cells and DCs is a specialized cell-cell adhesive junction characterized by stability and directed secretion (Dustin et al., 2002). The classical definition of the IS is based on a cell-cell interface in which leukocyte function-associated antigen 1(LFA-1) and intercellular adhesion molecule 1(ICAM-1) interactions as well as talin form a ring around a central cluster of TCR-MHCp (T-cell receptor-major histocompatibility complex molecule-peptide complex) interactions (Monks et al., 1998; Dustin et al., 1998).These structures were defined as supramolecular

activation clusters (SMACs). The TCR cluster marke the central (c) SMAC, whereas the LFA-1 ring marke the peripheral (p) SMAC (Fig.5).

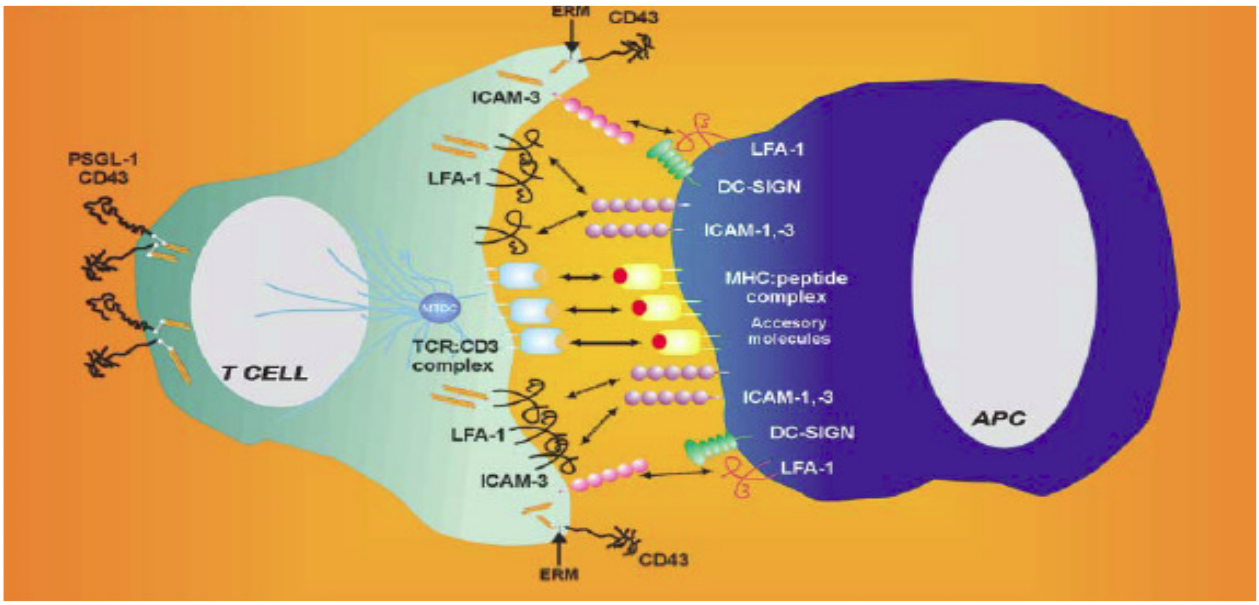


Fig.5: View of T-cell / APC conjugate. Localization of adhesion and adaptor molecules after antigen recognition of peptide-MHC complex by the TCR/CD3
(Montoya et al., 2002)

It has been proposed that the DC cytoskeleton plays an active role in shaping the T cell-DC immunological synapse, and there is direct evidence that the antigen-presenting cell (APC) cytoskeleton can modify the location of key molecules (Al-Alwan et al., 2003).

### 1.3.3.2. Different types of IS

Different types of APC not only differ in their morphology and in the structure of their actin cytoskeleton but also in their molecular properties, such as patterns of cell-surface adhesion-molecule expression and chemokine secretion. The impact of the type and activation status of the APC on the type and duration of cell-cell interaction seems to be inversely correlated with the co-stimulatory capacity and activation potency of the APC (Gunzer et al., 2004). For example, interactions between naive CD4+T cells and resting B cells usually last for several hours and are mainly of the stable type; however, although

these are the longest lasting interactions, they lead to efficient T-cell activation (Monks et al., 1998). By contrast, interactions between naive T-cells and activated B cells or DCs are less stable (lasting only minutes), more commonly involve dynamic phases and have a higher efficiency of T-cell activation (Gunzer et al., 2004). In addition, the stability and duration of T-cell-APC interactions seem to be inversely correlated with the morphological complexity and cytoskeletal activity of the APC, and they might further depend on cell-surface-receptor numbers and distribution (that is, their pre-clustering state at the surface of the APC).

According to diversity of molecular-interaction zone of the immunological synapse, four types of molecular arrangement at the immunological synapse are described (Friedl et al., 2002):

A monocentric immunological synapse has a stably adhesive junction with a fully segregated central supramolecular activation cluster (cSMAC) and peripheral SMAC (pSMAC), which lead to T-cell priming, T-cell receptor (TCR) downregulation and sustained signalling (Bromley et al., 2001)

A multicentric immunological synapse is an assembly of partially mobile molecular clusters that lack complete segregation into a pSMAC and cSMAC.

An unsegregated immunological synapse is enriched for TCR, co-stimulatory molecules and signalling molecules, yet it lacks pSMAC and cSMAC segregation.

A dynamic immunological synapse is an asymmetrical structure that is predicted to occur in T cells that are migrating across an antigen-presenting cell (APC); it is thought to involve receptor engagement at the leading edge of the cell and receptor exit at the rear of the cell (Friedl et al., 2002).

## 1.4. Aim of the work

Interaction with dendritic cells (DCs) is considered as central to immunosuppression induced by MV. MV-infected DC cultures do not support allogenic T cell expansion. Evidently, signalling by the viral glycoprotein complex accumulating on these cells is important for this phenomenon. Signalling processes in T cells targeted by surface interaction with this complex have been studied using UV-inactivated virus as effectors. In these cases, activation of the PI3K in response to serum factors, TCR ligation by antibodies, or cocultured mature DCs was severely compromised. Importantly, MV interaction alone has been linked to a collapse of T cell microvillar structures and the inability of T cells to organise a functional monocentric IS with mature DCs based on MTOC redistribution and centring of CD3. The latter experiments were performed based on the assumption that DC maturation induced by MV roughly corresponded to those by other maturation stimuli. We were interested in whether other parameters associated with DC maturation such as cytoskeletal rearrangements, integrin-dependent and dynamic adhesion were also affected by MV infection. Thus, we planned to look how MV infection modulates integrins and Rho GTPases activation and the velocity of infected DCs. MHC-II clustering on WTF-infected DCs was the next point of interest. In particular, the capability of WTF-DCs to stably conjugate to and to organise functional immune synapses with cocultured allogenic T cells was to be precisely analysed.

# 2. Materials

## 2.1. Cell lines

All cell lines used in this work were available in the institute.

| Cell line | cell type | medias | origin |
|---|---|---|---|
| **BJAB** | B cell, lymphoblastoid (homo sapiens) | RPMI 1640,10% FCS | Menezes et al. 1975 |
| **B95a** | EBV transformed, marmoset (Callithrix jacchus) B cell | RPMI 1640, 5% FCS | Kobune et al |
| **Vero** | fibroblast cell line (kidney) African green long-tailed monkey | MEM, 5% FCS | Yasumura, 1963 |

Table 1: Culture medium, cell lines and their origin

## 2.2. Primary cells

Human peripheral blood mononuclear cells obtained after elutration from healthy donors at the Institute for transfusion medicine and immune haematology of the University hospital Würzburg served as source for T cells and monocytes.

## 2.3. Viruses

The vaccine strain Edmonston and the wild type strain Fleckenstein were grown routinely in the laboratory. MGV is recombinant MV that contains the G protein of vesicular stomatitis instead of MV glycoproteins was kindly provided by Dr. E. Avota

| virus types | receptor | cell lines used |
|---|---|---|

| | | |
|---|---|---|
| wild type Fleckenstein (WTF) | CD150 | BJAB |
| vaccine straine Edmonston (ED) | CD46,<br>CD150 | Vero |
| recombinant MV that contains the G protein of VSV insted of MV glycoproteins (MGV) | | Vero |

Table 2: Viruses and cell lines used for passaging

## 2.4. Cell culture media

Cell culture media RPMI 1640, MEM, DMEM, HANKS and additions were produced in the institute. Different compounds were added to the media depending on the usage:

| Substance | concentration (final) | manufacturer |
|---|---|---|
| FIP | 200 µ M | Bachem |
| penicillin | 100 U/ ml | institute |
| streptomycin | 100 µg/ml | institute |
| GM-CSF | 500 U/ml | Berlex |
| IL-4 | 250 U/ml | Promo-Cell |
| Ciprofloxacin | 2 mg/ml | Bayer |
| FCS ( 5-10 %) | 5-10 % | Seromed |
| LPS | 100ng/ml | Sigma Aldrich |
| BSA | 0.5%, 1%, 5% | Applichem |

Table 3: Summary of additives used for the culture media

Solutions:

ATV (Adjusted trypsin-versene) (institute);

$NaHCO_3$ (sodium hydrogen carbonate) (institute)

**FREEZING MEDIUM**: 90% fetal bovine serum (FCS) and 10% DMSO (dimethyl sulfoxide)

## 2.5. Solutions and buffers used for cell separation

| | |
|---|---|
| AET solution: | for 1l (10 flasks) of SRBCs:<br><br>2g AET in 50 ml dd$H_2O$ adjusted to pH 9 with 4 N NaOH |
| SRBC ( Sheep red blood cells ) | 1l (10 flasks ) 1% SRBC was centrifuged (2000 rpm, 7 min, at 20° C).The four pellets were combined in 50 ml tubes and Alsevers was added, then centrifuged (2000 rpm, 7 min, at 20° C). |
| 4 % AET-SRBC solution: | SRBC-pellets were solved in AET, incubated in a water bath 20 min at 37° C, then cold PBS-/- was added. After 10 min centrifugation at 1500 rpm, at 20℃ was diluted to 4% with RPMI (10% FCS). |
| erythrocyte lysis buffer | 155 mM $NH_4Cl$, 10 mM $KHCO_3$, 0.1mM EDTA sterile filtered |
| ammonium chloride buffer | For 100 ml : 10 ml 10 x $KHCO_3$ (1 g/100 ml), 10 ml 10 x $NH_4Cl$ (8.3 g/100 ml), 20 µl of 0.5 M EDTA, (pH8) and diluted to100 ml with dH2O |
| Percoll solution: | |

| Gradient 1 ( for 10 ml) | Gradient 2 ( for 10 ml) | Gradient 3 ( for 10 ml) |
|---|---|---|
| 1 ml 1.5 M NaCl (1.076 g/m 5.442 ml Percoll (1.129 g/m 3.558 ml $dH_2O$ | 1 ml 1.5 M NaCl (1.059 g/ml) 4.124 ml Percoll (1.129 g/ml) 4.876 ml $dH_2O$ | 1 ml 1.5 M NaCl (1.045 g/ml) 3.039 ml Percoll (1.129 g/ml) 5.961 ml $dH_2O$ |

Table 4: Summary of solutions and buffers used for cell separation

## 2.6. Antibodies for purity determination of the isolated cell populations

| antibody | dilution | conjugated | manufacturer |
|---|---|---|---|
| CD3 | 1: 100 | FITC | Becton Dickinson |
| CD56 | 1: 100 | PE | Becton Dickinson |
| CD19 | 1: 100 | FITC | Beckman Coulter |
| CD14 | 1: 50 | FITC | Beckman Coulter |
| CD16 | 1: 100 | PE | Becton Dickinson |
| HLA DR | 1: 100 | FITC | Becton Dickinson |

Table 5: Antibodies for control stainings

## 2.7. Immunofluorescence

### 2.7.1. Antibodies for immunofluorescence

| antibody | dilution | conjugation | isotype | clone | manufacturer |
|---|---|---|---|---|---|
| CD3 | 1 : 50 | FITC | IgG1,k | UCHT1 | Becton Dickinson |
| CD19 | 1 : 100 | FITC | IgG2a,k | HIB19 | Becton Dickinson |
| CD14 | 1 : 50 | FITC | IgG2a,k | RM052 | Beckman Coulter |
| CD16 | 1 : 100 | PE | IgG1,k | 3G9 | Becton Dickinson |
| CD56 | 1 : 100 | PE | IgG1,k | B159 | Becton Dickinson |
| HLA-DR | 1 : 100 | FITC | IgG1,k | 5681 | Becton Dickinson |
| MV-H | 1:50 | - | IgG2a,k | K83 | Institute |
| MV-N | 1:100 | - | IgG2a,k | F227 | Institute |
| CD4 | 1:50 | PE | IgG1,k | RPA-T4 | Becton |

| | | | | | |
|---|---|---|---|---|---|
| | | | | | Dickinson |
| IgG1,k | 1:50 | PE | IgG1,k | MOPC-21 | Becton Dickinson |
| CD11a | 1:100 | PE | IgG1,k | HI111 | Becton Dickinson |
| CD11c | 1:50 | PE | IgG1,k | B-ly6 | Becton Dickinson |
| IgG( H+L ) | 1:100 | PE | - | - | Beckman Coulter |
| CD18 | 20µg/ml | - | IgG1,k | MEM 48 | Chemicon |
| Goat F(ab`)2 α-mouse | 1:50 | FITC | - | - | Dianova |
| Goat F(ab`)2 α-mouse | 1:100 | PE | - | - | Beckman Coulter |
| Goat α-mouse | 1:100 | Alexa 594 | - | - | Molecular Probes |
| CD29 | 1:100 | - | IgG2a,k - | - | Becton-Dickinson |
| Goat α- | 1:100 | Alexa 488 | - | - | Molecular |

| | | | | | |
|---|---|---|---|---|---|
| mouse | | | | | Probes |
| tubulin | 1:500 | - | - | DM1A | Sigma |
| LFA-1 | 1:100 | - | - | - | Department of Molecular Cell Biology and Immunology, Amsterdam |
| β1-activated | 1:100 | FITC | - | HUTS-4 | Bioscience |
| fascin mAb | 1:50 | - | - | - | Chemicon |
| CD-3-ξmAb | 1:100 | - | - | - | Santa Cruz |
| talin pAb | 1:200 | - | - | - | Santa Cruz |
| talin mAb | 1:200 | - | - | - | Sigma |
| FN1 (CDw78) | 10-20µg/ml | - | - | - | Dr.Steinar Funderud, Oslo |

| | | | | | |
|---|---|---|---|---|---|
| phalloidin | 1:40 | rhodamine-conjugated | - | - | Molecular Probes |

Table 6: Summary of the used antibodies.

### 2.7.2. FACS buffers

- standard FACS-buffer: 0.4 % BSA 0.02 % sodium acid in PBS $Ca^2+/Mg^2+$ PBS
- saponin-buffer: 0.33 % saponin in FACS-buffer, pH 7.4

## 2.8. In situ-immunlocalisation

### 2.8.1. Buffers for in situ-immunolocalisation

- PBS 500µM $Mg^2+$, 900µM $Ca^2+$
- PBS 500µM $Mg^2+$, 900µM $Ca^2+$, 2.5% BSA, 0.02 % sodium acid
- 1% BSA in PBS-/-, 0.02 % sodium acid
- 5% BSA in PBS-/-, 0.02 % sodium acid
- 0.1% Triton X -100 in PBS
- 4% Paraformaldehyd - in PBS
- PHEMO-buffer: 0.068 M PIPES, 0.025 M HEPES, 0.015M EGTA, 0.003M $MgCl_2$ x 6 $H_2O$, in DMSO pH=6.8

### 2.8.2. Reagents for in situ-immunolocalisation

- Poly-L-Lysin [100µg/ml] (Sigma)
- Phemo-fix (2x): 7.4% PFA, 0.1%GA (glutaraldehyde), 1% Triton-X-100 mixed in water to final volume of 200ml , finally mixed with 200 ml of PHEMO-buffer
- Fluoromount G (Biozol)

## 2.9. FN/ICAM-1 adhesion assays

### 2.9.1. Buffers for adhesion assays

- TSM buffer : 20 mM Tris, 150 mM NaCl, 1 mM $CaCl_2$, 2 mM $MgCl_2$,
- TSA buffer =TSM buffer + 0.5 % BSA

### 2.9.2. Reagents for adhesion assays

- fibronectin 20µg/ml (Sigma) in water
- ICAM-1 (recombinant human Intracellular Adhesion Molecule-1)/Fc Chimera 20µg/m ( R&D systems) in PBS
- 4% paraformaldehyd in PBS
- PMA 0.1µg/ml (Calbiochem) in RPMI 0% FCS

## 2.10. Kit for fast activated cell ELISA-based adhesion assay

FACE-Kit **(**Active Motif Europe) was used.

## 2.11. Cell lysis

Lysis buffer:

1% (w/w) Nonidet P-40 (NP-40)120mM NaCl, 10mM NaF, pH=7.2, 50mM Hepes, pH=7.4, 40mM β-glycerophosphat, 1mM EDTA, 1 tablet protease inhibitors cocktail per 50ml lysis buffer

- **RIPA buffer** lysis buffer

1% (w/w) Nonidet P-40 (NP-40), 1% (w/v) sodium deoxycholate, 0.1% (w/v) SDS, 0.15 M NaCl, 0.01M sodium phosphate, pH=7.2, 2mM EDTA, 50mM NaF, 1 tablet protease inhibitors cocktail per 50ml RIPA buffer

## 2.12. Determination of protein concentration

Performed by BCA- assay (Sigma)

## 2.13. Western Immunoblotting of proteins

### 2.13.1. Buffers for WB

blocking buffer: 5 % w/v skim-milk in PBS

washing buffer: PBS/0.05 % Tween-20

buffer for incubation with the primary antibody: 3 % w/v BSA in PBS/0.05 % Tween-20

buffer for incubation with the secondary antibody: 5 % w/v skim-milk in PBS/0.05 % Tween-20

10 x protein gel buffer for 1 l: 30.0 g Tris, 144 g glycin 10 g SDS, pH 8.7

cathode buffer for 1 l: 3.0 g Tris, 5.2 g hexane acid , 20 % v/v methanol, pH 9.4

30mM anode buffer for 1 l: 3.6 g Tris, 20 % v/v methanol, pH 10.4

300 mM anode buffer for 1 l: 36 g Tris, 20 % v/v methanol, pH 10.4

APS 10 % w/v in dH20.

SDS 20 % w/v in dH20.

loading buffer for SDS-PAGE gel: 200 mM Tris pH 6.8, 4 % w/v SDS 20 % w/v glycerol 0.02 % w/v bromophenolblue 200 mM DTT

protein standard marker for WB (Fermentas)

film: Super X-ray-film, Fuji

nitrocellulose membrane: (Protran®, Schleicher & Schuell)

chemiluminescence substrate: ECL (Amersham Biosciences)

### 2.13.2. Antibodies for WB

| antibodies | dilution | type | manufacturer |
|---|---|---|---|
| Fascin | 1:1000 | monoclonal | Chemicon |
| β1-integrin | 1:500 | monoclonal | Chemicon |
| β1-activated integrin clon(HUTS-4) | 1:500 | monoclonal | Chemicon |
| FAK | 1:500 | polyclonal | Santa Cruz |

| | | | |
|---|---|---|---|
| Erk | 1:1000 | monoclonal | Santa Cruz |
| P-Erk | | monoclonal | Cell Sygnaling Technology |
| Paxillin | 1:1000 | polyclonal | Cell Sygnaling Technology |
| P-Paxillin | 1:1000 | polyclonal | Cell Sygnaling Technology |
| PKC-α | 1:1000 | monoclonal | Santa Cruz |

Table 7: Antibodies for WB

### 2.13.3. SDS-polyacrylamide gel electrophoresis (SDS-PAGE)

Table 8 - Polyacrylamide Separating and Stacking Gels

| **SEPARATING GEL** | 8% | 10% | 12% |
|---|---|---|---|
| 30% acrylamide/bisacrylamide | 8.5 ml | 10.6 ml | 12.8 ml |
| 1.5 M TrisNaCl( pH=8.9 ) | 8 ml | 8 ml | 8 ml |
| $H_2O$ | 15.1 ml | 12.9 ml | 10.8ml |
| 20%SDS | 160 µl | 160 µl | 160 µl |
| TEMED | 10 µl | 10 µl | 10 µl |

| | | | |
|---|---|---|---|
| 10% APS | 280 µl | 280 µl | 280 µl |

| | |
|---|---|
| **STACKING GEL** | 4% |
| 30% acrylamide/bisacrylamide | 1.3 ml |
| 1 M TrisNaCl ( pH=6,8 ) | 1.25 ml |
| $H_2O$ | 6 ml |
| 20%SDS | 50 µl |
| TEMED | 10 µl |
| 10% APS | 100 µl |

**REAGENTS USED IN GELS**

Protease-Inhibitor Cocktail, 1 tablet in 50 ml lysis buffer (Roche)

SDS (1x) Sample buffer / non reducing conditions: 62.5 mM Tris-HCl (pH6.8), 10% glycerol, 50mM DTT, 0.01% w/v bromophenol blue

## 2.14. Kinase assay

### 2.14.1. Kinase buffer

10mM $MgCl_2$, 56mMTris-Cl pH=7.5, added $H_2O$ to 50ml added freshly: 1mM DTT, 0.1mM $Na_3VO_4$, protease inhibitors cocktail (1 tab.)

### 2.14.2. Washing solutions

- 0.5M $LiCl_2$ in PBS
- lysis buffer
- Tris-buffer saline (TBS): 136.8mM sodium chloride, 5mM potassium chloride, 0.9mM calcium chloride, 0.5mM magnesium chloride hexahydrate, 0.7mM dibasic sodium phosphat, 25ml 1M Tris, pH=7.4 and $H_20$ to 1l

## 2.15. Plasmids

### 2.15.1. Human MHCII-GFP plasmid

MHCII-GFP - plasmid was obtained from Dr. J. Neefjes, Netherland Cancer Institute, Amsterdam.

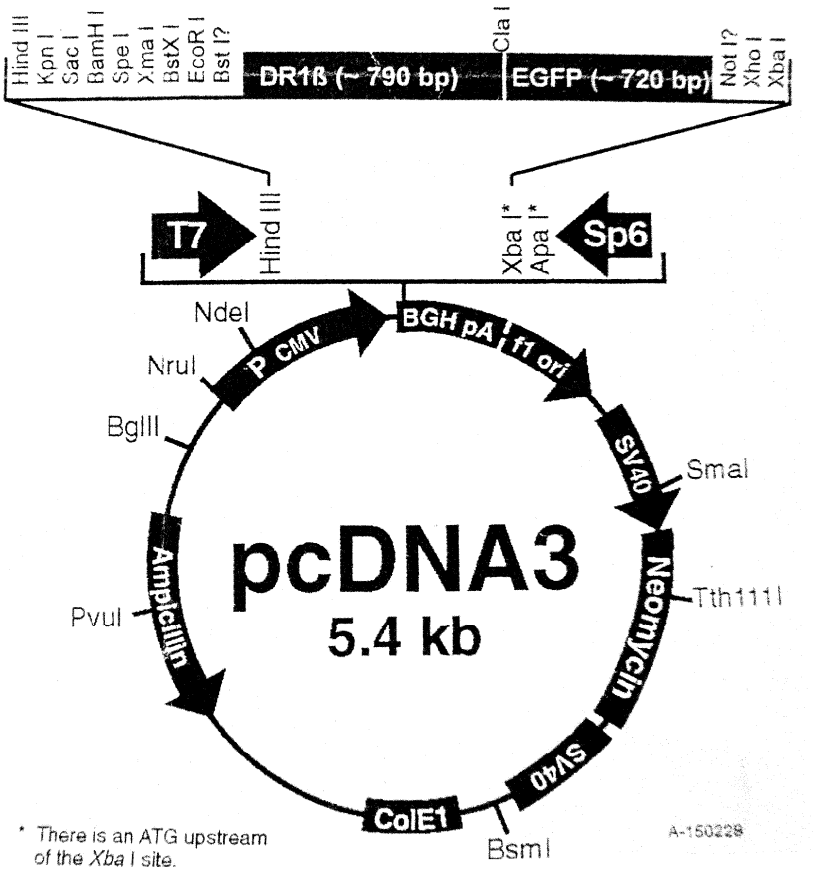

### 2.15.2. Human GTP-ases –GFP Plasmids

The GTP-ases –GFP plasmids were kindly provided by Dr. Francisco Sanchez-Madrid Servicio de Inmunologia, Hospital de La Princesa, Madrid, Spain

| | |
|---|---|
| human V14RhoA-GFP | ca RhoA-GFP |
| human V12Cdc42-GFP | ca Cdc42-GFP |
| human V12Rac1-GFP | ca Rac1-GFP |
| human RhoAN19-GFP | dn RhoA-GFP |
| human N17 Cdc42-GFP | dn Cdc42-GFP |
| human N17 Rac1-GFP | dn Rac1-GFP |

Table 9: Human GTP-ases –GFP Plasmids

The following reagents were used for amplification and purification of the plasmids:

- **LB medium:**

10 g/l Bacto-Tryptone 5 g/l yeast extract 10 g/l NaCl 5 ml/l Tris HCl; pH 7.5; pH= 7.4

- **agar plates:**

10 g/l Bacto-Tryptone, 5 g/l yeast extract, 10 g/l NaCl 5 ml/l Tris HCl; pH 7.5; 15 g/ml agar pH 7.4

ampicillin - 30µg/ml (MHCII-GFP – plasmid) or kanamycin - 30µg/ml (GTP-ases –GFP Plasmids)

- Endofree Plasmid Maxi Kit (Quiagen)

## 2.16. Transfection

DCs were transfected using the dendritic Cell Nucleofector Kit (Amaxa, Germany) according to the manufacturers' instructions.

## 2.17. Materials

| | |
|---|---|
| plastic scrapers | Hartenstein |
| Lab-Tek II Chamber slide System | Nalge Nunc |

Table 10: Materials

## 2.18. Devices

| | |
|---|---|
| FACScan | Becton Dickinson |
| fluorescence microscope | Leitz |
| confocal microscope | Zeiss |
| light microscope | Labovert FS |
| BIO-Photometer | Eppendorf |
| table centrifuge | Heraeus, Sepratech |

| | |
|---|---|
| cell chamber | Neubauer, Thoma |
| platform Shaker | Bühler |
| Nucleofector | Amaxa |
| harvester 96 | Tomtec |
| phosphoimager | FUJI, FLA-3000 |
| Scanning electron microscope | Zeiss DSM 962 |

Table 11: Devices

# 3. Methods

## 3.1. Cell culture

All cells were cultivated at 37°C in a humidified 5%$CO_2$ incubator.

### 3.1.1. Adherent cells

Medium from monolayer cell cultures was completely removed cells were washed once or twice with a small volume of 37°C - warmed medium. ATV was added and the bottle was placed on 37°C for 1 to 2 minutes. Complete medium was added to the detached cells. They were split 1/5 or 1/10 and transfered into a fresh culture bottle. Cultures were passaged 1-2 times weekly.

### 3.1.2. Passaging cells in suspension culture

Suspension cultures were grown in culture flasks and passaged 1-2 times weekly. Cells were transfered into a 50ml tube, centrifuged 5 minutes at 1200 rpm, the pellet was resuspended in small volume of fresh medium, then about one-third of the suspension wasremoved and discarded from the flask and replaced with an equal volume of prewarmed (37°C) fresh medium. Split cells were transferred into fresh culture flask.

### 3.1.3. Freezing and cryo-storage of cells

Cells were adjusted to a final cell concentration of $10^6$ or $10^7$ cells/ml. Freezing medium (4°C) was added and mixed thoroughly. The suspension was divided into aliquots (1ml) into cryovials, which were placed for 1 hour at –20°C, overnight at –70°C and finally were transferred to liquid nitrogen.

## 3.2. Isolation of primary human mononuclear cells

### 3.2.1. Elutriation

The advantage of Elutration method is that enrichment of primary human cells is according to their density, form and size by means of centrifugal strength.

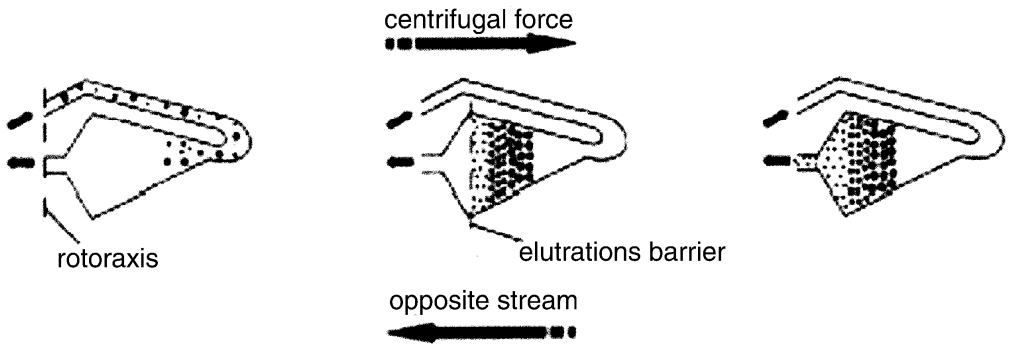


Fig 9. Elutriations process: 1.The medium including suspended cells was introduced into the separating chamber. 2. Cells reached the position, at which there was a balance of the strengths dependence of the cell size, form and density. 3. By rising of the fluid rate and down regulation of the rotor speed the separated cell fractions were washed from
the separating chamber and collected (Luttmann W., 2004)

After centrifugaiting procedure five fractions were obtained:

1st fraction: Mainly erythrocytes but also thrombocytes.

2nd fraction: Mainly T cells, mixed with erythrocytes.

3rd and 4th fraction: Mainly T cells (low number).

5th fraction: Contained mainly monocytes.

The monocyte fraction was directly frozen. The T cell fraction was depleted from erythrocytes by repeated treatment with erythrocyte lysis buffer for a short time (2-7 min). To avoid cell damage due to hypotonic effect of the lysis buffer, RPMI 1640/10% FCS was added and cells were centrifuged at 300 x g for 10 minutes at room temperature. Between

the individual lysis steps cells were washed twice with PBS -/-. Before freezing, aliquots were taken to determine the purity by FACS.

### 3.2.2. Density-gradient separation

The leukocyte cell concentrate separation was carried out in three steps:

1. PBMCs were separated from the leukocyte concentrate by Ficoll-Paque-gradient.

2. Isolation of CD2 positive cells was done by rosetting to AET treated SRBCs (sheep red blood cells).

3. Separating of monocytes by discontinuous Percoll gradients.

4. Staining of cells with a mixture of the monoclonal antibodies: CD3-FITC, CD14-FITC, CD19-FITC, CD16-PE, CD56-PE and HLA-DR-FITC

#### 3.2.2.1. Isolation of primary human mononuclear cells

To isolate PBMCs the leukocyte cell concentrate was first diluted (1:2) with Versene and layered on Ficoll-Paque (30 ml diluted leukocyte solution per 9 ml Ficoll-Paque), followed by density-gradient-centrifugation (30 min, 400 x g, 4°C). Cells were collected from the interphase and transferred into a 50 ml tube, washed 2 - 3 times with PBS-/- and centrifuged at 300 x g for 10 minutes at room temperature. An aliquot was taken for determination of the cell number and for FACS staining. About 30% of the PBMCs were centrifuged and frozen. The other PBMCs served as sourcel for isolation of T cells and monocytes.

#### 3.2.2.2. Isolation of primary T cells via rosetting

Enrichment of T cells was carried out via rosetting to the sheep erythrocytes, which express CD54 molecules (LFA-3) and via CD2 molecules (expressed on the T cells surface) bound the T cells.

For rosetting of the T cells, an 1% - sheep erythrocyte solution was first centrifuged (400 x g, 10 min, at room temperature), then cells were washed with Alsevers. The pellets were resuspended in 4% AET solution and activated for 20 minutes at 37°C in a water bath, which improves binding of CD2-positive T cells. The pellets were washed with PBS-/- repeatedly, centrifuged (10 min, 400 x g, at 20°C) and carefully resuspended with 10% FCS RPMI. Each 3 x $10^8$ PBMCs were mixed with 13 ml of AET treated sheep erythrocytes and 7 ml of FCS, then centrifuged for 5 minutes (200 x g, at 4°C). The pellets were incubated on ice for an hour. During this period the T cells bound to the erythrocytes. The cell pellets were resuspended by rolling and the suspensions put onto Ficoll Paque-gradients for 30min. at room temperature, then centrifuged (400x g, without brake). The interphases contained mostly monocytes, NK cells and B cells, while the T cells were in the pellets. The T cell fraction was depleted from erythrocytes before freezing by short (2-7 min) treatment with erythrocyte lysis buffer. Between the individual lysis steps cells were washed once with 50 ml 10% FCS/ RPMI and twice with PBS-/- to avoided cell damages.

### 3.2.2.3. Isolation and purification of monocytes

The interphase generated during the previous separation step contained monocytes, B cells and NK cells. A discontinuous percoll-gradient was performed to isolate the monocytes. Percoll solutions with different density (1.076 g/ml, 1.059 g/ml, 1.045 g/ml) were prepared. The solutions were carefully layered on a round bottom small polypropylene tube beginning with the solution with the lowest density. After washing with PBS-/- , the cell suspensions were applied onto the gradients and centrifuged for 30

minutes at room temperature, 400 x g without brake. The interphases were then transferred to fresh 50 ml tubes and washed with PBS-/- (for 10 min, at room temperature, 300 x g).

## 3.3. Cultivation of primary human cells

### 3.3.1. Dendritic cells

MoDC (monocyte-derived dendritic cells) were generated in vitro from monocytes. 2 x$10^7$ monocytes were resuspended in 3ml 10% FCS RPMI supplemented with IL-4 [250 U/ml] and GM-CSF [500 U/ml ] and plated at a density of 1.5 x $10^6$ cells/well into 6 well plates. Every two days 1 ml of the medium was removed from each well, collected, centrifuged and replaced with 1 ml of a fresh medium 10% FCS/RPMI with 750 U IL-4 and 1500 U GM-CSF for five to six days (monocytes, obtained by Elutration – for 3-4 days)**.**

### 3.3.2. T cells

Primary human T cells were thawed and propagated as described in the previous section in 10% FCS RMPI

## 3.4. Viruses

### 3.4.1. Wild type virus

The wild type virus was passaged on BJAB. 5 x $10^7$ BJAB cells were infected (a MOI of 0.01) by applying of virus in 0% FCS RPMI and incubated 1-4 hours at 37°C. The cells-virus suspension was repeatedly inverted during the infection period. Cells were centrifuged (5 min, room temperature, 300 x g), resuspended in 100 ml 10% FCS RPMI and grown in a vertically stationary culture bottle in the incubator for two to three days. As soon as a syncytia formation was recognizable, the pre-infection was divided onto fresh

BJAB cells in 550 ml culture bottles. Infection cultures were collected (5 min, room temperature, 300 x g) as soon as a clear syncytia formation could be recognized. Cell pellets were resuspended in PBS -/- and frozen at -20°C overnight. For the extraction of virus particles, cell suspensions were thawed fast and then centrifuged (15 min, 0° C, 1000 x g) to deplete the cell debris from virus stock. The virus stock was divided into aliquots and stored at -80°C.

Parallel to the virus cultivation uninfected BJAB cells were grown under analogical conditions, harvested and also divided into aliquots. These frozen aliquots were also stored at –80°C and served in all tests as mock control.

### 3.4.2. Vaccine strain Edmonston

Vaccine strain Edmonston was passaged on Vero cells, (2 x $10^7$ cells / per culture bottle) infected with a MOI of 0.01. For this, the culture medium was removed and the corresponding volume virus was resuspended in 10 ml 0%FCS/ MEM and applied in each bottle. The cells were infected by incubation 1-4 hours at 33° C. After replacement of the inoculum into 5% FCS/ MEM cells were cultured at 37°C until clear syncytia formation could be recognized. Subsequently medium was removed and replaced by 2 ml PBS-/- . The cells were frozen overnight at -20° C, then thawed rapidly at 4°C, scraped from the culture bottles, resuspended, centrifuged (15 min, 0°C, 1000 x g) and collected in cryo tubes (stored at –80°C ).

The TCID50 (tissue culture infectious dose 50%) indicates the dilution of a virus stock, which is sufficient to infect 50% of the cells in the culture. For the determination of the TCID50/ml by 50% end-point titration, 5 x $10^4$ B95a cells were incubated in 5% FCS/RPMI (100 µl/well), cultured overnight at 37°C. For the infection eight to ten virus stock dilutions

were prepared and resuspended in 0% FCS RPMI and placed on ice. To infect the cells, the culture medium of the B95a cells was replaced by a 100 µl/well of diluted virus stock. After one to three hours incubation at 37° C the medium containing virus was replaced by 100 µl/well fresh 5% FCS/RPMI (100 µl/well). After three to five days the number of CPE-positive wells was determined by light microscopy and the TCID50 was calculated according to the formula (by Spearman and Kärber).

$$\log TCID_{50} = x_{p=1} + \frac{1}{2}d - d\sum p$$

$x_{p-1}$ = highest log dilution giving all positive responses

d = decadic logarithm of the dilution factor

p = CPE positive wells on each dilution step

$\Sigma$ p = the sum of values of p for $x_{p-1}$ and all higher dilutions , which have CPE

$$SE\ \log\mathrm{TCID}_{50} = \sqrt{d^2 \sum \frac{p(1-p)}{n-1}}$$

d = decadic logarithm of the dilution step

p = CPE positive wells on each dilution step

n = the numbers of wells on each dilution step

Calculation of the Standard error of the TCID50 (by Spearman and Kärber) per dilution step.

### 3.4.3. Infection of Monocyte derived Dendritic Cells

Immature DCs were collected into a 50 ml tube and centrifuged (5 min, 300 x g, room temperature). The pellet was resuspended in a small volume and the cell number was determined. DCs were divided into tree tubes, centrifuged (5 min, 300 x g, room temperature) and each pellet was resuspended in 100 µl 0%FCS/ RPMI containing IL-4 and GM-CSF. Corresponded volume of virus was applied to the first tube to distinguish the desired MOI. An equal volume of mock - suspension was added to the second tube. LPS at a final concentration of 100 ng/ml was added to the third tube, used as positive control. All tree tubes were vortexed and incubated at 37° C for 1-2 hours, then washed, centrifuged (5 min, 300 x g, room temperature) and resuspended in 10% FCS /RPMI containing IL –4 and GM-CSF. LPS (100 ng/ml ) was added to the positive control culture. To abolish syncytia formation, FIP (fusion inhibitory peptide) in a final concentration 200 µM was added to the medium. The efficiency of the infection was controlled after 24h by microscopy or FACS after staining of DCs with MV-H or MV-N specific antibodies.

## 3.5. Molecular biological methods

### 3.5.1. Amplification of Plasmids

#### 3.5.1.1. Transformation

A 100 µl aliquot of E. coli competent cell (f.e. XL1 Blue) was thawed on ice, then 50ng of plasmid DNA was added, mixed well and incubated for 45 min. on ice. The next step was heat shock by incubation for 10 min at room temperature (or 45 seconds at 42°C) followed by addition of 1 ml LB-medium without antibiotics. The mixture was incubated 1h at 37°C, followed by short centrifugation step (1min) and 1ml of the supernatant was removed. The bacterial pellet was mixed well in the remaining fluid and seeded onto the agar plates with

ampicillin (MHCII-GFP – plasmid) or kanamycin (GTP-ases –GFP plasmids). The agar plates were incubated overnight at 37°C.

#### 3.5.1.2. Mini- culture and maxi- culture

Mini- culture was prepared according to the manufacturers using Quiagen EndoFree Plasmid mini Kit (Qiagen GmbH). To obtain a proper yield of plasmid DNA, maxi-preparations were performed using Quiagen EndoFree Plasmid maxi Kit (Qiagen GmbH). The concentration of the DNA was determined photometrically.

#### 3.5.1.3. Transfection

Immature dendritic cells (1-2x$10^6$) were transfected with 1-5µg of different GTP-ase-GFP plasmids/ MHCII-GFP or pmax-GFP – control plasmid, according to the manufacturers (Nucleofactor TM Kit, Amaxa, Germany). The efficiency of the transfection was detected microscopically 20-24h after transfection (100µl aliqot with 1.$10^5$ cells was taken from the transfected culture, seeded, fixed with 4%PFA/PBS, washed and covered. 100 cells of 4 different fields were counted and the number of GFP-positive cells was determined. The percentage of GFP-positive cells in the transfected culture was calculated).

## 3.6. Biochemical methods

### 3.6.1. Preparation of cell lysates

Cells were washed with ice-cold PBS and ice-cold RIPA or lysis buffer was added. The plate was incubated on ice and cells were scraped off. The lysis buffer- cells mixture from each well was transferred into tube and vortexed then incubated on ice for 20 minutes. The lysate was centrifuged at 14 000 x g at 4°C for 20 minutes. The supernatant was transfered to a fresh tube and placed on ice. The cell lysate was diluted at 1:10 before

determining the protein concentration and the aliquots were stored at –20℃ or used directly.

### 3.6.2. Determination of protein concentration

Performing BCA- assay (Sigma):

Solution I (bicistronic acid) was diluted 1:50 with Solution II (cupper-II-sulfate). 5 µl of each probe was added to 995 µl BCA-Solution-mix. 5 µl Standard-protein-solution was diluted in 995 µl BCA-Solution-mix and served as control. Probes were incubated 15 min at 60℃, transferred into cuvets and the optical density of the colour reaction was measured at 562nm using an Eppendorf-Photometer with an integrated standard curve.

### 3.6.3. Western Blot

A nitrocellulose membrane was soaked in 30 mM anode buffer and the SDS-gel was soaked in cathode buffer. On the bottom plate of transfer apparatus were placed 2 paper sheets soaked in cathode buffer, the SDS-PAGE gel, the nitrocellulose membrane, 2 paper sheets soaked in 30 mM anode buffer and 2 paper sheets soaked in 300mM anode buffer. The transfer was run for 1 h with a current of 110 mA. After the transfer the nitrocellulose membrane was washed 1 x with PBS/0.1% Tween, incubated 1 h at room temperature in blocking buffer and washed with PBS/0.1%Tween. The membrane was incubated over night at 4℃ with the primary antibody diluted in 3 % w/v BSA in PBS/0,1 % Tween, washed (3 times) by incubation with washing buffer for 10 min at room temperature and incubated 1h at room temperature with the secondary antibody diluted in 5% milk/PBS/0.1%Tween and washed with PBS/0.1%Tween (3 times).

The membrane was incubated for 1 min with the chemiluminescence solution (ECL), placed in plastic wrap and fixed in the cassette. The membrane was exposed to film in the dark room. Signal intensity was quantified by using AIDA software program, Version 4 (Raytest, Straubenhard, Germany)

### 3.6.4. Immunoprecipitation /Co- Immunoprecipitation

DCs were lysed in lysis buffer on ice. To prepare protein A agarose, the beads were washed twice with PBS. Pre-clearing was done by adding 10µl of either protein A or G agarose/sepharose bead slurry per 100µl of cell lysate and incubation 10 min at 4°C on an orbital shaker. To remove the beads cell lysates were centrifuged at 14 000 x g for 10 min at 4°C. The final concentration of the cell lysates was adjusted to 1µg/µl and each sample was mixed with 5µl PKCα antibody and gently rocked for 2 hours or overnight at 4°C. 20µl protein A agarose beads slurry were added to each sample and rocked at 4°C for 1-3 hours, centrifuged 5 seconds at 14 000 rpm, the supernatants were discarded, the beads were washed with ice-cold RIPA buffer (or lysis buffer) 3 time. The agarose beads were resuspended in 25µl/sample 6x loading buffer (without SDS and β-mercaptoethanol), vortexed, boiled for 5 min to dissociate the immunocomplex from the beads. The beads were collected by centrifugation. The supernatants were loaded on SDS-PAGE (10-12%) using nonreducing conditions (without SDS and β-mercaptoethanol).

## 3.7. Cell biological methods

### 3.7.1. Scanning electron microscopy

DCs were washed in PBS-/-, centrifuged 5min/1600g, resuspended in small volume (80-

100µl) PBS-/- or TSM buffer, applied to the PLL (1:1 in $dH_2O$) or fibronectin (20µg/ml in

TSM buffer ) coated chambers and incubated for 1h at 37° C. Cells were subsequently fixed with 6.25% glutaraldehyde in cacodylate buffer 0.1 M, pH =7.4, for 30 min at 37°C (or 1h at room temperature). After washing with cacodylate buffer, cells were postfixed with a mixture of osmic tetroxide ($OsO_4$) 1% and potassium ferrocyanate 1.5% in cacodylate buffer for 30 min. at 4°C. Cells were dehydrated in increasing concentrations of ethanol, critical point dried and sputtered with platin/paladium beror and analyzed on SEM - scanning electron microscopy (SEM) (Zeiss DSM 962).

### 3.7.2. Cell adhesion assay

$1x10^5$ DCs per well were resuspended in 100µl TSM buffer, seeded onto chamber slides, covered with FN (20µg/ml) or ICAM-1 (20µg/ml, recombinant human Intracellular Adhesion Molecule-1/Fc Chimera/ R&D systems), at 37°C for 10, 20 or 60 min and fixed with 4% PFA/PBS for 20 min at room temperature or 10 min with Phemo Fix for MTOC analyses, washed and incubated with 0,1% Triton X-100 in PBS for 5 min. at 4°C . After washing steps with PBS(3x) DCs were blocked with 5% BSA in PBS-/- for 1h at room temperature and cortical actin was visualised by staining with Phalloidin-594, (Molecular Probes). The number of adhered DCs was calculated.

### 3.7.3. FACE method by using FAK Kit

Step 1: The 96-well culture plate was coated with FN for 60 min at 37 °C, and washed twice with PBS. The DCs were seeded at 85 000 cells/well, stimulated 60 minutes at 37°C, fixed by replacing the medium by 4% PFA in PBS for 20 minutes at room temperature, washed 3 x wash buffer (supplied), incubated 20 min at room temperature with quenching buffer (supplied) and blocked for 60 minutes at room temperature with blocking buffer

(supplied). NIH3T3 cells were starved by incubation in 0.2% FCS, DMEM for 16h at 37°C, then seeded, stimulated 60 minutes at 37°C on FN and served as positive control.

Step 2: Binding of primary (for 3 hours or overnight) and secondary antibodies (for 1 hour)

Step 3: Chemiluminescent detection was performed immediately after adding the room temperature chemiluminescent working solution to each well. A CCD camera system and AIDA programme were used to readout the chemiluminiscent (Raytest, Straubenhard, Germany).

### 3.7.4. Immunofluorescence

DCs were counted and $1x10^5$ DC/well were resuspended in 100µl TSM or 0% RPMI, plated on fibronectin- or Poly L-Lysin-coated chamber slides and allowed to adhere for different periods. After fixing in 4% PFA/ PBS for 20 min at room temperature, a permeabilisation step with 0.1% Triton X-100/PBS for 5 min on ice was performed (for intracellular staining) prior to blocking with 5% BSA/ PBS for 30 min at room temperature. Antibodies were added over night at 4°C (or 60 min at room temperature), followed by incubation for 45 min with (1:200) Alexa-488 or Alexa-594 conjugated / secondary antibodies. All antibodies were diluted in 1% BSA/PBS. After 3 washing steps with PBS, chamber slides were mounted in Fluoromount - G mounting medium, covered and sealed with nail varnish. Confocal images were obtained using a Zeiss LSM 510 confocal microscope equipped with x40, x60, x100 immersion lens. Acquisitions and differential interference contrast (DIC) were performed using Zeiss LSM (version 3.0) software, and processing were completed using Photoshop 7.0 (Adobe Systems, San Jose, CA)

### 3.7.5. Extra- and intra- cellular FACS staining

5 x 104 cells were used per FACS staining. Cells were harvested on ice and washed with cold FACS buffer by centrifugation (5 min at 4° C/1500 rpm). Pellets were resuspended with the first antibody, vortexed and incubated in the dark on ice for 30 min. After washing step at 4°C (5 min /1500 rpm) cells were incubated for further 30 min with secondary FITC or PE antibodies in the dark on ice. After washing step andcentrifugation (5 min at 4° C/1500 rpm), cells were analysed by FACScan flow cytometer (CellQuest, Becton Dickinson). For intracellular FACS staining before staining with the primary antibody cells were fixed with 4%PFA for 20 min at room temperature, washed with cold FACS buffer and permeabilised with saponin buffer for 10 min.

### 3.7.6. Conjugate formation between DC and T cells

Chamber slides were coated with PLL 0.1% w/v in dH2O and incubated for 15 minutes at 37°C. Each $5x10^5$ DCs resuspended in 100µl 0%FCS/ RPMI were seeded in each well and incubated for 20-30min at 4°C. DCs were pulsed with SEA 1µg/ml and SEB 1µg/ml in 10%FCS/RPMI, incubated at 37°C for 30 minutes. T cells ($2x10^5$ /well) were resuspended in 10-20µl 10%FCS/RPMI and added to the DCs. Conjugation was allowed by incubation for 30 minutes at 37°C and stopped by fixation with 4%PFA at room temperature for 20 minutes or with Phemo Fix for 10 minutes, at 37°C.

### 3.7.7. Deconvolution /XY/analyses; 3-D confocal images

Tree dimensional image was acquired in 10 focus intervals with a optical difference of 0,5 microns (stack), illuminated by an Argon/2 (488) and / or a HeNe (543) laser exitation source. 3D-image was visible at the image margin. Section of the XZ plane though the

stack: above the XY image. Section of the YZ plane though the stuck: right of the XY image. Section of the XY plane center image - section of the XY plane though the stack: center image.

### 3.7.8. Fluo-4 loading of T cells

To analyse the $Ca^2$+influx in the T cells after contact with DCs, T cells were loaded with Fluo-4. T cells (2x10 $^6$ cells/ml) were washed with 5%FCS/10mM Hepes /HANKS (without $Ca^2$+), pH=7.5, resuspended in 1ml 5%FCS/10mM Hepes /HANKS (without $Ca^2$+) and 1µl/ml Fluo-4 (from stock-1mM Fluo-4 in DMSO; Molecular Probes) was added. Cells were incubated for 30 minutes at 37°C, washed in 1ml PBS -/- (- $Ca^2$+, - $Mg^2$+), centrifuged 5 min at 1600 g, resuspended in 1ml HANKS (without $Ca^2$+), incubated 30min at 37°C, centrifuged /1600 for 5 min and resuspended in 1ml 5%FCS/10mM Hepes /HANKS (with $Ca^2$+). 1x10$^5$ T cells (in 50µl) were applied to the each well with DCs and immediately after adding T cells acquisitions were performed (each 15s for period of 10 minutes). An aliquot of T cells stimulated with ionomycin (final concentration 10µM) was used as positive control for Fluo-4 loading.

### 3.7.9. Live-cell imaging

1x10$^4$- 1x10$^5$ DCs were transfected with different GTPases-GFP or control plasmid –GFP. 4 hours after transfection cells were infected with WTF (moi=2) or treated with LPS or mock. FIP (final concentration 200µM) was added in 10%PRMI with IL-4/GM-CSF to all cultures and DCs were incubated for 18-20h at 37°C, then captured on PLL-coated slides, incubated 30 minutes in 0%FCS/RPMI at 4°C and pulsed with SEB 1 µg/ml and SEA 1 µg/ml for additional 30 minutes in 10% FCS RPMI at 37°C. 10-20µl with 1x10$^5$ - 4x10$^5$ T-cells/well were resuspended in 10%FCS PRMI buffer (for clustering assays); or in

5%FCS/10mM Hepes/HANKS buffer (for $Ca^2$+influx experiments) or in TSA buffer (for tracking experiments). Images were acquired each 15 seconds for entire period of 10 minutes (for $Ca^2$+ influx), each 1 minute for entire period of 25-30 minutes (for clustering assays) or each 2 minutes for entire period of 30 minutes (for tracking experiments)

### 3.7.10. Cell tracking

To analyse the changes in velocity of DCs tracking experiments were performed. Thus, $1x10^4$- $1x10^5$ DCs were transfected (according to the manufacturer's protocol, Amaxa) with different GTPases-GFP (see 3.5.1.3) or control plasmid (pmax-GFP). 4 hours later cells were infected with WTF (moi=2) or treated with LPS (100ng/ml) or mock, resuspended in 10%PRMI with IL-4/GM-CSF supplied with FIP (200µM) and incubated for 18-20 hours at 37°C. Some DCs were pre-incubated with Rac-inhibitor (Bachem) in different concentrations (25µg/ml, 50µg/ml, 75µg/ml, 100µg/ml) for 4 hours at 37°C in 10%PRMI. DCs resuspended in 100µl of TSA buffer were added into fibronectin-coated coverglass slides (Nunc, Lab Tek II) placed at 37°C into a chamber of the confocal laser scanning microscope - LSM Meta, Zeiss based on an inverted microscope (Axiovert 200 M, Zeiss) through an objective (40x, oil, NA = 1,3 Plane-Neofluor). An Argon/2 (488 nm) laser was used as excitation source for GFP positive cells, which were tracked by acquiring an images each 2 minutes for entire period of 30 minutes, transferred to a workstation (Compaq XP100) to calculate the tracking speed. Cell trajectories were analysed by cell image segmentation methods and tracking algorithms, which were run on the Compaq XP100 and the cell movement trajectories were visualised from X and Y coordinates by Illustrator software (10.0)

# 4. Results

## 4.1. DCs morphology and adhesion

### 4.1.1. Morphology and adhesion of WTF- DCs on Poly-L-Lysin (PLL)

It was previously shown (Klagge at al., 2001) that MV infection induced upregulation of cell surface molecules, including MHC class I and II, CD80 and CD86, CD40, CD54 and CD83. DC maturation was more pronounced by wild-type MV (WTF). Morphological changes during DC maturation are characterized by numerous long arborizing processes known as dendrites. The formation of these processes by DCs, both in the periphery and in lymphoid organs, is believed to contribute to the efficiency with which they take up, and after processing, present antigen to T cells. To investigate whether, or to what extent, MV infection induced morphological changes, immature DCs were infected with MV wild-type strain at a moi=0,5. MV-induced fusion was prevented by including with inhibitory peptide (FIP), which was added immediately after infection and also to the control cultures (immature DCs exposed to mock preparations or LPS stimulated DCs). Six hours, 12 hours or 24 hours after infection / treatment, DCs were captured on PLL and surface stained for F-actin by using Alexa 594 direct conjugated phalloidin, and additionally stained for MV protein H followed by secondary Ab-Alexa 488 (Fig.10 a), and then analysed by confocal microscopy. LPS treated DCs had typical long dendrites and the morphology of mock DCs was comparable to those of the infected cultures. Infected DCs were rounded without dendrites.

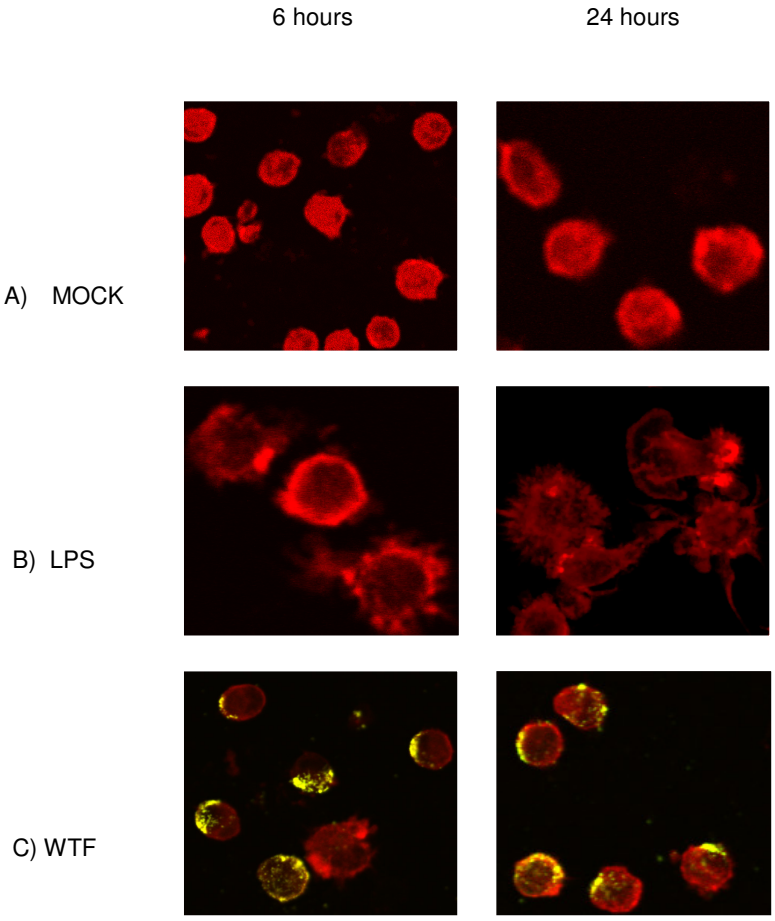


Fig.10: a) Immunofluorescence images of mock- (A), LPS- (B) and WTF infected DCs (moi=0,5)(C), 6 hours (left panels) and 24 hours (right panels) after treatment / infection, were captured on PLL coated slides, fixed and stained for F- actin by phalloidin / Alexa 594, and for MV-H by anti-MV-H – mAb / Alexa 488. Each 100 cells per culture were analysed. Images from one representative experiment out of three independent experiments are shown.

Adhesion assays on PLL coated slides were made to analyse whether MV-WTF infection altered the adhesion properties of DCs. Fig.10 b) summarises the data from three independent experiments. The observed reduction of adhesion in WTF-infected cultures was about 50%, and was similar in mock cultures (66%), as opposed to LPS cultures, in which about 90% of the cells were attached.

### 4.1.2. Morphology and adhesion of WTF-infection DCs on FN and ICAM-1

Cell-to-substrate adhesion assays were used to examine the ability of MV-DCs to attach to extra cellular matrix (ECM) proteins such as fibronectin or ICAM-1.

To find out how the major dynamic rearrangements of the actin cytoskeleton were modulated by MV-WTF infection in DC, we started with immunofluorescence analysis of F-actin using confocal microscopy and adhesion assays of mock-, LPS- or WTF-DC cultures on FN.

Most of the mock-DCs (Fig.11 A) appeared highly elongated and adherent. The morphology was typical for immature DC (Burns et al., 2001). Some infected cells were round with multiple membrane ruffles covering the surface. A high proportion of WTF-infected DCs were polarised with leading-edge lamellipodia (Fig.11 C, indicated by white arrow). In LPS cultures, a large proportion of DC were also polarised with large leading-edge lamellipodia (Fig.11 B, indicated by white arrow). A part of the LPS-DCs were round, lacked podosomes and clumped in small groups of 4-6 cells. There was great similarity between cell morphology in WTF-infected and LPS treated cultures.

Our investigation was continued by scanning electron microscopy analysis. When seeded onto FN-coated slides (for 1 hour at 37°C), cells of heterogeneous morphology were seen by scanning electron microscopy in mock-, LPS-, and WTF-DCs (after infection / treatment for 24 hours) cultures and which scored in appearances ranged from polarised migratory to immobile, ruffled phenotypes (Fig.12, panel I-IV). As expected (from FN attached DCs confocal microscopy data), mock-DCs and LPS-DCs differed with regard to their representation within these categories, and based on these morphological criteria WTF-infected DCs strongly resembled LPS-DCs. Most mock-DCs were small, rounded, adherent (45%) or had a ruffled nonpolarised phenotype (37%) (Fig.12, categories II and IV). WTF-infected DCs were polarised with typical migratory phenotype (67%) like LPS-DCs (70%) (Fig.12, bottom graph, category I). Just 15% of infected cells were small, rounded and adherent (Fig.12, category II). Twelve percent of them had extended

lamellipodial protrusions (Fig.12, category III). Ruffled, nonpolarised phenotype was observed in 4.5% of infected cultures (Fig.12, category IV).

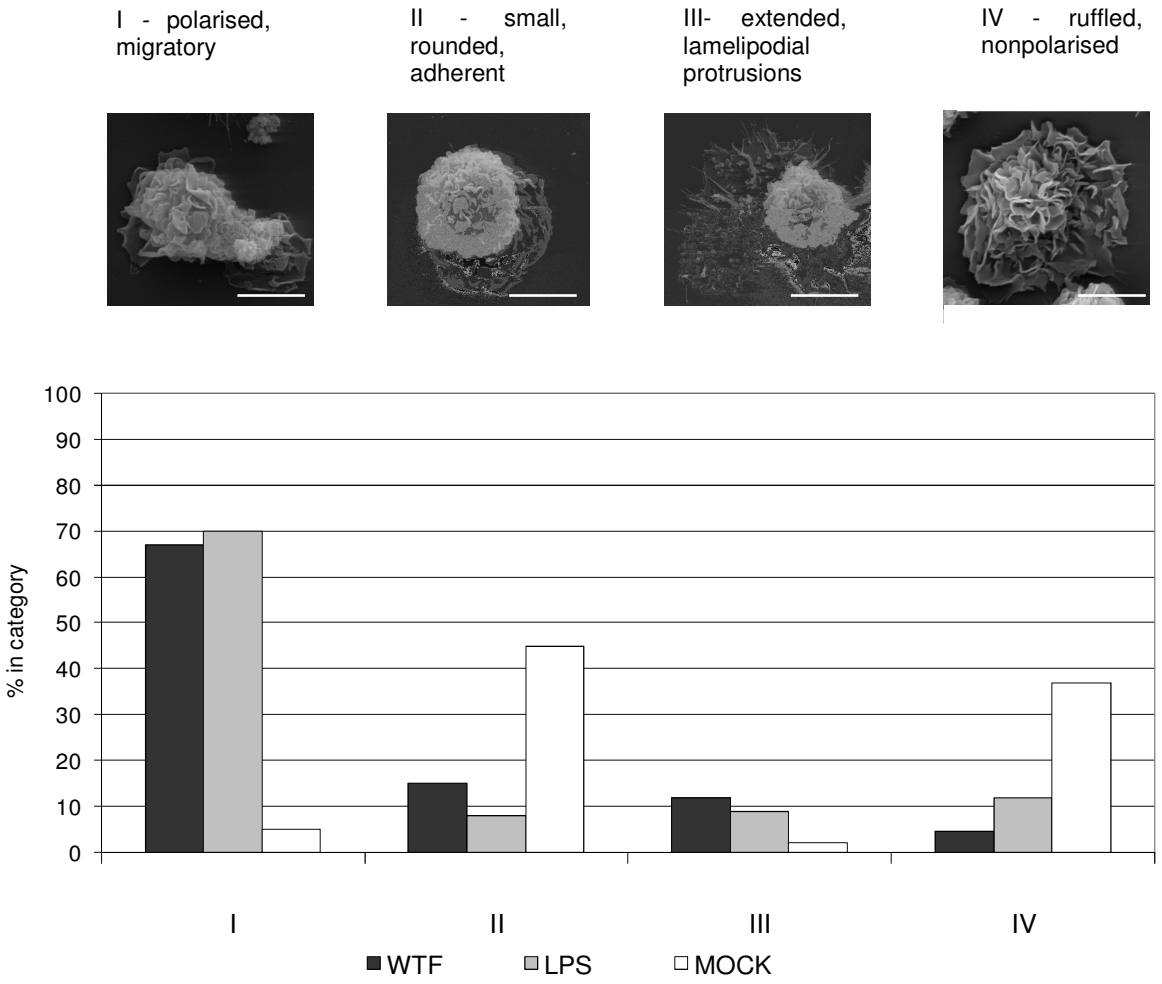


Fig.12 Mock- (white bars), LPS- (black bars) or WTF-DCs (grey bars) were seeded on FN coated slides, fixed and analysed by scanning electron microscopy. Cells were scored into four morphological categories (I: polarised, migratory phenotype; II: small, rounded, adherent; III: extended, lamelipodial protrusions; IV: ruffled, nonpolarised; magnifications: categories I to III: 3000x; category IV: 5000x; bars indicated 5 µm) and the fraction of cells distributed into these categories in each culture (each 300 cells were recruited into the analysis) was determined (%)(bottom graph).

For the adhesion assay mock-, LPS- or WTF-DCs were seeded onto FN or ICAM-1, allowed to attach for 60 minutes, and subsequently stained for F-actin and analysed. Fig.13 shows representative data of three independent experiments. In each case, 100 cells in different fields of view were scored. Changes in morphology were closely

associated with a quantitatively reduced ability of matured DCs to adhere to FN and ICAM-1 (de Vries et al., 2003). This was confirmed in our adhesion assays, where 69% of LPS matured DCs attached on FN, compared to 90% of immature mock-DCs. For WTF-infected DC, only 55% of the cells were attached on FN, even less than with LPS-DCs. The same was true for ICAM-1 coated surfaces, where just 40% of WTF-infected DCs and 60% of LPS-DCs adhered, compared to 97% of mock DCs. Thus, WTF induced a loss of adhesive properties (Fig.13) and acquisition of motile morphology (Fig.12) in infected DCs.

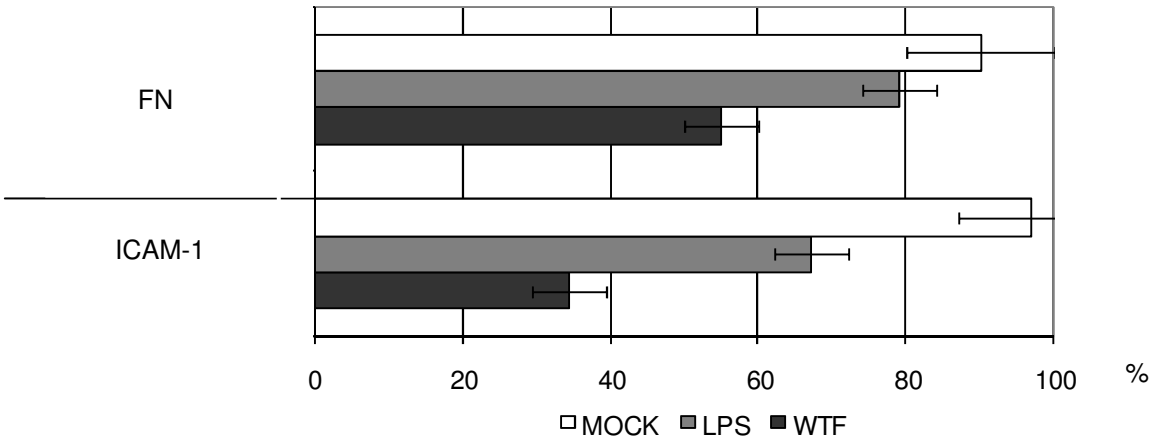


Fig.13 Each 1 x $10^5$ mock- (white bars), LPS- (grey bars) or WTF - DCs (black bars) 24 hours after treatment / infection were seeded onto slides, coated with FN (upper panel) or ICAM-1 (bottom panel) for 1 hour at 37°C and fixed in triplicate assays and the percentage of adherent cells was determined (n=100 cells / culture). The values represented were the means of three independent experiments with standard deviations indicated.

## 4.2. Integrin β-1 in DCs

Both β1 and β2 integrins were expressed by DC and their expression levels weren't changed by maturation (Burns et al., 2004). We were interested to study the expression of integrins on the surface of WTF-infected DCs, as compared to LPS- and mock-DCs, and how these were regulated after ligation by FN- for β1- integrin.

### 4.2.1. β-1 and activated form of β1-integrin expression levels on DCs were not affected by attachment on FN

To study whether MV entry into the cells, or MV replication modulated the adhesion properties of these cells, we used UV-inactivated WTF for treatment or live WTF virus for infection of DCs. Immature DCs were exposed to mock preparations, LPS stimulated, treated with UV-inactivated virus, or infected with WTF (at moi of 2) for 1 hour at 37°C and finally FIP treated. Twenty four hours later, mock-, LPS-, UV-inactivated WTF treated- and WTF infected-DCs were kept in suspension, or were stimulated by attachment on FN for 10, 20 or 60 minutes. Immature DCs in suspension were stimulated with PMA (final concentration 0,1μg/ml) for 20 minutes at 37°C, and served as a positive control. All cells were harvested and stained for surface β1-integrin (Fig.14).

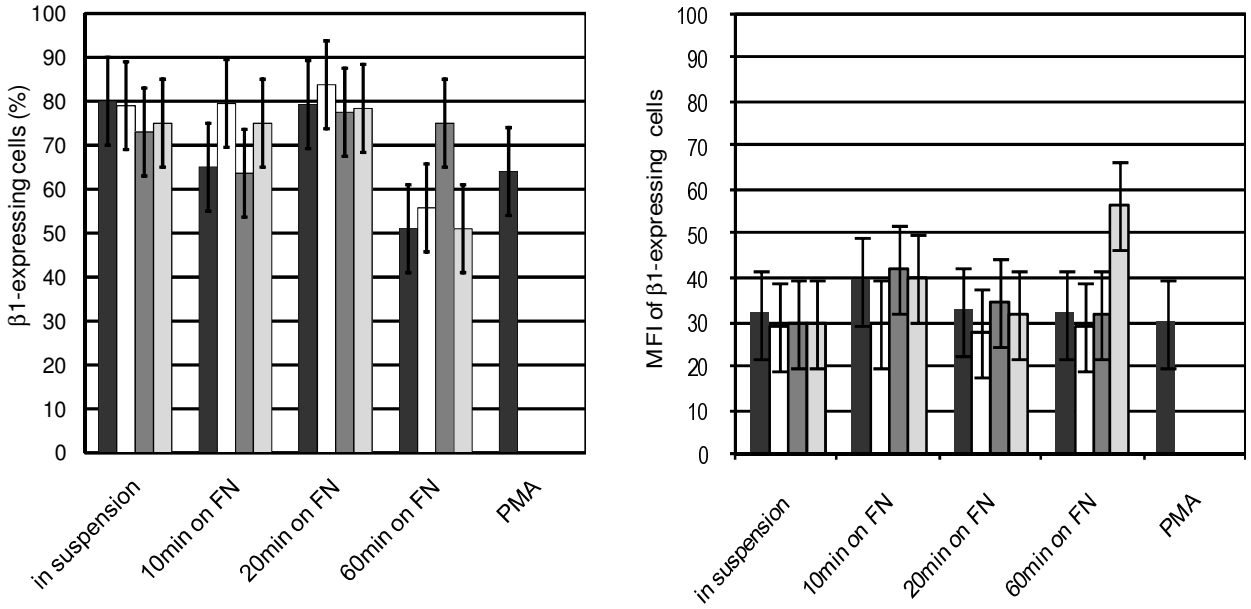


Fig.14
Left panel: The percentage of cells expressing β1-integrin 10, 20 and 60 minutes after FN interaction or left in suspension was determined by flow cytometry (mock-DCs, black bars; LPS-DCs, white bars; UV-inactivated WTF treated DC, dark grey bars; WTF-infected DCs, grey bars). PMA-stimulated (20 minutes at 37°C, concentration 0,1μg/ml) immature DCs served as a positive control, and an IgG1k-specific antibody served as an isotype control.
Right panel: Mean fluorescence intensity of β1-integrin expressing DCs

In suspension mock-, LPS-, UV-inactivated WTF- or WTF-DC cultures, about 80% of the cells expressed β1-integrin on their surfaces. Stimulation of all DC-types by FN ligation had no effect on the β1-integrin expression levels (Fig.14 left panel). Also, except for the value of WTF infected DC after 60 minutes of FN stimulation (Fig.14 right panel), the MFI did not vary. Thus, previously observed differences in adhesion of these DC cultures could not be explained with modulation of β1-integrin levels.

Integrin activation is often mediated by intracellular signals that change the affinity of some integrins for their ligands, termed inside-out signalling (Hughes and Pfaff, 1998). Thus, we asked whether WTF infection or UV-inactivated WTF-treatment could induce affinity modulation in DCs. To determine this, we used mAb clone HUTS-4, which detects the highly activated form of β1 integrin and repeated the previous experiment. All types of DC-cultures (in suspension or FN activated mock-, LPS-, UV-inactivated WTF-, WTF- and PMA stimulated DCs) were harvested and stained for surface activated β1-integrin.

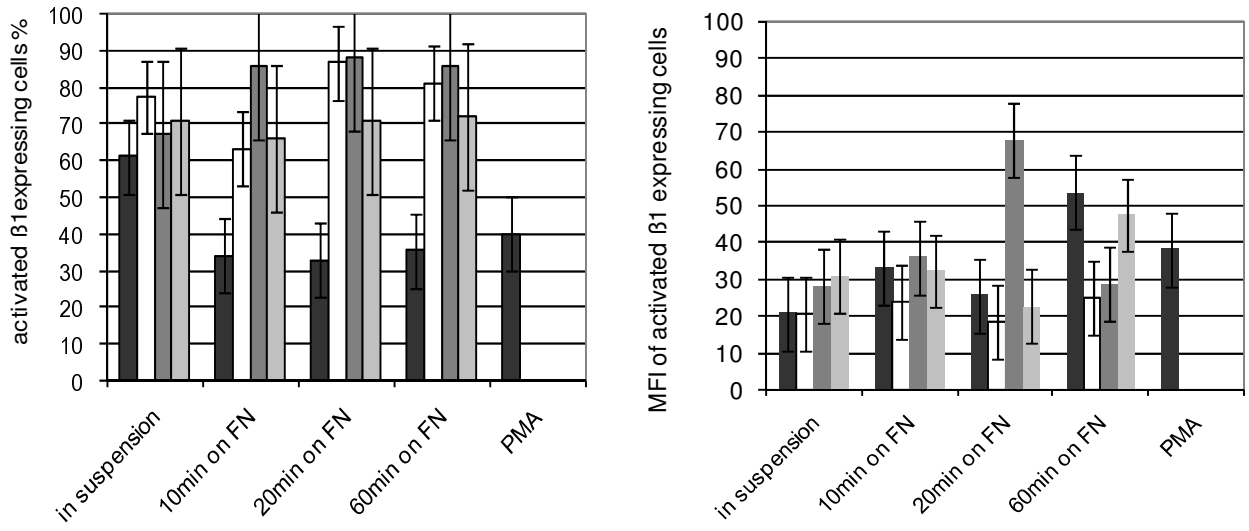


Fig.15 Left panel: The percentage of cells expressing activated β1-integrin 10, 20, 60 minutes after FN interaction or left in suspension was determined by flow cytometry (mock-DCs, black bars; LPS-DCs, white bars; UV-inactivated WTF treated DCs, dark grey bars; WTF-infected DCs, grey bars). PMA-stimulated (20 minutes at 37°C, used concentration 0,1μg/ml) DCs served as a positive control and an IgG2-specific antibody served as an isotype control.
Right panel: Mean fluorescence intensity of activated β1 expressing DCs

Flow cytometry data shown in Fig.15 were determined in three independent experiments. In all cultures 60% to 80 % of suspension DCs expressed the activated form of β1 – integrin. Additional activation for 10, 20 or 60 minutes by FN ligation caused a reduction to 30% in mock cultures. However, in WTF infected DCs, UV-inactivated WTF treated-DCs and LPS–DCs, no effect of activated β1 – integrin expression was detected (Fig.15 left panel). The same was observed for the MFI levels. In comparison to suspension cells, only in DCs treated with UV-inactivated WTF, MFI did increase after 20 minutes of FN stimulation (Fig. 15 left panel: dark grey bars). We concluded that FN adhesion had no impact on the expression of activated β1-integrin, neither on the rate of expressing cells nor the MFI**.**

### 4.2.2. Activated β1-integrin distribution in WTF-DCs

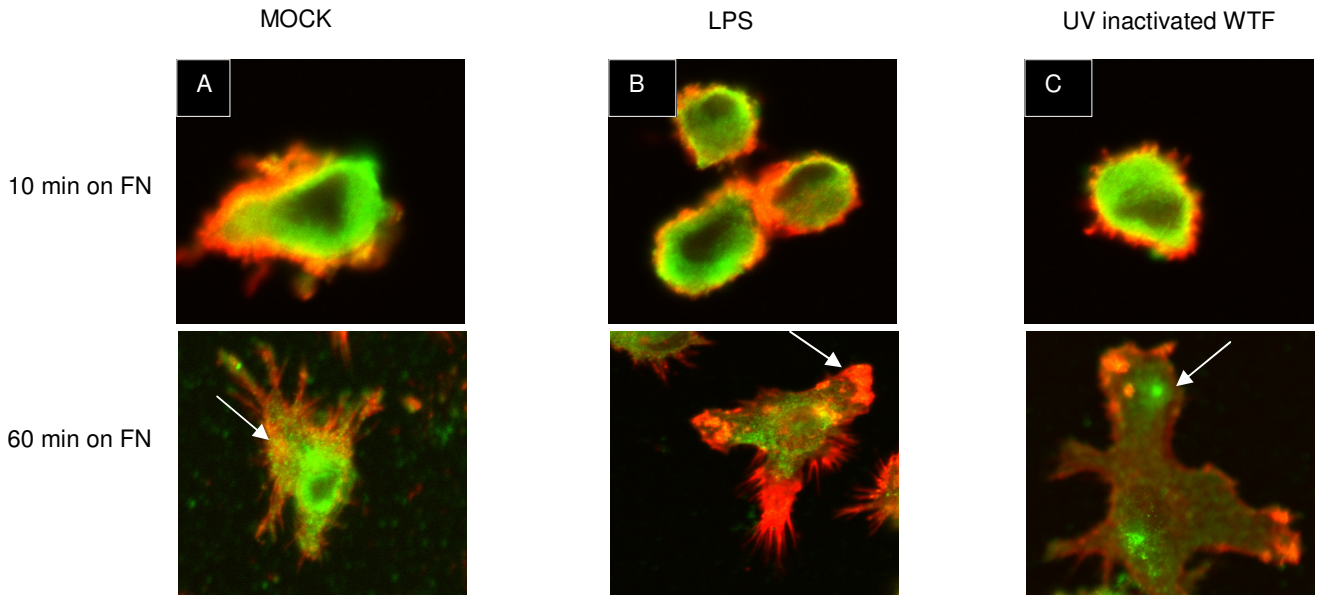


Fig.16 Representative images of mock-(A), LPS-(B), WTF-(not shown) and UV-inactivated WTF treated DCs (C) 24 hours after treatment / infection seeded onto FN for 10 minutes (upper row) or 60 minutes (bottom row), fixed and stained for F- actin detected by phalloidin-Alexa 594 and for β1 activated-integrin detected by anti- β1activated (clone HUTS-4) mAb / secondary Ab-Alexa 488. Each 100 cells / culture were analysed. Images from one representative experiment out of three independent experiments are shown.

Next, we looked at the subcellular localisation of activated β1-integrin in FN seeded WTF-DCs, UV-inactivated WTF-DCs, LPS-DCs and mock-DCs by immunofluorescence analysis. Images of representative mock-, LPS- and UV-inactivated WTF DCs, attached for 10 or 60 minutes on FN are shown in Fig.16 (A, B and C). WTF-infected DCs were also FN attached (for 10 or 60 minutes) and analysed, but images are not shown, because they looked like UV-WTF DCs (Fig.16 C upper and bottom row). At the early time point, where DCs were stimulated for 10 minutes F-actin and the activated form of β1- integrin co-localised in all DC cultures. Later, after 60 minutes stimulation, spotted distribution of activated β1-integrin and co-localisation with F-actin in these patched structures was seen in mock-DCs (Fig.16 A, shown with white arrow). The same was rarely detected in LPS-, WTF-infected and UV-inactivated WTF-DC cultures. In WTF-infected (images not shown), UV-inactivated-WTF treated DCs (Fig.16 C, shown with white arrow), and LPS-DCs, large lamellipodia with concentrated F – actin at the leading edge (Fig.16 B, shown with white arrow), but without co-localisation with activated β1-integrin were observed. In WTF-infected, like in UV-inactivated WTF-DC, β1-activated integrin was only detected in adhesion aggregates (Fig.16 C, shown with white arrow).

## 4.3. Signalling pathway and regulation of integrins in DCs

Our investigation was focused on the intracellular signalling pathways, regulating integrin recruitment. Ligand binding to integrins leads to integrin clustering and recruitment of actin filaments and signalling proteins to the cytoplasmic domain of integrins (Hynes, et al. 2002; Adams et al. 1997) (Fig.17). These ECM attachment and signalling centres were

termed focal complexes (FCs) when they were still nascent, and focal adhesions (FAs) when they matured into larger complexes (Hynes, et al. 2002). In our further investigation, we analysed proteins that structurally or functionally link integrins with the actin cytoskeleton in mock-, LPS- and infected-DCs (Fig.17).

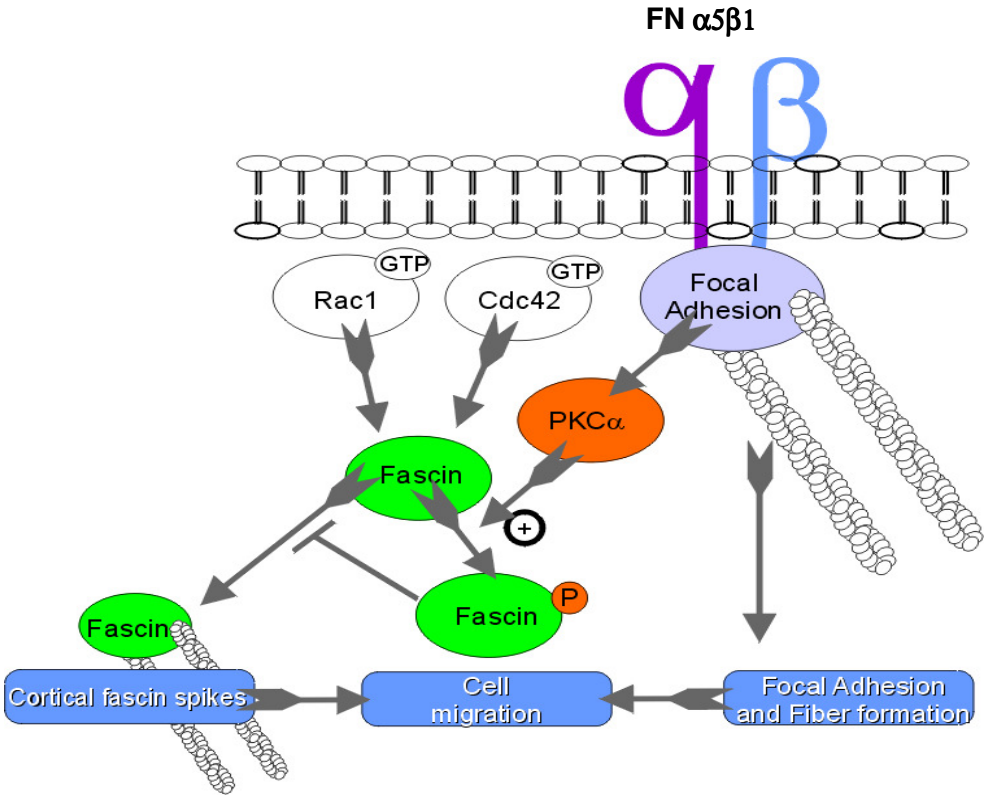


Fig.17 Schematic representation of β1– integrin signalling (Adams et al. 1997)

### 4.3.1. Focal adhesion kinase activity in infected DCs

Activation of FAK triggers the formation of protein complexes that can modify the actin cytoskeleton. We were interested in investigating whether the phosphorylation levels of FAK in mock-, LPS- and WTF-DCs vary. Thus, we stimulated mock-, LPS- and WTF-DCs by attachment on FN coated wells (Fig.18 A, black bars), or kept them in suspension in the wells for 1 hour at 37°C (Fig.18 A, white bars). Further, all DC-cultures were analysed by using the ELISA-based–method. Here, after fixation cells were incubated with the primary antibodies, which recognised phosphorylated FAK or total FAK. This was followed by a HRP–conjugated anti-rabbit IgG secondary antibody, and finally incubated with developing solution). NIH3T3 cells which were left in suspension (unstimulated) or attached on FN for 1 hour at 37°C (stimulated) (Fig.18 A, upper and bottom row) served as a positive control. Suspension- or FN attached-NIH3T3 cells, which were incubated with secondary antibody alone, served as a negative control (Fig.18 A, middle row). All DC-cultures were scanned with a CCD camera system, which was used to readout the chemiluminescence (Fig.18 A). Total-FAK or FAK-phosphorylation levels were quantified by using AIDA software (Fig.18 B). The phosphorylation level of stimulated NIH3T3 cells was taken as a 100% value (Fig.18 B, the last black bar), and wells without cells were taken to quantify the background (Fig.18 A, middle row on the right side). The experiment was done in triplicate and data are shown in Fig.18. One representative image out of three is shown (Fig.18 B).

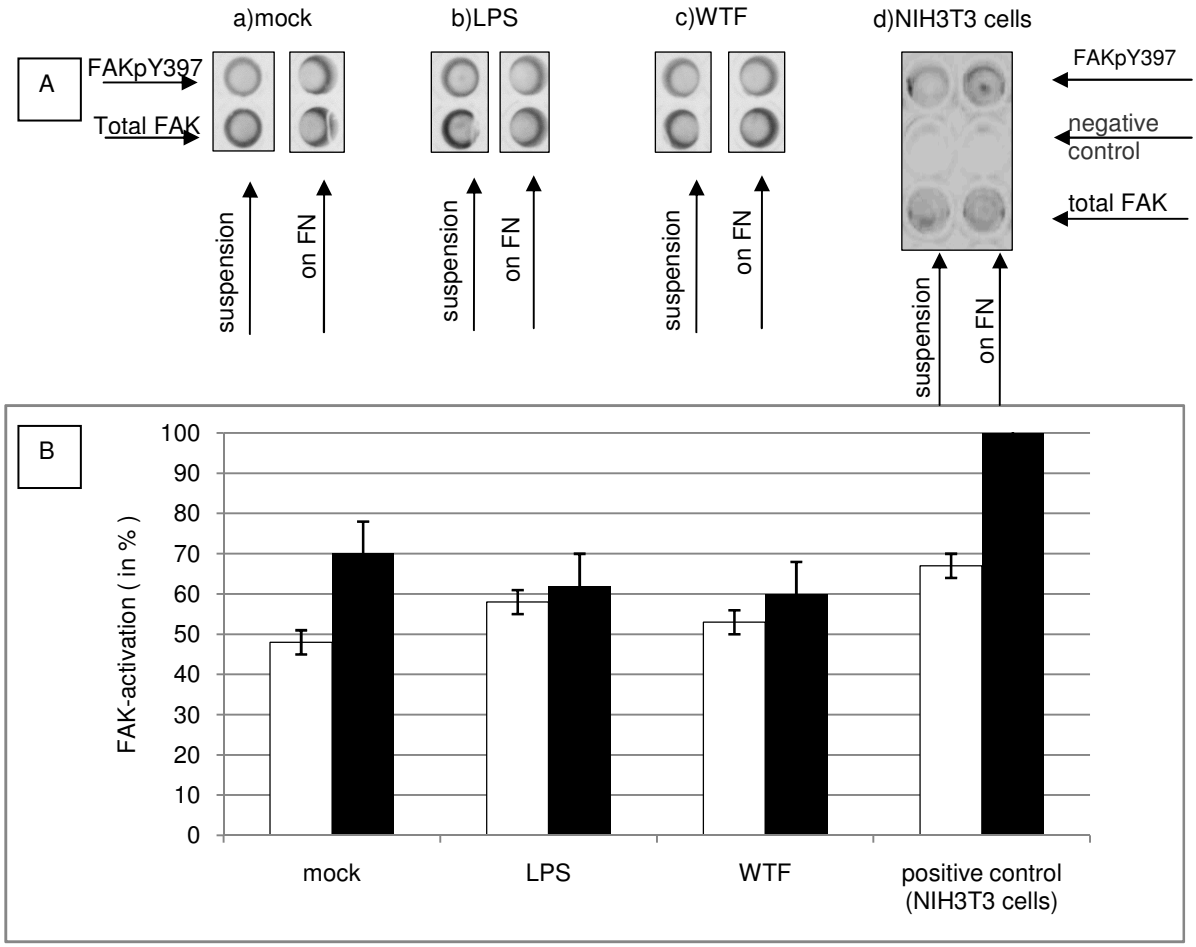


Fig.18 Mock- (a), LPS- (b), WTF-DCs (c) and NIH3T3 cells (used as positive control)(d) in suspension (left panels), or after 1 hour of FN stimulation (right panels) were stained for P-FAK by specific pAb-FAK pY397 (upper row), or stained for total FAK by specific pAb-FAK (bottom row). Suspension (d)(left panel) or FN stimulated (for 1 hour) NIH3T3 cells (d)(right panel) were stained just with secondary antibody and served as a negative control. All DC-cultures were stained with HRP-conjgated anti-rabbit IgG secondary antibody, followed by a chemiluminiscent solution, and the chemiluminescence was read with a CCD camera system.
A) Images of the scanned wells, which visualised the signal intensity in the cells incubated with p-FAK or FAK antibodies were obtained from a CCD camera system. Wells without cells were scanned and taken as background. One representative experiment out of three independent experiments is shown.
B) Quantification of FAK-activation (in %) detected by total FAK in suspension mock-, LPS-, WTF-DCs and NIH3T3 cells (white bars) or after FN (1 hour, at 37°C) stimulation detected by pY397-FAK (black bars) was made with the AIDA programme. The values represented were the means of three independent experiments with standard deviations indicated.

In mock-DCs, FN stimulation induced elevated FAK autophosphorylation (Fig.18 B, first pair of white/black bars). In LPS- and WTF-DCs, FAK phosphorylation was high and was not upregulated after FN stimulation (Fig.18 B, second and third pair of white/black bars).

### 4.3.2. Fascin expression in MV-infected DCs

Fascin is a small globular protein that plays an important role in formation of cell protrusions and cytoplasmic actin bundles. Fascin is a protein specifically expressed in mature DCs and has been found necessary for T cell stimulation (Al-Alwan et al., 2001). WTF infected-, LPS-treated and mock-DCs were lysed 24 hours or 36 hours after infection/treatment. Lysates were separated by 10% SDS-PAGE. Proteins were transfered to the membrane and analysed by Western blotting for fascin or moesin with specific mAbs (Fig.19).Lysed HeLa cells were used as a positive control, lysed T cells served as a negative control.

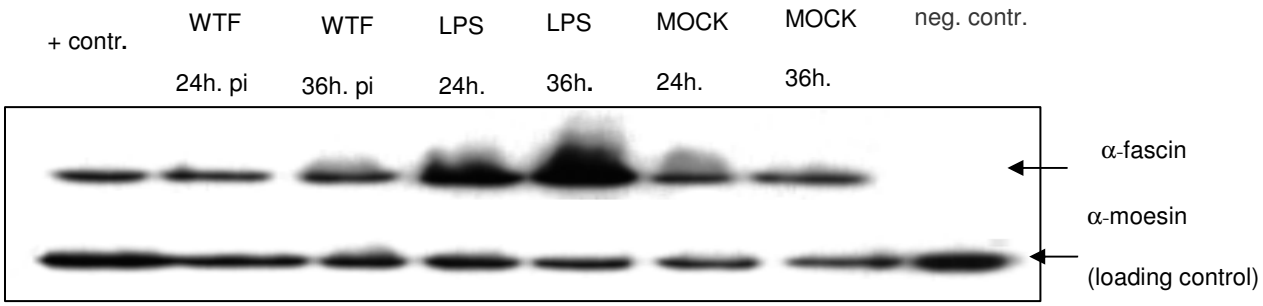


Fig.19 Fascin expression in mock-, LPS- and WTF infected- DCs, which were lysed 24 hours or 36 hours after treatment / infection. Lysates were separated by SDS-10% polyacrylamide gel electrophoresis. Proteins (fascin and moesin) were detected by Western blotting with specific mAb α- fascin (upper part) and with mAb α- moesin (bottom part) used as loading control. HeLa cells served as a positive control and T cells as a negative control. One representative experiment out of three independent experiments is shown.

Consistent with maturation dependent expression of this protein, fascin was expressed at low levels, both 24 hours or 36 hours of culture in mock DCs. By contrast, fascin was upregulated over time in LPS-DCs. WTF-DCs showed an intermediate phenotype in that overall fascin levels remained substantially lower than in LPS-DCs. Next, we determined the percentage of fascin positive cells in mock-, LPS- and WTF-DCs (moi=0,5 or moi=1) 36 hours after treatment / infection by IF. For each experiment (n=3), DCs were stained

with specific mAb-α-fascin, followed by Alexa 488-conjugated secondary antibody, and 100 cells per culture were counted (Fig.20 A and B). The percentage of MV-infected cells in WTF-DC-cultures was determined by immunostaining with MV-human serum, followed by Cy3-conjugated anti-human secondary antibody, and subsequently stained with mAb-α-fascin, followed by Alexa 488-conjugated secondary antibody. Each 100 cells per infected culture were analysed. The represented means of three independent experiments are shown in Fig.20 bottom part: (a) and (b). We observed a correlation between infection efficiency and fascin expression in WTF infected cultures: 25 % (Fig.20 A) or 45 % (Fig.20 B) of the cells expressed fascin 36 hours after infection using moi of 0,5 or moi of 1, respectively.

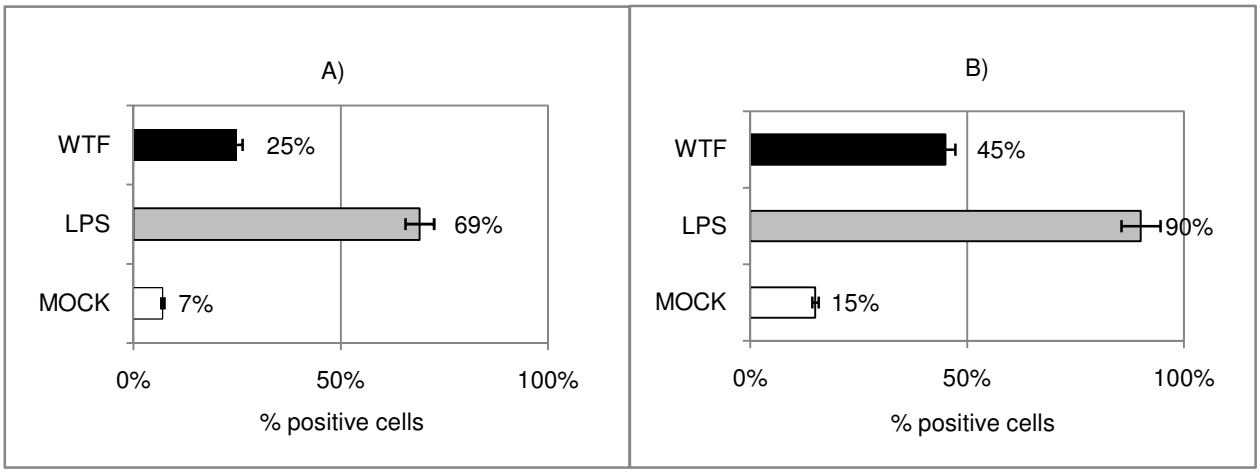


a) 22% MV-WTF infected DCs

b) 45%MV-WTF infected DCs

Fig.20 The percentage of DCs expressing fascin was determined in mock- (white bars, A and B), LPS– (grey bars, A and B) and WTF infected DCs (black bars; A: moi=0,5; B: moi=1) 36 hours after treatment or infection, by using a specific mAb-α-fascin, followed by Alexa 488-conjugated secondary antibody by IF analysis. Each 100 cells per culture were counted. The values represented, were the means of three independent experiments with standard deviations indicated.
Bottom part: The percentage of MV-infected cells (at moi of 0,5 (a) or moi of 1 (b)) in WTF-DC-cultures was determined by staining with MV-human serum, followed by Cy3-conjugated anti-human secondary antibody and subsequently stained with mAb-α-fascin, followed by Alexa 488-conjugated secondary antibody. Each 100 cells per infected-culture were analysed, and the means of three independent experiments are shown (a, b).

### 4.3.3. In FN stimulated WTF-DCs fascin interacted with PKCα

The actin bundling activity of fascin depends on its capacity to crosslink actin monomers and this is inhibited by phosphorylation on S39 (Adams et al., 2004). In cell lines seeded on FN, PKCα mediated phosphorylation of S39 (Anilkumar et al., 2003) and led to the dissociation of fascin from F-actin bundles, as well as a diffuse localisation of fascin. However, in DCs it has not been explored whether PKCα could directly bind fascin. Next, we investigated the interaction between PKCα and fascin in infected DCs by co-immunoprecipitation using nonreducing conditions (see methods). Twenty four hours after WTF-infection (moi of 1,5), LPS- or mock- treatment DCs were attached on FN or left in suspension for 60 minutes, lysed, and the final protein concentration was adjusted to 1μg/μl. Precipitated fascin and PKCα were detected by using specific antibodies (mAb α–fascin and mAb anti-PKCα). In all unstimulated (in suspension) DC cultures (Fig.21, lines 4, 5, 6) and in FN stimulated mock-DCs,just a small quantity of fascin was co-precipitated with PKCα (Fig.21, line 3). In LPS-DCs FN stimulation induced strong fascin-PKCα association (Fig.21, line 2), where in WTF-DCs fascin associated moderately strong with PKCα (Fig.21, line 1).

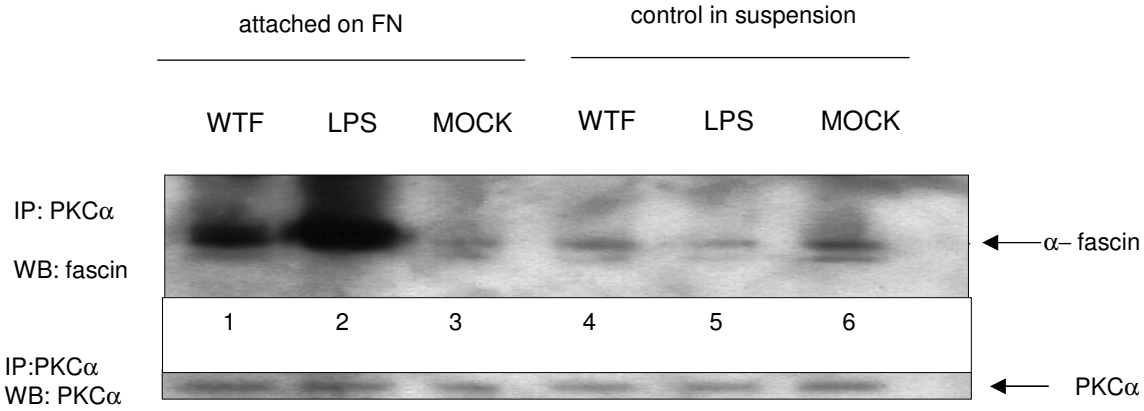


Fig.21 Co-immunoprecipitation between PKCα and fascin detected by mAb α-fascin (upper panel) and a loading control, detected by mAb PKCα (bottom panel). WTF infected DC, LPS–DCs and mock-DCs were attached on FN (bands 1, 2 and 3) or left in suspension (bands 4, 5 and 6) for 1 hour and lysed. Lysates were immunoprecipitated (IP) with an anti-PKCα antibody, followed by anti-fascin immunoblotting (WB) (upper panel) and anti-PKCα reblotting (bottom panel). The results of one representative experiment out of three independent experiments are shown.

Further, we looked for colocalisation between fascin and F-actin by immunofluorescence analysis. Thus, 24 hours after WTF infection (moi=1,5), LPS- or mock-treatment DCs were attached on FN for 1 hour, fixed and stained with specific mAb for fascin, followed by Alexa-488, and for F-actin by phalloidin / Alexa 594, and then imaged by confocal microscopy. LPS-DCs and WTF-infected DCs were large and polarised, and fascin was distributed diffusely (Fig.22 B and C middle panels). Their migratory phenotype was characterised by the disappearance of cortical fascin spikes. F-actin and fascin co-localised on leading edges of these cells (Fig.22 B and C bottom panels, merge, seen in yellow and labelled with white arrows). In mock-DCs, multiple focal contacts (Fig.22 A bottom panel, merge, seen like yellow dots and labelled with white arrowheads) and long thin processes were apparent.

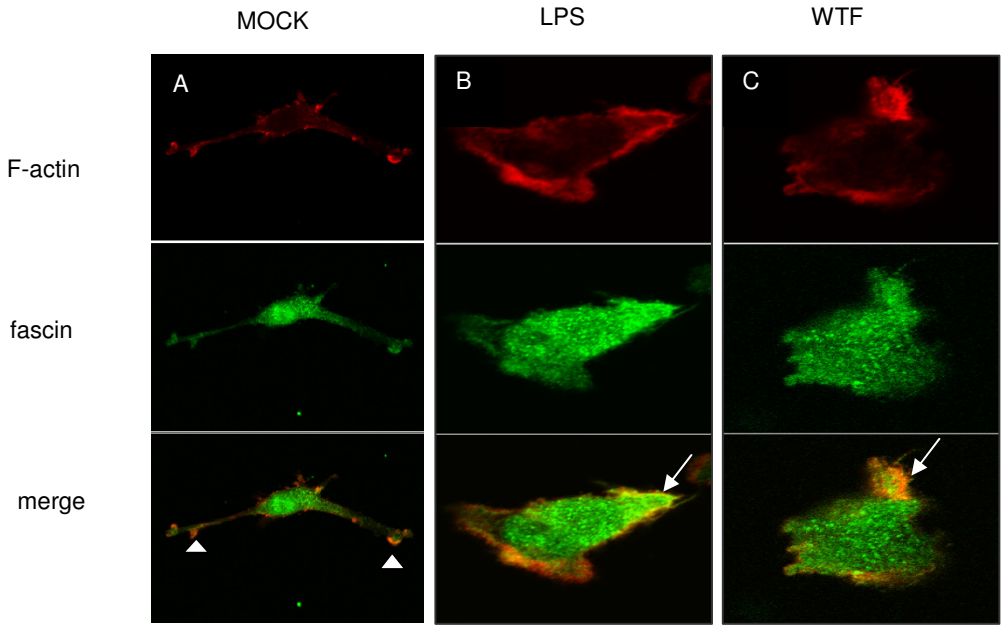


Fig.22 Immunofluorescence images of mock- (A), LPS- (B) and WTF infected DCs (C) 24 hours after treatment / infection were attached on FN coated slides for 1 hour, fixed and stained for fascin and F-actin. F- actin was detected by phalloidin / Alexa 594 (first row panels) and fascin by mAb α-fascin/ Alexa 488 (second row panels). F-actin and fascin colocalisation was shown in the merge images (third row panels). Original magnification: 40x. Leading edges in LPS-DCs and WTF-DCs were shown with white arrows (B and C, merge images). The focal contacts in mock-DCs (A, merge image) were shown with white arrowheads. Each 100 cells per culture were analysed and representative examples are shown. Original magnification: 100x.

## 4.4. Role of Rac1-GTPase in adhesion and movement of DCs

Acquisition of a migratory capacity is associated with DC maturation, and for murine DCs on FN, this is RhoGTPase Rac associated (Benvenuti et al., 2004b). To analyse whether this also applied to human DCs, and if so, was affected by WTF-interaction, mean velocities and trajectories of these cells were tracked at a single cell level on FN coated slides by scanning microscopy. Immature DCs were transfected to express GFP-tagged constitutively active (ca) Rac1 or dominant negative (d.n.) Rac1. For control, DCs were transfected with a pGFP-control plasmid, and 4 hours later, infected with WTF (moi=2), treated with LPS, or mock treated for 18-20 hours. When indicated, Rac1-inhibitor was applied to DC cultures for four hours. Tracking was performed immediately after seeding of resuspended cells onto FN-coated chambered coverglass slides, which were placed into a chamber, and then on the stage of the confocal laser scanning microscope at 37°C. Cell images were scanned through the lens of a Laser Scanning system, which was mounted on an inverted microscope. Scanning was done at 37°C. An Argon/2 (488nm) laser was used as an excitation source for GFP+ cells and for differential interference contrast (DIC). Frames were acquired every 2 minutes for 30 minutes and transferred to a workstation (Compaq XP100) to calculate the tracking speed of the GFP+ cells. Twenty cells per type were analysed. The mean velocity of DC in μm/min is shown in Fig.23 A. Since these experiments were performed in the absence of added chemoattractants, the trajectories followed for mock-, LPS-, or WTF-DC cultures were random, rather than directional. The high motility of immature DCs, transfected to express GFP-tagged constitutively active (ca)

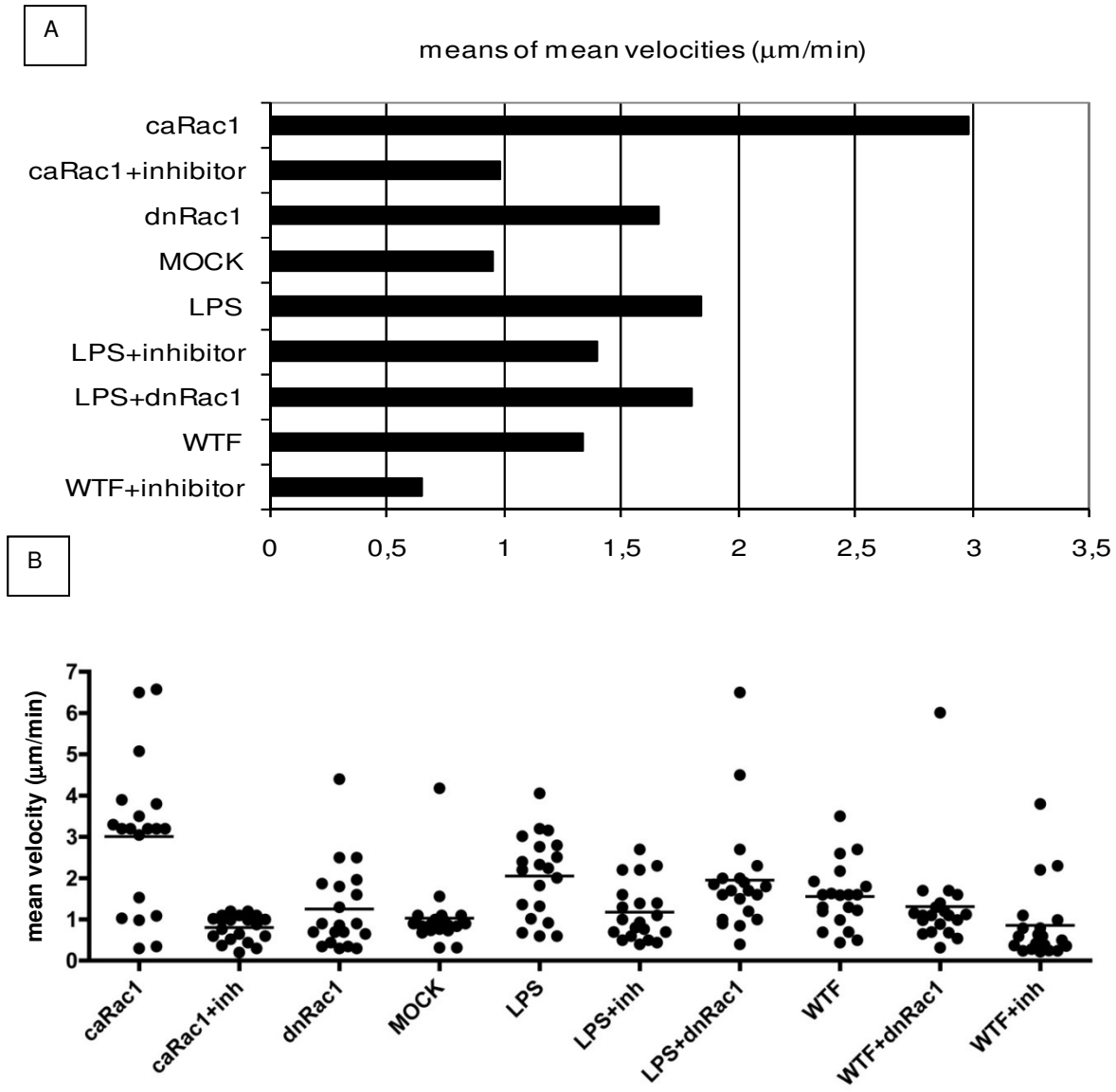


Fig.23 A. Mean velocities were determined by recording movement of GFP+ cells in cultures of immature DCs, transfected to express constitutively active (ca) Rac1-GFP (left untreated or pre-exposed to 100 µg/ml Rac1-inhibitor for 4 hours), dominant negative (dn) Rac1-GFP or pGFP transfected mock-, LPS- or WTF-DCs (pretreated or not with 100 µg/ml Rac1 inhibitor) immediately after seeding on FN for 30 minutes (frames were acquired every 2 minutes). n= 20 per sample.
B. Individual mean velocities for transfected (caRac1, dnRac1 or pGFP, respectively), mock-, LPS-, and WTF-DCs in the presence or absence of 100 µg/ml inhibitor are shown.

Rac1 was lost dose-dependently by inclusion of a Rac-inhibitor to approach values determined for immature and mock-DCs transfected with a pGFP-control plasmid (Fig.23

A and B). This confirmed that migration of human DC also involved Rac activity. In common with murine DCs (Benvenuti et al., 2004b), mean velocities of human LPS-DCs exceeded those measured for mock-DCs by about two fold: 1,84 μm/min versus 0,85 μm/min (Fig.23 A). For both, LPS-DCs and WTF-DCs, mean velocities were rather variable with the latter migrating overall about 30% slower than LPS-DCs 1,84 μm/min (Fig.23 A) and 1,3 μm/min, respectively (Fig.23 B). Corroborating the importance of Rac activity, motilities of LPS- and WTF-DCs were sensitive to the Rac-inhibitor (Fig.23 A and B). The motility of immature DCs transfected to express GFP-tagged dominant negative (dn) Rac1 did not decrease. Also, the motility of LPS- and WTF-DCs transfected to express dn Rac1 did not vary from that of nontransfected LPS-DCs and WTF-DCs. Overall, however, WTF-infection affected Rac-dependent dynamic interaction of DCs with FN only to a moderate extent.

## 4.5. DC/T cell immunological synapse (IS)

### 4.5.1. MTOC orientation in WTF-DC/T cell conjugates

Next, we analysed the ability of superantigen (SA)-loaded WTF-DCs to stably conjugate to and organise functional immune synapses (IS) with cocultured allogenic T cells after 25 minutes. For this, mock-, LPS- and WTF-DC (24 hours after infection / treatment) were SA-loaded allowed to conjugate with T cells for 25 minutes, and after fixation, stained with α-tubulin mAb, finally analysed by confocal microscopy. Compatible with the formation of a functional IS, LPS-DCs, but surprisingly also WTF-DCs, efficiently redistributed the T cell MTOC towards the interface (Fig.24 C and B). This suggests that WTF-DCs should be able to promote T cell activation.

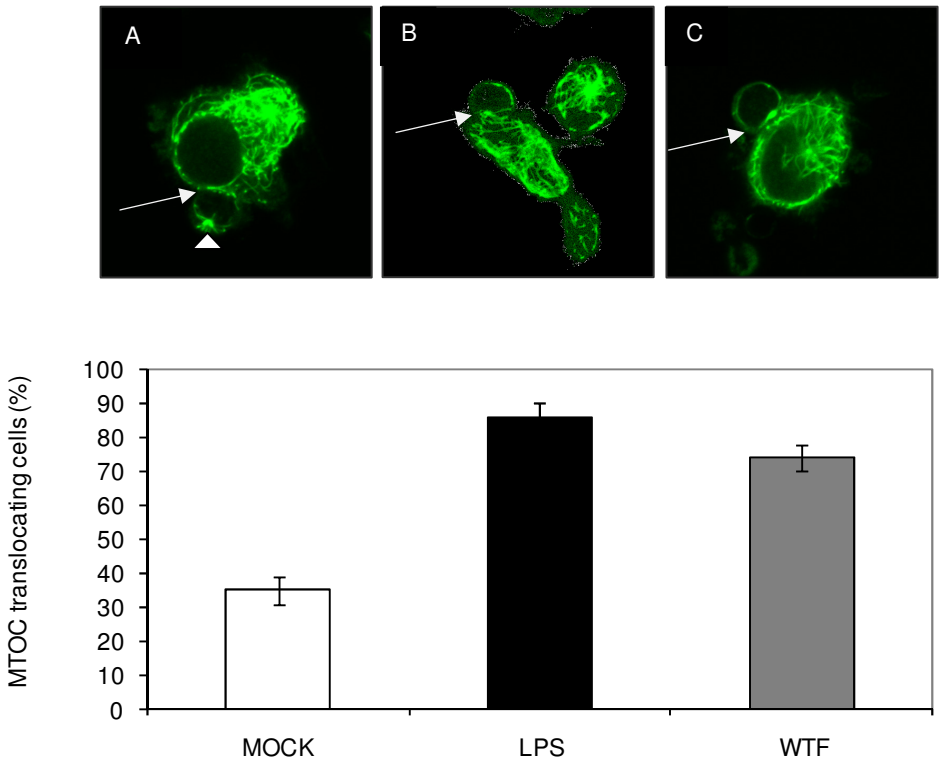


Fig.24: Upper panels: Conjugates formed between SA-loaded mock- (A), LPS- (B) or WTF-DCs (C) and allogenic T cells after 25 minutes at 37°C were fixed and analysed for subcellular localisation of α-tubulin by confocal microscopy, using staining with mAb α-tubulin / Alexa 488. In (A) the position of the MTOC was indicated by an arrowhead, and the interface by a white arrow which marks the position of the MTOC in the interface in (B) and (C). Original magnification: 100x
Lower panel: The percentage of cells redistributing the MTOC towards the interface was determined for each culture mock-DCs (white bars), LPS-DCs (black bars) and WTF-DCs (grey bars) by confocal microscopy (n=100 conjugates / culture).

Our data revealed that in 80% of the conjugates between WTF-DCs and T cells, the MTOC of T cells correctly translocated towards the contact surface (Fig 24 lower panel, grey bars). The same was true in 90% of the LPS-DC/T cell conjugates (Fig 24 lower panel, black bars). By comparison, just 30% of the T cell - MTOC were correctly translocated to the contact interface in mock-DC/T cell conjugates.

### 4.5.2. Analyses of the IS architecture

In the classical (APC/T cell), IS were defined structures, termed supramolecular activation clusters (SMACs) (Monks et al., 1998; Dustin et al., 1998). On a cell-cell interface, LFA-1(leukocyte function-associated antigen 1) and ICAM-1 (intercellular adhesion molecule 1), as well as talin formed a ring (termed peripheral synapse region - pSMAC) around a central cluster of TCR-MHCp (T cell receptor - MHC-peptide complex), termed central synapse region - cSMAC (van-der Merwe et al., 2000).

#### 4.5.2.1. LFA-1/talin distribution in DC-T cell conjugates

To study the architecture of the IS in our system in more detail, we stained DC/T cell synapses for LFA-1 and talin, which were both representative marker proteins of a pSMAC. To do this, we allowed conjugate formation between (SA)-loaded mock-DCs, LPS-DCs or WTF-DCs (moi = 2) (24 hrs after treatment/infection) and allogenic T cells for 25 minutes, fixed, stained by using specific antybodies (pAb $\alpha$-talin / Alexa 594 and mAb $\alpha$-LFA-1 / Alexa 488), and analysed by confocal microscopy. Images of the conjugates interfaces (red lines, indicated with arrows) were deconvoluted and analysed with Zeiss software. The intensity profiles for distribution of LFA-1 and talin were shown as histograms under the synapse (Fig.25 A, B, C and D panels). Identified conjugate interface types were scored into four categories: central, peripheral, multifocal and homogeneous. The central distribution of LFA-1 and talin was rarely observed in any of the three DC cultures (less than 10%) (Fig.25 A and E). The peripheral ring formed by these two proteins was observed in 20% of LPS-DC/T cell conjugates, and in less than 10% of mock-DC/T cell and WTF-infected DC/T cell conjugates (Fig.25 B and E). Most of the analysed DC/T cell conjugates (about 70%) formed multifocal pSMACs (Fig.25C and E), where co-

localised talin and LFA-1 were organised into multiple small patches. The distribution of LFA-1 and talin was homogeneous in 20% of the WTF-DC/T cell and mock-DC/T cell conjugates, and in just 10% of the LPS-DC/T cell conjugates (Fig.25 D and E). Overall, no differences in the LFA-1 and talin distribution in the three types of DC/Tcell conjugates were found.

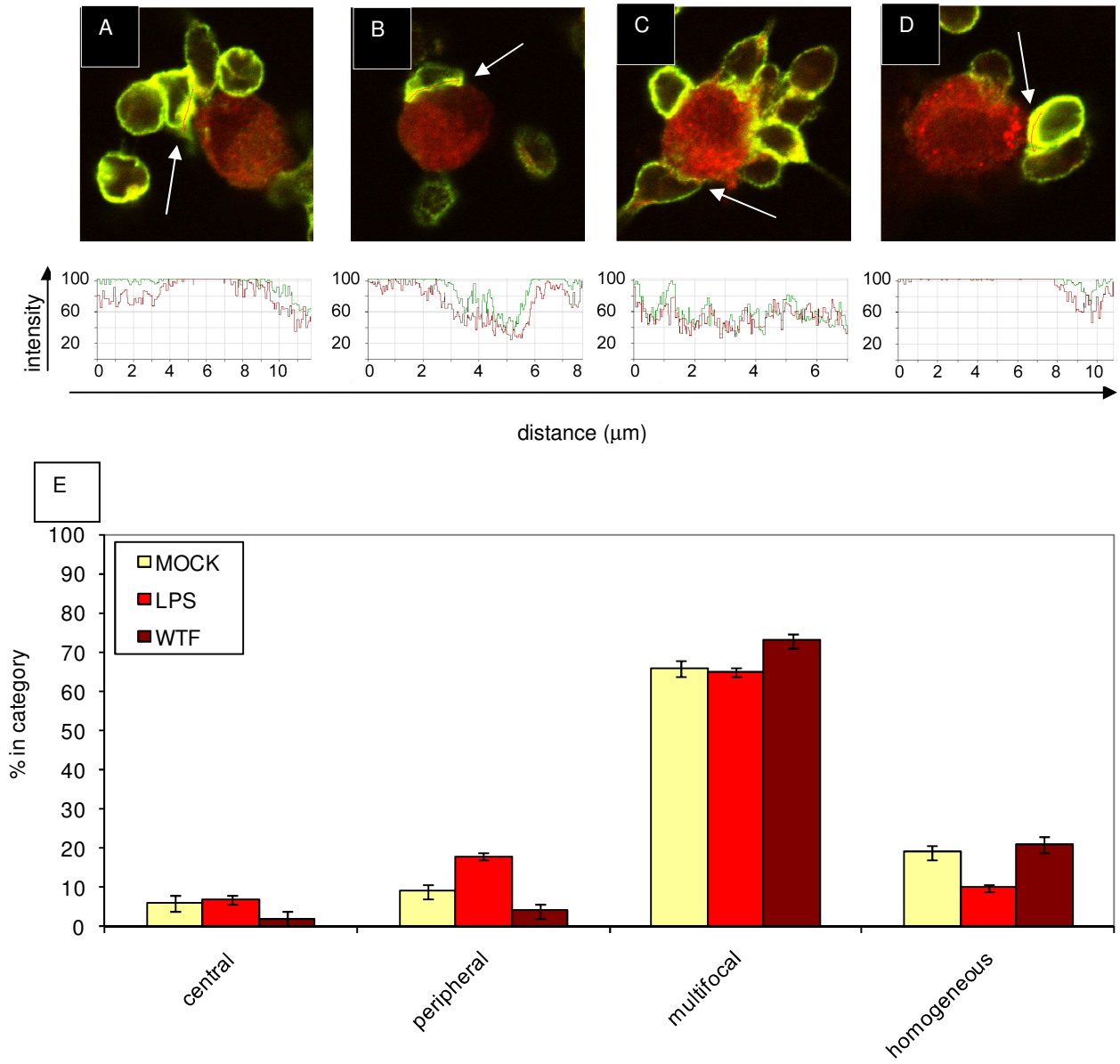


Fig.25 A – D. Interface organisation in conjugates formed between SA-loaded mock-, LPS- or WTF-DCs 24 hours after treatment/infection and allogenic T cells (which were cocultured for 25 minutes at 37℃ and fixed) was categorised after double labeling for LFA-1 / Alexa 488 and talin / Alexa 594 (A-D) (illustrated for central organisation in A, peripheral organisation in B, multifocal organisation in C and homogeneous organisation in D). In panels A - D, the interface analysed was indicated by arrows. The intensity profiles for distribution of both antigens are shown as histograms under the synapse (red line, indicated by white arrows).
E. Quantitative analysis of DC-Tcell conjugates: the percentage of synapses of each category was determined in cocultures with mock- (yellow bars), LPS- (red bars) and WTF-DCs (brown bars), (n= 20 conjugates / culture for LFA-1/talin).

#### 4.5.2.2. CD3/talin distribution in DC-T cell conjugates

Stable conjugates between (SA)-loaded mock-, LPS- or WTF-DCs (24 hours after treatment/infection) and allogenic T cells cocultured for 25 minutes were fixed and analysed for spatial distribution of CD3 and talin by confocal microscopy. Conjugates were stained with mAb-CD3ζ /Alexa488 (green) and pAb-talin/Alexa594 (red). Images of the conjugates interfaces were deconvoluted and analysed for the intensity profiles of CD3 and talin distribution. A more precise *en face* view of the IS was provided by pseudocolor images and 3D reconstructions of XY and XZ planes, performed with Zeiss software. Fig.26 A to D shows XY and XZ pseudocolored reconstruction of the *en face* view with hues ranging from blue (low) to red (high). As for LFA-1/talin, types of IS detected were scored into four categories (central, peripheral, multifocal and homogeneous). The percentage of cells seen in individual cultures revealing these IS types were determined. The typical bulls eye distribution (Fig.26 A), where CD3 was in the middle surrounded by a ring of talin was seen in 10% of LPS-DC/T cell conjugates (Fig.26 E, blue bars), and in less than 6% of WTF-DC/T cell conjugates (Fig.26 E, bright blue bars), but not in mock-DC/Tcell conjugates (Fig.26 E, dark blue bars). The peripheral type of CD3/talin distribution was infrequent in all cultures (Fig.26 B and E). A multifocal pattern for CD3/talin was mainly detected with LPS-DCs (60%) or WTF-DCs (55%) (Fig.26 C and E). Interestingly, homogeneous distribution of these proteins, as predominantly seen in more than 80% of mock-DC/Tcell conjugates, also occurred in about 20% of WTF-infected DC/T cell conjugates (Fig.26 D and E). Overall, however, the spatial organisation of the interface was similar for WTF- and LPS-DCs.

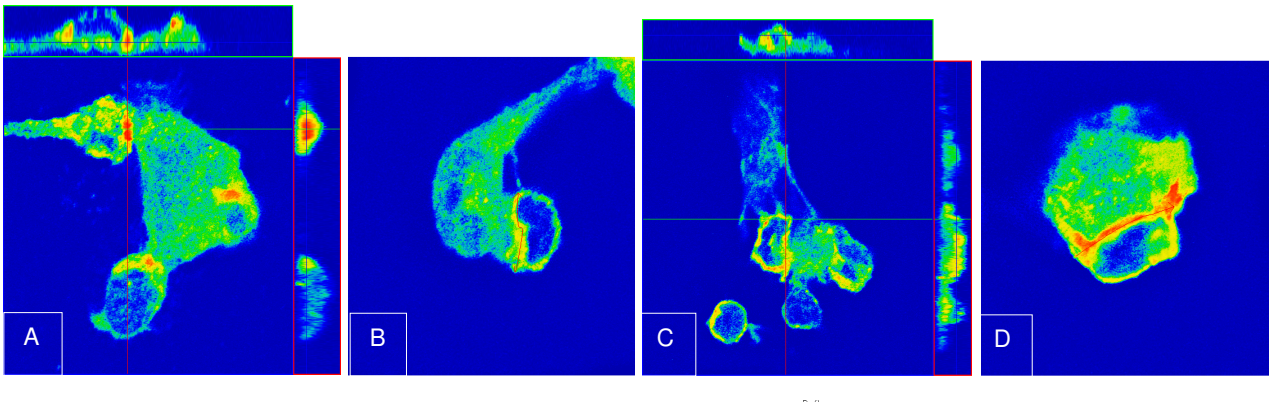


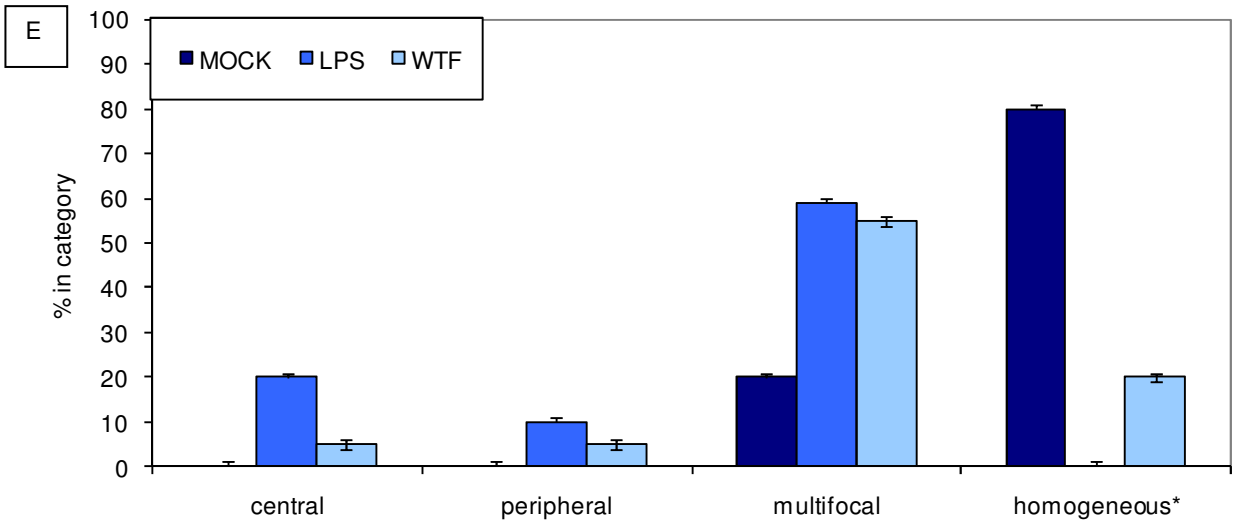


Fig.26 A-C. Interface organisation in conjugates formed between SA-loaded mock-, LPS- or WTF-DCs and allogenic T cells after 25 minutes at 37°C, fixed and was categorised after double labeling for CD3 and talin. Representative examples of each 20 conjugates analysed per culture were shown (A to C).
Central (A), peripheral (B), multifocal (C) and homogeneous (D) distribution of CD3/talin: XY and XZ pseudocolored reconstruction of the *en face* view (Zeiss Software, Ortho), with hues ranging from blue (low) to red (high).
E) The percentage in synapses of each category was determined in cocultures with mock- (dark blue bars), LPS – (blue bars) and WTF-DCs (bright blue bars) (n=each 20 conjugate / culture). Original magnification: 100x.

#### 4.5.2.3. MHCII / CD3 distribution in DC-T cell conjugates

Next, we examined the MHCII distribution in DCs towards the T cell interface. Immature DCs were transfected with pMHCII-GFP (green), 4 hours prior to exposure to mock- or LPS- or WTF infection. After 20 hours, they were SA-loaded and allowed to conjugate with T cells for 25 minutes. To localise the c-SMAC, the fixed conjugates were further incubated with CD3ζ–mAb (conjugated with secondary Ab-Alexa 594), and then analysed by confocal microscopy (n=20 synapses per culture). In LPS-DC/T cell conjugates, MHCII appeared as big green clusters, which colocalised with the CD3 (red) in yellow dots (Fig.27 B, white arrow). By comparison, smaller MHCII clusters formed in infected DCs, which colocalised with CD3 in green-yellow dots (Fig.27 C, white arrows). In mock DC/T cell conjugates, MHCII was homogeneously distributed and CD3 clusters were not orientated towards the DC interface (Fig.27 A, white arrow here shows the contact surface, without CD3 clusters).

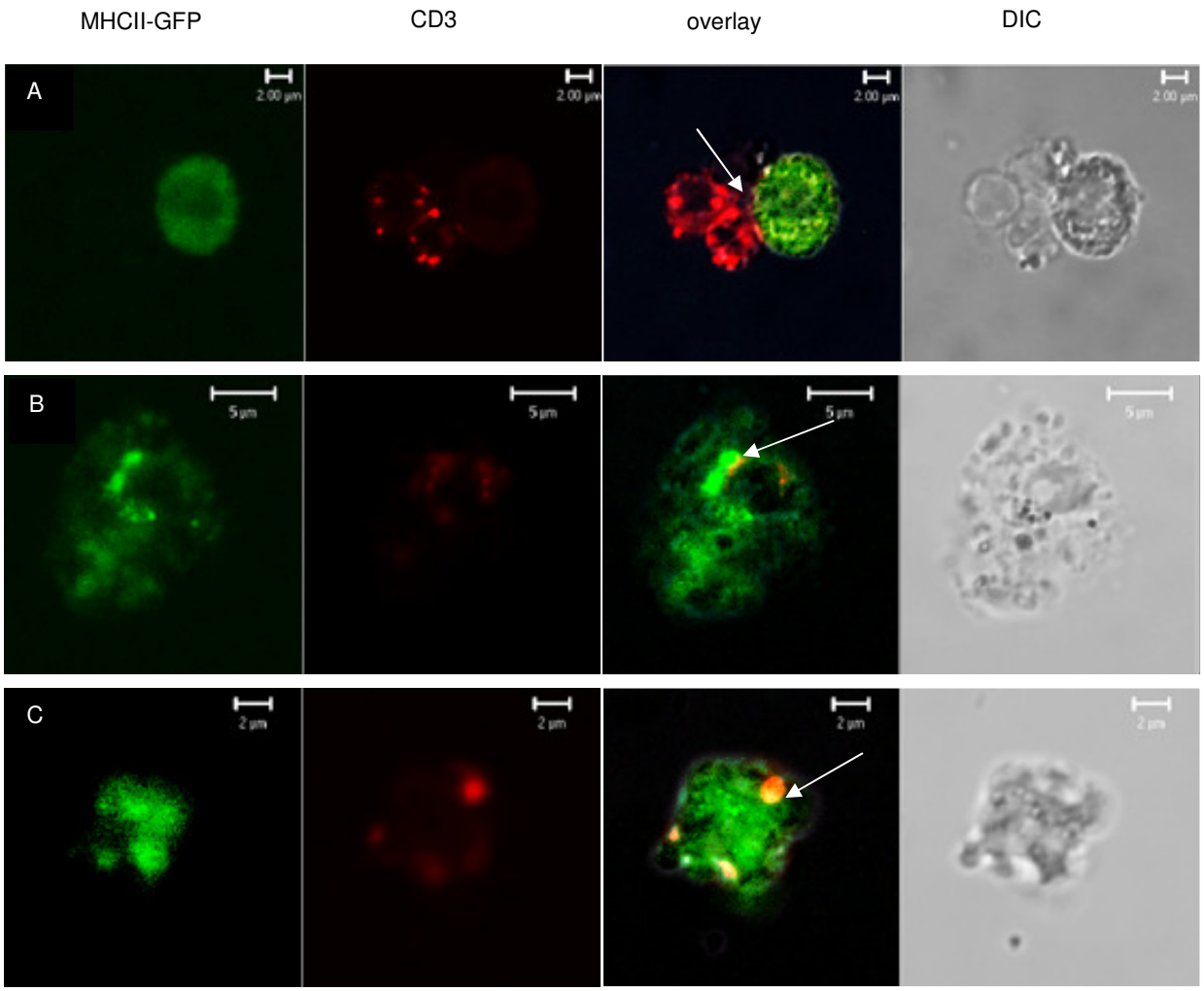


Fig.27 DCs were mock- (A), LPS-exposed (B) or WTF infected (C) 4 hours after transfection with pGFP-MHC-II (first column of panels), SA-loaded and after conjugation (for 25 minutes) with added allogenic T cells were fixed and stained with mAb-CD3 / Alexa 594 (second column of panels). In the overlay (third column of panels) were shown clusters at the interface, where CD3 co-localised with MHC-II (indicated by white arrows) in (B) and (C). In (A) CD3 did not co-localise with MHC-II. Here the contact surface was indicated by a white arrow. Differential interference contrast (DIC) images were shown in the fourth column of panels. Representative examples of each 20 conjugates analysed per culture are shown. Original magnification: 100x.

### 4.5.3.1. WTF infection up-regulated surface expression of HLA-DR, but not FN1-reactive MHC-II

The majority of MHCII is concentrated by incorporation into lipid rafts or tetraspannin-rich microdomains in intracellular compartments (Kropshofer et al., 2002) and redistributes to the cell surface upon DC maturation or T cell contact (Boes and Ploegh, 2004). We investigated how MV infection alters these processes. The expression levels of HLA-DR and tetraspannin associated MHC-II on the DCs surface were analysed by flow cytometry staining with specific mAb α-HLA-DR and mAb α-FN1 (Fig.28). It was apparent, that WTF infection upregulated HLA-DR efficiently (Fig.28 A, the green line), like in LPS-DCs (Fig.28 A, the red line). Surface expression levels of tetraspannin-associated MHCII, specifically detectable with the FN1 antibody, greatly increased in LPS-DCs (Fig.28 B, the red line), while only a low percentage of WTF-infected DCs (51%) displayed considerable amounts of FN1-reactive MHC-II (Fig.28 B, the green line) as compared to 41% on mock-DCs (Fig.28 B, the blue line).

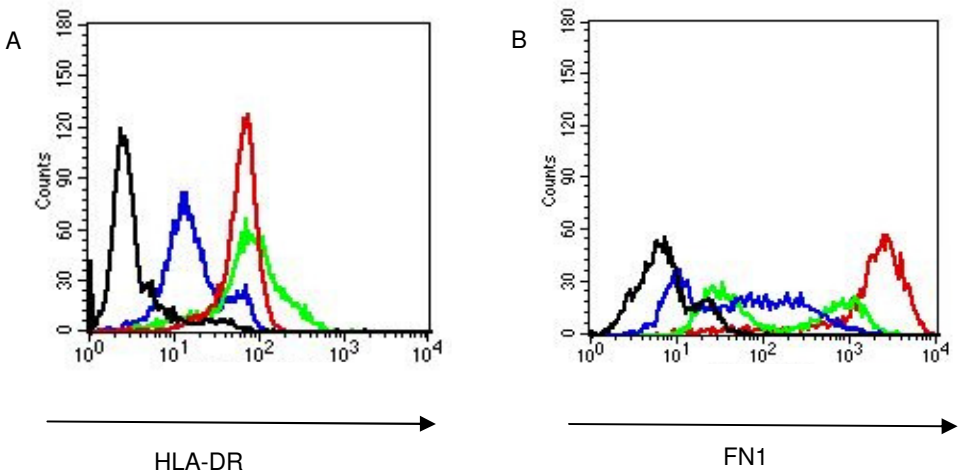


Fig.28 Surface expression levels of pan- (A) or FN1-reactive MHC-II (B) were determined on mock- (blue line), LPS- (red line) and WTF-DCs (green line) by flow cytometry. IgG2a.k and IgG1k-specific antibodies served as an isotype control (black lines)

### 4.5.3.2. The distribution of tetraspannin associated MHC-II in WTF-infected DC/T cell synapses

Mock-, LPS- or WTF-infected DCs were SA-loaded, captured on PLL, allowed to conjugate with T cells for 25 minutes at 37°C, fixed and stained by using specific mAb-FN1 / Alexa 488 and F-actin by phalloidin / Alexa 594.

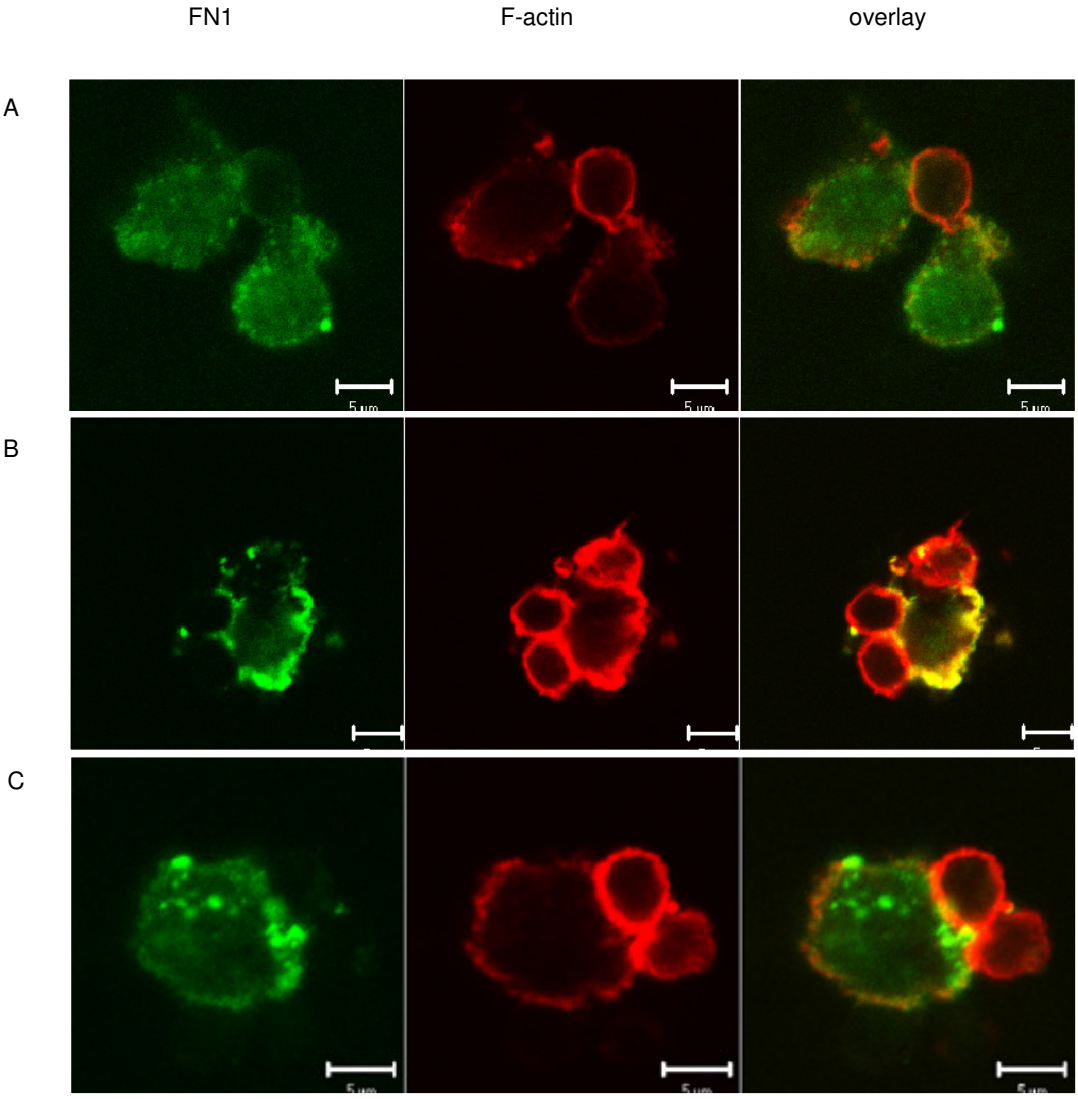


Fig.29 Conjugates formed between SA-loaded mock- (A), LPS- (B) and WTF-DCs(C) and allogenic T cells were stained for tetraspannin-associated (FN1/reactive) MHC-II by mAb-FN1/Alexa 488 (first column), and for F-actin by Alexa 594-conjugated phalloidin (second column) after fixation. The colocalisation between FN1/reactive MHC-II and F-actin was shown in yellow in the overlay panels (third column). Representative examples of each 20 conjugates analysed per culture were shown. Original magnification: 100x.

When analysed by confocal microscopy, FN1 reactive MHC-II was almost exlusively associated with cortical actin at the plasma membrane in LPS-DCs with no obvious preferential redistribution towards the T cell interface (Fig.29 B), while in mock-DCs it mainly localised in membrane proximal intracellular compartments (Fig. 29 A). Consistent with its low accumulation level on most WTF-DCs (Fig.28 B, green line), a substantial fraction of FN1 reactive MHCII subset was retained in these compartments. However, those redistributing to the plasma membrane apparently also distributed towards the pre-synaptic interface (Fig.29 C)

#### 4.5.3.3. Surface accumulation of clustered MHCII occurred inefficiently in WTF-DCs

MHCII redistributed to the DC surface upon maturation (Boes et al., 2003) or by contact with T cells. To evaluate whether MV-infection alters the organisation of the DC/T cell synapse, we studied the MHCII recruitment to the contact site. To analyse trafficking of MHCII and potential functional differences in detail, DCs were transfected to express GFP-tagged MHCII 4 hours prior to mock- or LPS-exposure or WTF-infection for 20 hours. DCs were further captured on PLL, SA-loaded and allowed to contact with allogenic T cells. The recruitment of MHCII molecules to the contact site was monitored by live cell imaging of DC-T cell conjugates. Series of images in one minute intervals, for entire 30 minutes were acquired. Five different categories of DC/T cell contacts duration and MHCII clustering were detected. Four categories were with clustering: short (2 minutes), middle long (7-9 minutes), middle long (10-14 minutes) or long contacts (more than 25 minutes) and one category was without clustering. Here, the contacts were short (2 minutes). In mock-DCs, GFP-MHCII clustered inefficiently at the interface, and interactions were mainly transient (Fig.30 A and D). In LPS-DCs, MHCII converged into large clusters, which accumulated at the T cell contact site (Fig.30 B and D), and the interactions were usually stable, typically

lasting for more than 25 minutes. In WTF-infected DC/T cell conjugates, MHCII clusters remained substantially smaller (Fig.30 C and Fig.30 D right side). Here, 53% of the analysed contacts were only transient. This was similar to those seen in the absence of detectable interface MHC-II clusters, where the majority of mock-DCs, but only 10% of all contacts in infected cultures revealed characteristics typically seen with LPS-DC/T cell.

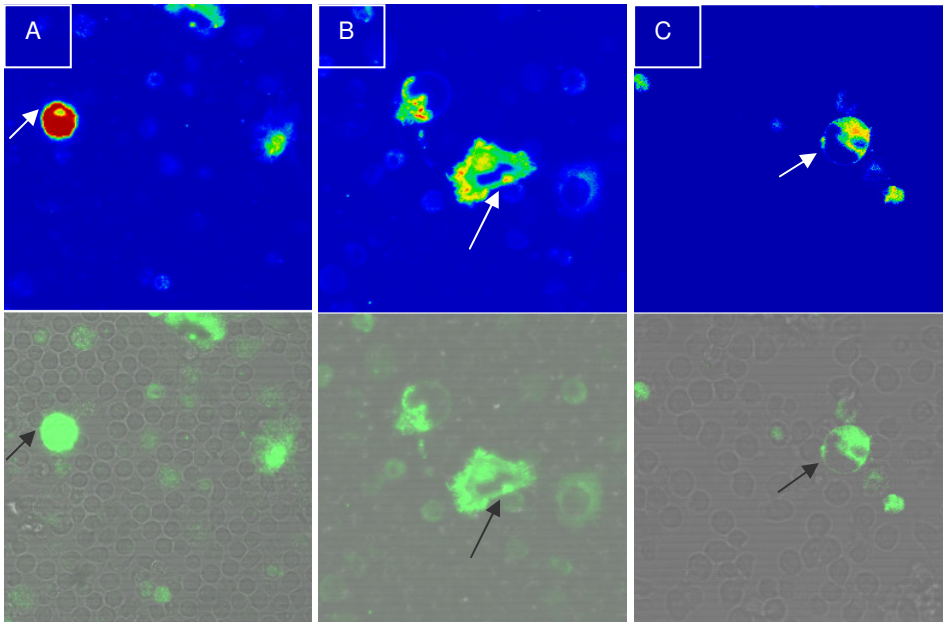


Fig.30 DCs were mock-, LPS-exposed or WTF infected 4 hours after transfection with pGFP-MHCII, captured on PLL coated slides and SA-loaded. After addition of allogenic T cells, redistribution and accumulation of MHCII clusters and contact kinetics were recorded by dynamic scanning in 1 minute intervals for 30 minutes. The intensity signal in the clusters at the interface (indicated by white arrows in (B) and (C)) was pseudocoloured (upper row). Typical examples of the category prevailing in mock-DCs (A: short contact, no clustering (2 minutes*), LPS-DCs (B: long contact, large clusters (> 25 minutes) or WTF-DCS (C: short contact, small clusters (2 minutes)) are shown (the T cells of interest were labeled by black arrows; A-C, bottom row). For any culture, a total of 20 contacts was analysed and categorised (D). Original magnification: 100x.

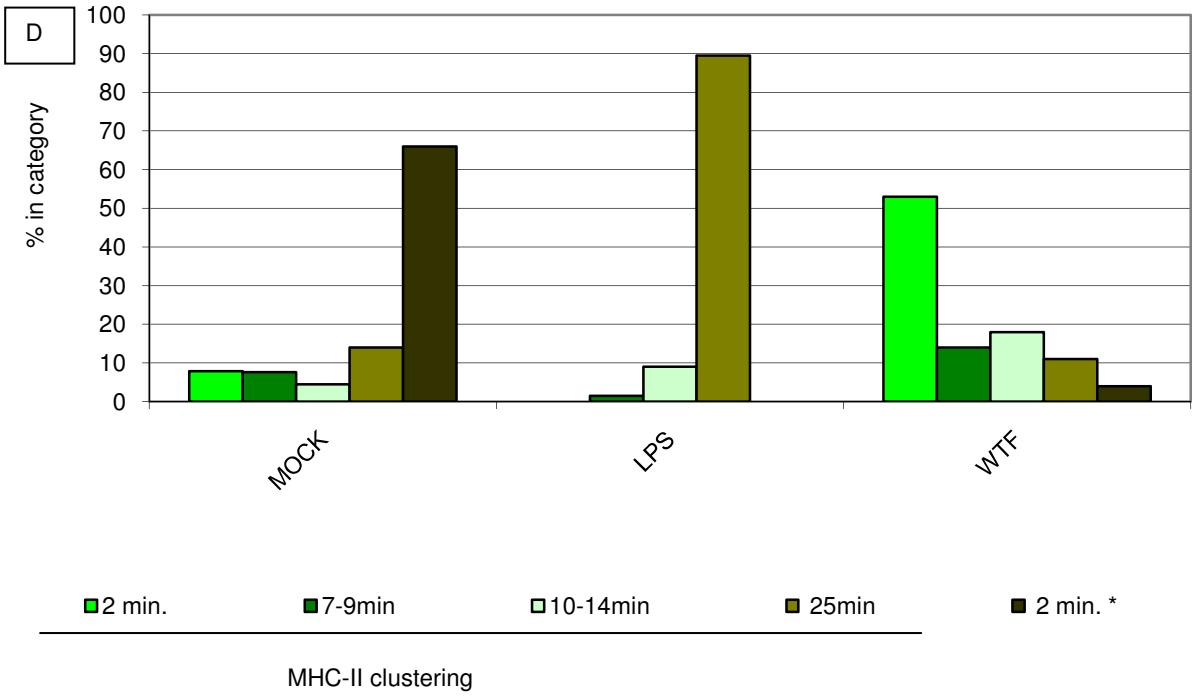


D) Quantitative analysis of the contact kinetics and MHC-II cluster redistribution and accumulation in DC/T cell interaction, recorded by dynamic scanning in 1 minute intervals for 25 minutes in mock-DC/T cell, LPS-DC/T cell and WTF-DC/T cell conjugates (n=20 conjugates/culture, shown in %). Shown are: short contacts with clustering (green bars), middle long contacts with clustering (dark green bars), middle long contacts with clustering (light green bars), long contact with clustering (light brown bars), short contact without clustering (brown bars).

### 4.5.3. Most of the WTF-infected DCs failed to promote sustained T cell activation

Since calcium mobilisation directly mirrors T cell activation, we aimed to characterise the calcium response of T lymphocytes, which contacts with WTF-infected, LPS- or mock-DCs at the single cell level.

We performed real-time differential interface contrast (DIC) (Fig. 31 A, B, C and D each bottom rows), coupled with calcium imaging for individual contacts between SA-loaded mock-, LPS- or WTF-DCs captured on PLL coated chambers, and allowed them to interact with Fluo-4 loaded T cells at 37°C for 25 minutes. Calcium-dependent changes in fluorescence (shown in a pseudocolor scale in Fig. 31 A, B, C and D each upper rows) and contact kinetics were traced for 10 minutes after initiation. Frames were acquired at 15 sec. intervals (by using LSM-software). In all cultures, interactions differing in duration and efficiency to flux calcium were observed. They could be categorised into sustained (>10 minutes, 100% activation (I), Fig.31 A and E; and (III) >10 minutes, <50% activation (Fig.31 C and E) and short contacts (<2 minutes 25% activation (IV); Fig.31 D and E; and <2 minutes 100% activation (II), Fig. 31 B and E).

As expected, activatory category I type contacts, which induced sustained calcium activation, prevailed for LPS-matured DCs, while in mock DC cultures, short-lived contacts with inefficient calcium flux were mainly seen (Fig.31 F). Less than 20% of WTF-DC/T cell contacts were stable and sustained calcium flux (category I), while most contacts were non-activatory. Remarkably, category type II predominated. It was seen almost exclusively with WTF-DCs, but only infrequently with LPS-DCs (Fig.31 F). Thus, more than 60% of interactions (categories II and III) with WTF-DCs did not sustain calcium fluxing, and therefore, T cell activation and proliferation.

Fig.31 A

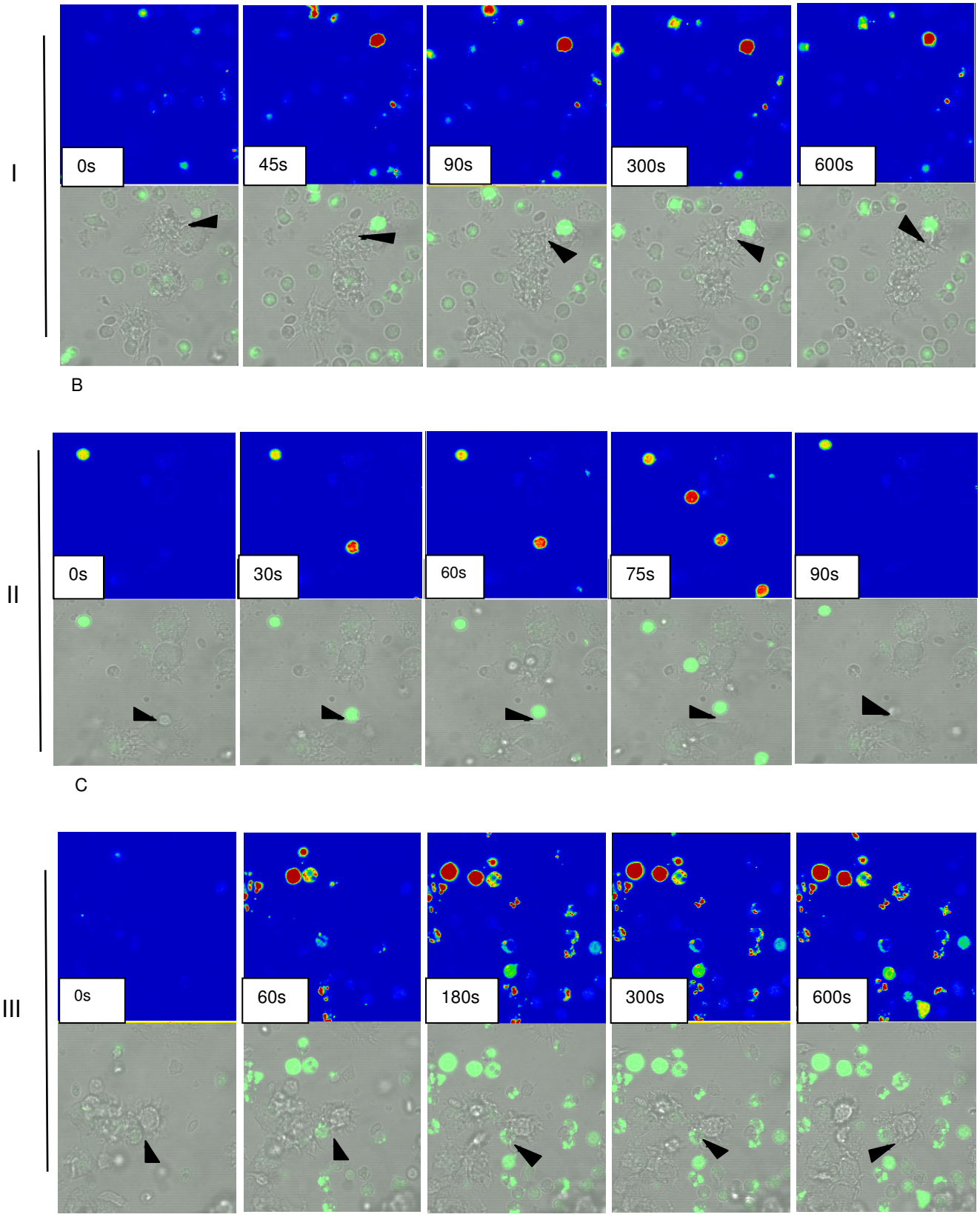
I
0s
45s
90s
300s
600s
B
II
0s
30s
60s
75s
90s
C
III
0s
60s
180s
300s
600s

D

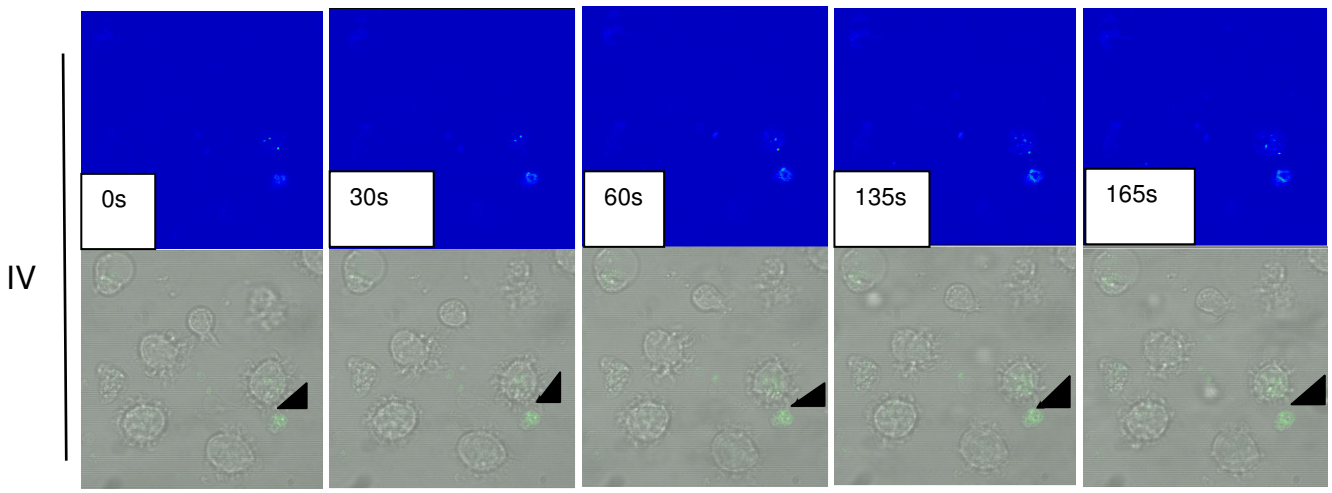
IV
0s
30s
60s
135s
165s

E

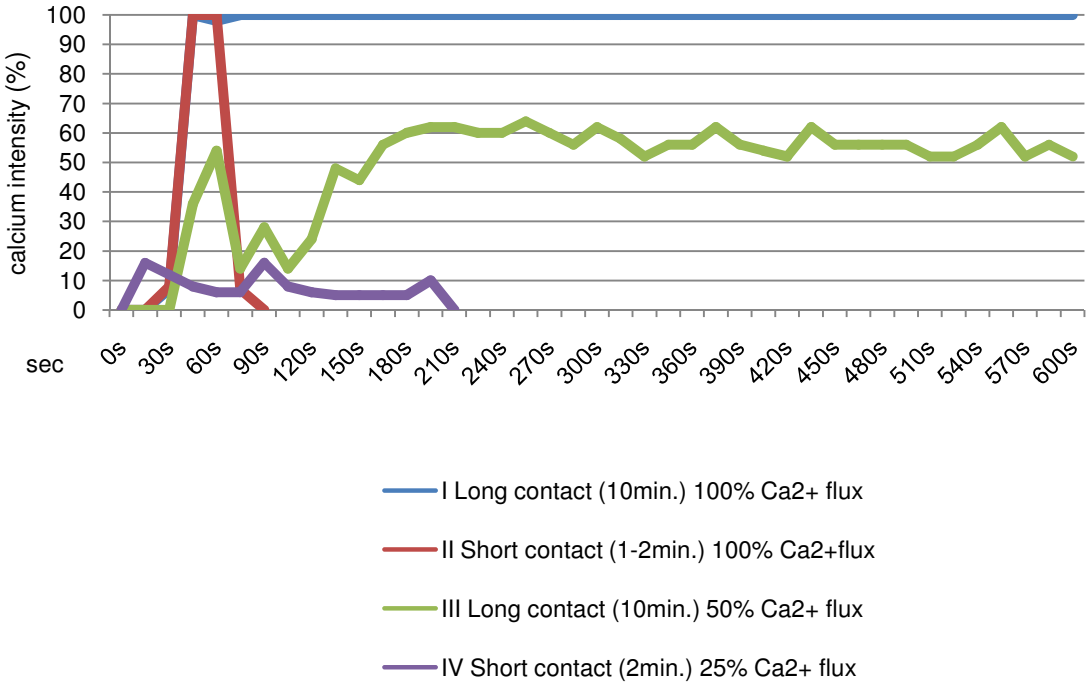
calcium intensity (%)
100
90
80
70
60
50
40
30
20
10
0
sec
0s
30s
60s
90s
120s
150s
180s
210s
240s
270s
300s
330s
360s
390s
420s
450s
480s
510s
540s
570s
600s
I Long contact (10min.) 100% Ca2+ flux
II Short contact (1-2min.) 100% Ca2+flux
III Long contact (10min.) 50% Ca2+ flux
IV Short contact (2min.) 25% Ca2+ flux

F

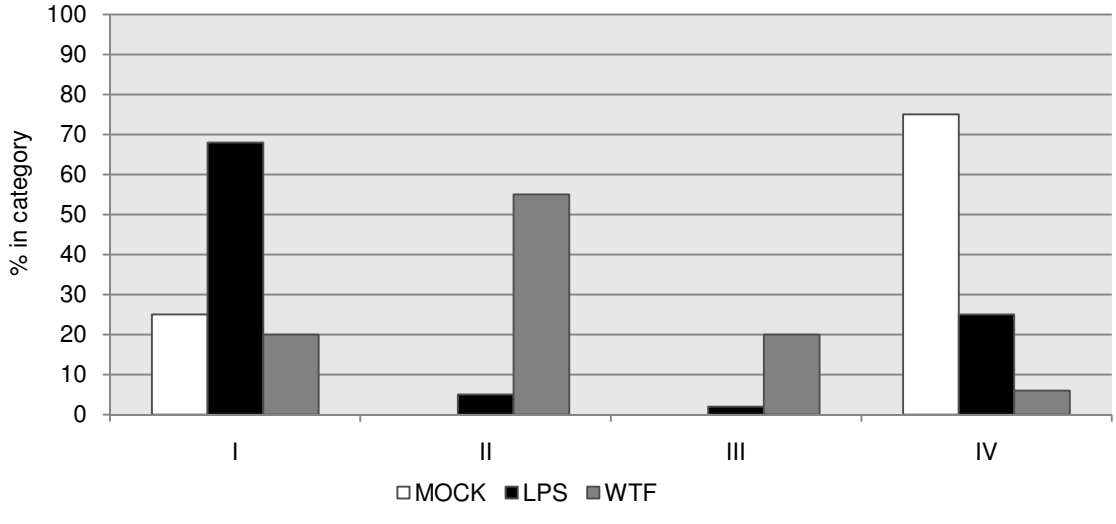
% in category
100
90
80
70
60
50
40
30
20
10
0
I
II
III
IV
MOCK
LPS
WTF

Fig.31
(A, B, C and D) Shown are: single frames of time-lapse series of DIC images (each bottom rows) and Fluo-4 images (each upper rows) of T cells interacting with SA-loaded mock-, LPS- or WTF-DCs, which were captured on PLL coated chambers. The T cells of interest were labeled by black arrowheads in the DIC images. Calcium influx as revealed by changes of the Fluo-4 emission spectrum at 488 nm were shown in a pseudocolor scale (low: blue; high: red) (original magnification: x 40). Serial images were acquired in 15 second intervals immediately after initiation of a T cell contact for 10 minutes in all cultures.
E) Major contact categories were based on both duration and Ca-mobilisation (I: sustained (long) contact and 100% Ca-flux (blue line) (A); II: short contact and 100% Ca-flux short (red line) (B); III: long contact and 50% Ca-flux (green line) (C); IV: short contact and 25% Ca-flux (violet line) (D)).
F) Quantification of contact categories (E) seen in each culture (mock-DCs (white bars), LPS-DCs (black bars) and WTF-DCs (grey bars)) were determined in % (n= 20 each).

### 4.5.4. Localisation of MV-H and MV-N proteins in the IS

For MV, surface contact with viral glycoprotein complex on virions or infected cells (including DCs) has been found to be important in T cell inhibition (Kerdiles et al., 2006; Schneider-Schaulies and Dittmer, 2006). The MV gp complex ,expressed on the surface of the infected human DCs, is known to be essential for ablation of the allostimulatory activity of DCs (Dubois et al., 2001), which indicates that this complex could potentially contribute to conjugate destabilisation directly. Thus, we analysed the MV-H protein and for control, MV-N protein localisation in the IS. WTF-infected DCs were SA-loaded, captured on PLL, allowed to conjugate with T cells for 25 minutes, fixed and double-stained (surface or intracellular) by using specific mAb-H–Alexa 488 and F-actin by Alexa 594-conjugated phalloidin, or by using specific mAb-N-Alexa 488 and F-actin by Alexa 594-conjugated phalloidin.

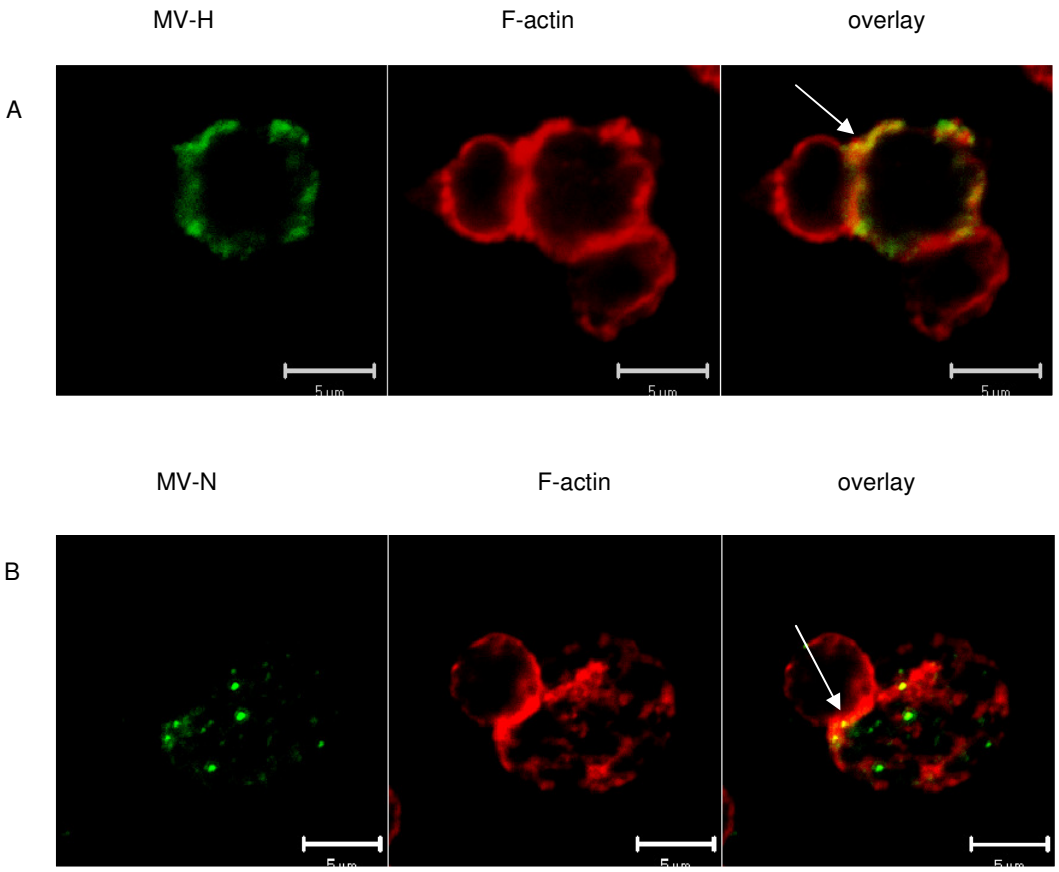


Fig.32 MV-H protein (A) or MV-N protein (B) and F-actin were co-detected in fixed WTF-DC/T cell conjugates, which were trapped on PLL 25 minutes after culture initiation. Twenty conjugates per culture were analysed. Representative examples of WTF-DC/T cell for MV-H/F-actin (A) and MV-N/F-actin (B) were shown. Protein co-localisation at the contact surface was labeled by white arrows (in overlay panels). Original magnification: 100x.

Representative images of MV-infected DC/T cell conjugates were shown in Fig.32. Clusters of H protein accumulated on the surface of WTF-DCs, also including the synaptic interface and co-localised with F-actin (Fig.32 A, overlay, labeled by a white arrow). Small clusters of MV-N protein were seen at the contact surface (Fig.32 B, overlay, labeled by a white arrow). Some larger clusters of MV-N protein, which did not co-localise with F-actin, were also observed in the infected-DCs (Fig.32 B, overlay).

### 4.5.5. MGV infection up-regulated surface expression of HLA-DR, but not FN-1

Further, we looked at whether the observation that H protein clustered in the synaptic surface (from 4.5.5) could be relevant for the destabilisation of infected DC/T cell interaction. Immature DCs infected (at a moi of 2) with a recombinant MV (expressing VSV G instead of the MV gp complex) or LPS-treated, or mock-DCs were fixed 24 hours after infection/treatment and stained by flow cytometry with specific mAb α-HLA-DR or mAb α-FN1(Fig.33 A and B). Infection efficiency was analysed by flow cytometry by intracellular staining with N specific mAb. More than 85% of the cells in MGV-DCs culture were MV-N protein positive (not shown). MGV-infected DCs were known to support expansion of allogenic T cells (Klagge et al., 2000; Schnorr et al., 1997)

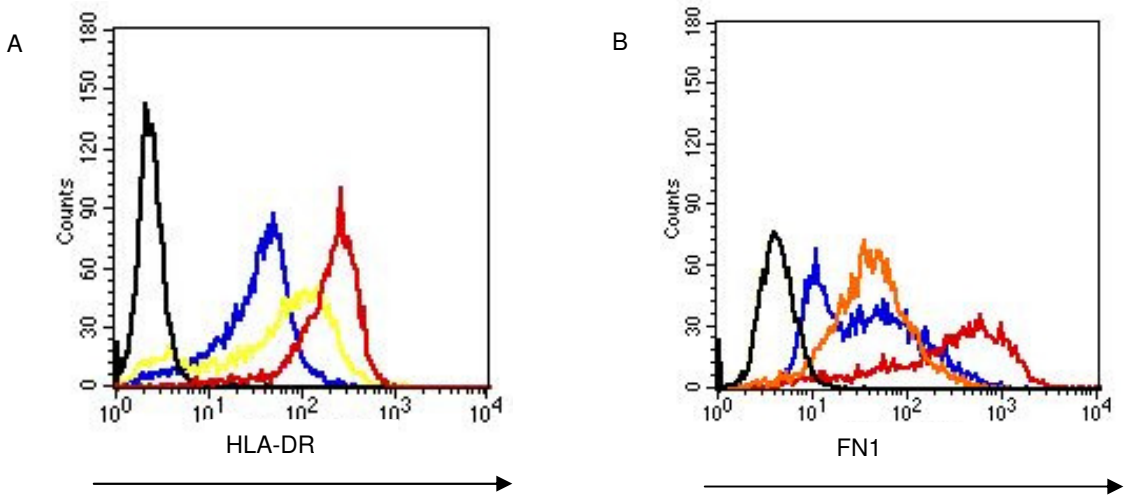


Fig.33 Surface expression levels of HLA-DR (A) or FN1-reactive MHC-II (B) were determined on mock- (blue line), LPS- (red line) and MGV-DCs (orange line; >85% MV N positive) by flow cytometry. IgG2a,k and IgG1k-specific antibodies served as isotype controls (black lines).

Since its backbone is that of an attenuated MV strain, MGV induces phenotypic DC maturation more slowly than WTF (Klagge et al., 2000; Schnorr et al., 1997). Thus, within 24 hours HLA-DR accumulated at lower levels on MGV- (Fig.33 A, yellow line) than on

WTF-DCs (Fig.28 A, green line). Interestingly, MGV-infection caused only very moderate surface accumulation of FN1 reactive MHC-II (Fig.33 B, orange line).

### 4.5.6. MGV-infected DC/T cell conjugation pattern differed from WTF-DC/T cell

We asked if DCs infected with MGV-MV should be able to at least partially rescue conjugate stability and calcium influx in the conjugates with allogenic T cells. We performed real-time differential interface contrast (DIC), coupled with calcium imaging for individual contacts between SA-loaded mock-, LPS- or MGV-DCs. They were captured on PLL coated chambers and allowed to interact with Fluo-4 loaded T cells at 37°C for 25 minutes. Calcium-dependent changes in fluorescence and contact kinetics were traced for 10 minutes after initiation with frames being acquired at 15 sec intervals, using LSM-software. In all cultures, interactions differing in duration and efficiency to flux calcium were observed which categorised into five categories (Fig.34 upper panel). About 55% of T cells conjugating to MGV-DCs scored into activatory categories I and I*. Here, a rapid calcium flux at a 100%level, or at an 80% level was sustained (Fig.34 bottom panel). Transiently high activation levels, as predominantly seen in WTF-DCs (category II, shown in Fig.31 B and E; from 4.5.4) were also observed. However, this was the case for less than 20% of contacts, which were also slightly prolonged (3 to 6 minutes instead of 2 minutes)(Fig.34 bottom panel, category II*). Thus, surface expression of the MV glycoprotein complex on DCs, most likely at the interface, essentially contributes to destabilisation and functional impairment of the IS.

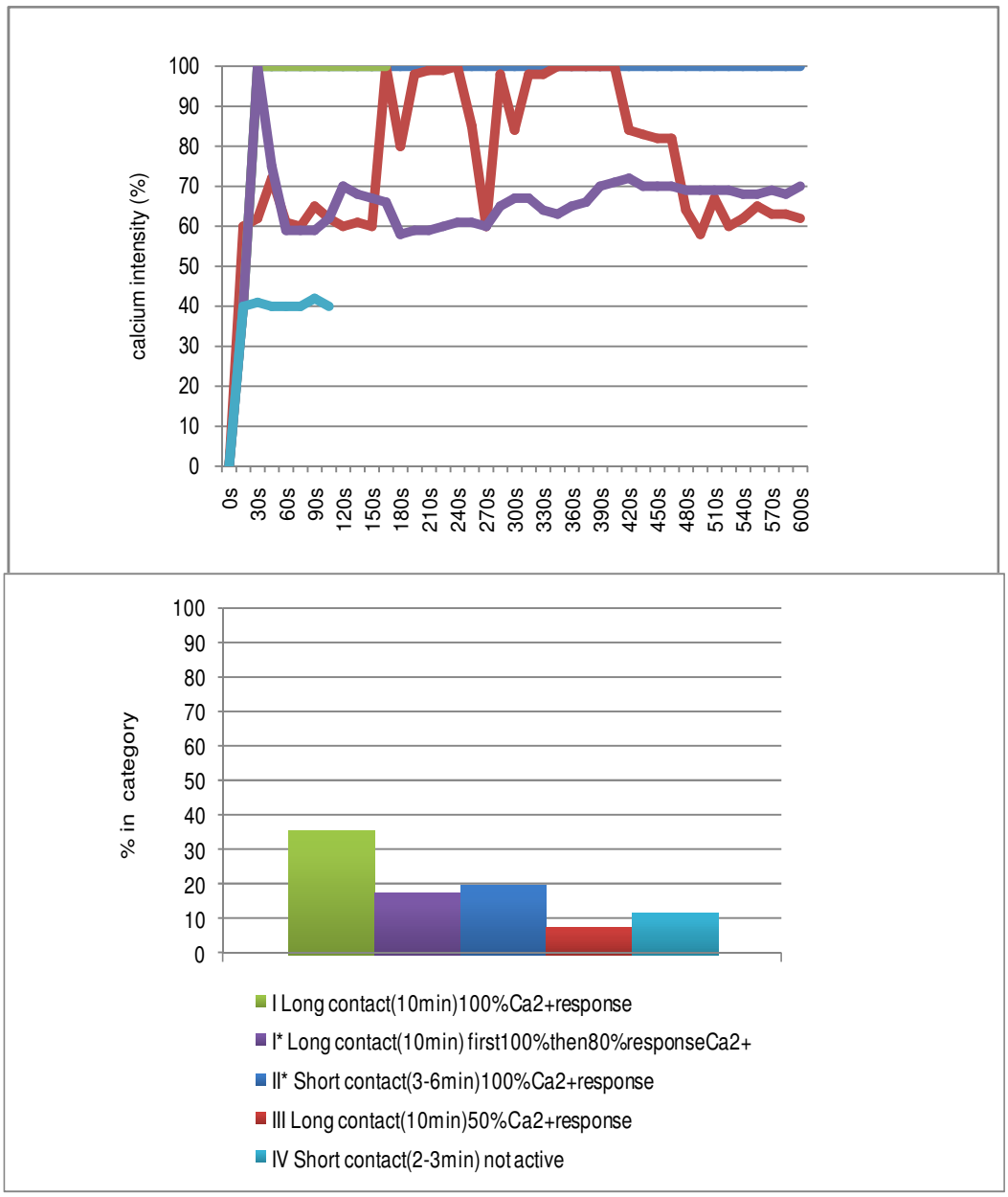


Fig.34: Major contact categories based on duration and calcium mobilisation, for T cell conjugated with MGV-DCs were SA-loaded, captured on PLL coated chambers. Serial images were acquired in 15 sec intervals immediately after initiation of a T cell contact for 10 minutes.
Category I: sustained (>10 minutes), 100% Ca-flux (green line); I*: long (>10 minutes), 100% Ca-flux for 2 minutes, then sustained at 80% (violet line); II*: short (3-6 minutes), 100% Ca-flux (blue line); III: long (>10 minutes), 50% Ca-flux (red line); IV: short (< 2 minutes ), 25% Ca-flux (turquise line) (upper panel).
Quantification of contact categories seen in the MGV-DC/T cell culture were determined (in %): I (green bar); I* (violet bar), II* (blue bar); III (red bar) and IV (turquoise bar) (bottom panel). A total of 20 contacts were analysed per culture.

# 5. Discussion

DCs have been coined as central to initiating and determining the antiviral immune responses (Steinman et al., 2003; Banchereau and Steinman 1998) but also for viral transport and transmission to T cells as targets for viral immunomodulation (Polara et al., 2005; Rinaldo and Piazza, 2004). The general suppression of immune responses to secondary infections induced by MV is associated with lymphopenia, cytokine imbalance and general loss of the ability of peripheral blood T cells to expand in response to polyclonal and antigen-specific activation (Schneider-Schaulies and ter Meulen, 2002b; Borrow and Oldstone, 1995). This effect is not reflected by the frequency of infected lymphocytes and thus DCs are believed to be important targets of viral interference in MV immunosuppression (Schneider-Schaulies et al., 2003; Servet-Delprat et al., 2003; Schneider-Schaulies and ter Meulen, 2002a). CD150, expressed at low levels on iDCs or upregulated in response to pro-inflammatory signals supports MV entry into these cells, and this is enhanced by DC-SIGN interaction (Bieback et al., 2002; Kruse et al., 2001; Minagawa et al., 2001 Swetman Andersen et al. 2006). MV replicates in DCs as revealed by accumulation of viral proteins. MV infection has been related to developmental and functional impairment (Servet-Delprat et al., 2000) but also maturation of DCs. This is indicated by upregulation of costimulatory molecules, as well as induction of cytokine synthesis (Klagge et al., 2004; Dubois et al., 2001; Klagge et al., 2000; Steineur et al., 1998; Grosjean et al., 1997; Schnorr et al., 1997). As other viruses, MV infection abrogates DC-capability to promote expansion of allogenic T cells (Pollara et al., 2005; Dubois et al., 2001; Servet-Delprat et al., 2000; Fugier-Vivier et al., 1997; Grosjean et al., 1997; Schnorr et al., 1997). Surface contact with the viral N protein or the glycoprotein complex on virions, or infected DCs has been established to be important for this

phenomenon (Kerdiles et al., 2006; Schneider-Schaulies and Dittmer, 2006). But the underlying mechanisms on a cellular level have not yet been addressed in detail.

To approach this particular interaction, we investigated the effect of MV wild type strain infection on DCs and their ability to recruit T cell into functional conjugates. Signalling processes in T cells, targeted by surface interaction of the glycoprotein complex, have been studied using UV-inactivated virus as effector. There, activation of the PI3K in response to serum factors, TCR ligation by antibodies or co cultured LPS-DCs was severely compromised (Avota et al., 2006, 2004, 2001). MV interaction alone induced collapse of T cell microvillar structures and inability of T cells to organise a functional monocentric IS with LPS-DCs based on MTOC redistribution and centering of CD3 (Müller et al., 2006). Further experiments were performed based on the assumption that DC maturation induced by MV roughly corresponded to that of other maturation stimuli. This was supported by studies addressing accumulation of MHC-I, MHC-II and costimulatory molecules collectively associated with maturation on these cells (Zilliox et al., 2006, Dubois et al., 2001; Ohgimoto et al., 2001; Klagge et al., 2000; Servet-Deprat et al., 2000; Schnorr et al., 1997).

In this work, we described first the DCs morphology and static adhesion on PLL (Fig.10a/b). Infected DCs were rounded without dendrites, cell morphology comparable to that of mock-DCs, while LPS matured DCs possessed typical long dendrites (Fig.10a). It appears that WTF-DCs were slightly less adhesive to PLL than LPS-DCs, compared to mock-DCs which have not reduced adhesive properties. (Fig.10b). Next, we determined how MV-WTF infection modulated DCs morphology and dynamic adhesion on extra cellular matrix proteins such as FN or ICAM-1. Our confocal microscopy data (Fig.11) as well as scanning electron microscopy data (Fig.12) show heterogeneous morphology of DCs, which were seeded onto FN-coated slides (Burns et al., 2001). Mock-, LPS- and

WTF-DCs were placed in four morphological categories: polarised, migratory phenotype (Fig.12 a-I), small, rounded and adherent (Fig.12 a-II), extended with lamellipodial protrusions (Fig.12 a-III) and ruffled, nonpolarised (Fig.12 a-IV). Predictable, mock-DCs and LPS-DCs differed with regard to their representation within these categories, and based on these morphological criteria, WTF-DCs resembled LPS-DCs (Fig.12 b). We also distinguished, that associated with their mature phenotype, both LPS-DCs and WTF-DCs adhered less efficiently to the FN support (Fig.13-upprt part) or ICAM-1 (Fig.13-bottom part).

Both β1 and β2 integrins were expressed by DC and their expression levels weren't changed by maturation (Burns et al., 2004). Neither MV entry nor replication affected β1-integrin levels on the DC surface (Fig.14). Ligation of integrins induced multiple signalling events (Zamar and Geiger, 2001; Plow et al., 2000) and suggested the important role of integrins activation in the rapid attachment and detachment of DCs (van Berg et al., 2001; Walzer et al., 2005). Stimulation of all DC-types (mock-, LPS-, UV-inactivated WTF- or WTF-DCs) by FN ligation had no effect on the β1-integrin expression levels (Fig.14, left panel). Also, most of the MFI did not vary. Thus, previously observed differences in adhesion of these DC cultures could not be explained with modulation of total β1-integrin levels. Integrin activation is often mediated by intracellular signals that change the affinity of some integrins for their ligands, termed inside-out signalling (Hughes and Pfaff, 1998). We found that in the investigated UV-inactivated WTF-, WTF-infected and LPS-treated DC cultures, FN adhesion had no impact on the expression of activated β1-integrin, neither on the rate of expressing cells, nor on the MFI (Fig.15). However, FN ligation caused a reduction of the percentage of cells expressing activated β1-integrin up to 30% in mock cultures (Fig.15, left panel). Recent work (Grose et al., 2002; Ballestrem et al., 2001) has revealed that the integrin-actin cytoskeleton connection is highly dynamic and subjected to

many regulatory processes, like cell polarity, spreading and motility. Furthermore, it has become clear that the interaction between integrins and the actin cytoskeleton is differentially regulated in different locations of the cell. At the leading edge of migrating cells, integrins bind the ECM, recruit the actin cytoskeleton and initiate local reorganization of the actin network, promoting membrane protrusion. At the rear of the cell, integrins detach from the ECM, dissolve the link to the cytoskeleton and are, at least partially, recycled to the front of the cell (Ballestrem et al., 2001). In WTF-infected (images not shown), UV-inactivated-WTF treated DCs (Fig.16 C, shown with white arrow) and LPS-DCs, large lamellipodia with concentrated F–actin at the leading edge (Fig.16 B, shown with white arrow), but without co-localisation with activated β1-integrin were observed. In WTF-infected, like in UV-inactivated WTF-DCs, β1-activated integrin was only detected in adhesion aggregates (Fig.16 C, shown with white arrow). Therefore, we detected by confocal microscopy focal expression of activated β1-integrin, which was upregulated with similar kinetics in UV-inactivated WTF-, WTF-infected and LPS-treated DC cultures. The formation of cell adhesion complexes assures substrate adhesion, as well as targeted location of actin filaments and signalling components (Hynes, et al. 2002; Adams et al. 1997) (Fig.17). These ECM attachment and signalling centres were termed focal complexes (FCs) when they were still nascent or focal adhesions (FAs) when they matured into larger complexes (Hynes, et al. 2002; Song Li et al. 2005). FAK is a tyrosine kinase that is critical component of the FA and provides both structural and kinase activity to the focal contact present in the FAs. Based on binding of FAK to peptides of the β1 cytoplasmic domain and precipitation experiments, FAK is thought to bind integrins directly (Chen et al., 2000). Upon cell attachment to the ECM, FAK becomes autophosphorylated at Tyr397 either directly by integrin clustering or after phosphorylation of tyrosines 576 and 577 by Src (Schaller et al., 2001).

We observed that in mock-DCs FN stimulation induced elevated FAK autophosphorylation (Fig.18 B, first pair of white/black bars). In LPS- and WTF-DCs FAK phosphorylation was high and was not upregulated after FN stimulation (Fig.18 B, second and third pair of white/black bars). These results suggest that integrin function in infected- and LPS-DCs could be affected on the level of FAK phosphorylation like in mouse DCs, where LPS treatment induced focal adhesion kinase (FAK) phosphorylation and rearrangement of the actin cytoskeleton (Walzer et al., 2005). Also, FAK phosphorylation is associated with integrin activation, i.e., cells expressing active integrins contain a high proportion of Y397-phosphorylated FAK (Burridge K. et al., 1992; Guan J. et al., 1992; Hanks S. et al., 1992; Lipfert L. 1992; Schaller M. et al., 1992).

Activated FAK can bind and phosphorylate a range of different substrates, which allows further recruitment of adaptor and signaling molecules. Fascin is a monomeric actin filament–bundling protein that participates in the DC dendrite formation (reviewed in Edwards and Bryan; René Geyeregger et al., 2007) and it has been found necessary for T cell stimulation (Al-Alwan et al., 2001).

Consistent with maturation dependent expression of this protein, fascin was upregulated over time in LPS-DCs, in contrast to mock DCs (Fig.19). However, WTF-DCs showed an intermediate phenotype in that overall fascin levels (Fig.19). Our WB data (Fig.19) were confirmed by morphological analyses. Infected and uninfected DCs were studied by fluorescence microscopy after double staining of fascin and MV (by using human serum) (not shown). We observed morphological similarity between LPS-DCs and infected DCs which expressed high level of fascin. It is important to take into account, that in the infected cultures were detected DCs, which expressed fascin at low level. The observed correlation between infection efficiency and fascin expression in WTF infected cultures

(Fig.20 A and B), could be completed after double staining by flow cytometry, which was not done (because of technical reasons).

The association between fascin and PKC-α is detectable by protein–protein binding *IN VITRO*, by coimmunoprecipitation from cell extracts, and in live cells as fluorescence resonance energy transfer detected by fluorescence imaging lifetime microscopy (Anilkumar et al., 2003) and is of functional importance for the balance between fascin protrusions and focal adhesions on FN (Adams et al., 1997; Adams and Schwartz, 2000). In cell lines PKC-α mediated phosphorylation of S39 was induced by FN (Adams, 1995; Adams et al., 1999) and led to the dissociation of fascin from the F-actin bundles (Vuori and Rouslahi 1993; Mirauti et al., 1999), as well as diffuse localisation of fascin ( Anilkumar et al., 2003). In all unstimulated DC cultures (Fig.21, lines 4, 5, 6) and in FN stimulated mock-DCs, only a small quantity of fascin was co-precipitated with PKC-α (Fig.21, line 3). In LPS-DCs, FN stimulation induced strong fascin-PKC-α association (Fig.21, line 2), whereas in WTF-DCs fascin associated moderately strong with PKC-α (Fig.21, line 1). Fascin is concentrated in leading edge protrusions of migrating cells, and fascin-containing protrusions function in the motility and cell–cell interactions of many differentiated cells (reviewed by Kureishy et al, 2002). In line with this, we observed that F-actin and fascin co-localised on leading edges of WTF-infected DCs and LPS-DCs (Fig.22 B and C bottom panels, merge, seen in yellow and labelled with white arrows). In mock-DCs, multiple focal contacts (Fig.22 A bottom panel) and long thin processes were apparent. Taken together, these data indicate that although fascin levels in WTF-DCs remained substantially lower than in LPS-DCs their overall morphology were similar. Our results suggest also that cell spread, formation of actin containing dendrites, as well as the surface expression levels of β1- and activated β1 integrin on FN are not detectably different in WTF-DCs and LPS-DCs. We could not explain the reduced adhesion of WTF-

DCs compared to mock-DCs, as well as the small difference between the adhesion properties of the infected and LPS treated DCs. If WTF infection affects β2-integrin expression levels in DCs on ICAM-1, should be analysed. In immature DC, failure to form podosomes or selective inhibition of the CD18 (β2) component of podosomes resulted in a similarly reduced ability to adhere to ICAM-1, indicating that podosomes, through CD18, are necessary for tight adhesion to this ligand (Burns et al., 2004). In line with this finding, the specific recruitment of β2 integrins by podosome assembly in infected DCs should be looked at in detail. The FAK activation, as well as the interaction between fascin and PKC-α did not differ in infected and in LPS-treated DCs. The precise mechanism by which the activity of PKC influences cell motility involved components of the focal complexes, such a talin, paxillin and ERK, as well the small GTPases and actin cytoskeleton-binding proteins (Zigmond et al., 1996) should be investigated. Also, a large number of PKCα substrates have been identified and are conceivable candidates for mediating the PKC-α effects on the cytoskeleton (Ng et al., 2001).

Rho GTPases were placed downstream of integrin signalling and were chronologically or coincidentally activated during dynamic adhesion and (human T) cell spreading (Nurmi et al., 2006). Rho GTPases regulated the release of adhesions to the substratum and associated cellular contraction (Garrett et al., 2000), as well as polarised formation of lamellipodia at the leading edge (Pellinen and Ivaska, 2006; Swetman Andersen et al., 2006; Burns et al., 2004). DC motility is enhanced upon maturation (Shutt et al., 2000), and consistent with their importance to dynamic integrin interactions, expression of Rac1/2 was found to be critical for migration of mature murine bone marrow derived DCs on FN (Benvenuti et al., 2004b). In line with these observations, also human LPS-DCs, and more so, DC transfected to express constitutively active Rac1 were the most motile DC-species analysed. The motility was effectively reduced upon inclusion of a Rac1 specific inhibitor

(Fig.23). The sensitivity of the velocity of WTF-DCs to Rac-inhibitor indicates that their dynamic interaction with FN is Rac-driven (Fig.23). Perhaps, Rac activation in response to integrin activation is not generally compromised. This could be detect by pulldown experiments (de la Fuente et al., 2005), which we did not perform (due to technical reasons). However, the velocity of WTF-DCs on FN is below that of LPS-DCs, signifying that maturation induced by WTF may be insufficient to completely promote integrin signaling, which leads to Rac activation. In the mouse system (Benvenuti et al., 2004b) cell motility of mature Rac1/2-/- knockout DCs (mean velocities 0.12 μm/min) decreased about 10 times in comparison to the wt control DCs (mean velocities 1.03 μm/min). The motility of immature DCs, transfected to express GFP-tagged dominant negative (dn) Rac1, did not decrease, like in inhibitor treated DC cultures as we expected. Nor did the motility of LPS- and WTF-DCs, transfected to express dn Rac1, vary from that of nontransfected LPS-DCs and WTF-DCs (Fig.23A and B). Taken as a whole, however, WTF-infection affected Rac-dependent dynamic interaction of DCs with FN, just to a moderate extent.

The spatial IS organisation can vary considerably depending on the system analysed (Dustin et al., 2006; Friedel et al., 2005) and was, however, determined by the maturation stage of the DC to a major extent (Friedman et al., 2006; Benvenuti et al., 2004a,b; Gunzer et al., 2004; Al-Alwan et al., 2001 and Al-Alwan et al., 2003).

Repositioning of the MTOC is a complex event dependent on TCR signaling that involves the shortening or sliding of microtubules (MTs) and the subsequent anchoring of MTOC at the site of TCR engagement (Noa et al., 2006). Our confocal microscopy data demonstrate, that compatible with formation of a functional IS, LPS-DCs, but unexpectedly also WTF-DCs efficiently caused redistribution of the T cell microtubule organising center (MTOC) towards the interface (Fig.24). These analyses are, however, biased in the selection of stable conjugates. Thus, it cannot be excluded that T cells conjugating to WTF-DCs are

compromised in their ability to efficiently redistribute CD3 into mature, functional synapses, as was observed previously in conjugates formed between MV preexposed T cells and LPS-DCs (Müller et al., 2006). This hypothesis was further supported by analysis of the spatial organisation of the interface, where again T cell conjugates with WTF-DCs bear a resemblance to those with LPS-DCs (Fig.24-lower part).

DC/T cell synaptic interfaces can differ to a great extent (Brossard et al., 2005). Classical monocentric synapses revealing central CD3- or LFA1- co-clustering with the cytoskeletal linker protein talin (Fig.25 A), as well as, synapses with peripheral clusters of both molecule pairs (Fig.25 B) were represented only in a minor fraction of conjugates formed in all DC cultures (Fig.25 E). Multifocal clustering of LFA1 and talin was predominant in all DC species, which were examined (Fig.25C and E). Nevertheless, a multifocal pattern for CD3/talin was mainly detected with LPS- or WTF-DCs (Fig.26C and E). Interestingly, homogenous distribution of these proteins as mostly seen with mock-DCs, also occurred in about 20% of conjugates with WTF-DCs (Fig.26D and E). In general, however, the spatial patterning of the interface was similar for WTF-DCs and LPS-DCs. This is consistent with efficient T cell activation based on MTOC redistribution (Fig.24-upper part) while it is not consistent with the finding that MV-infected DC cultures do not support expansion of allogenic T cells. The majority of MHC-II is preconcentrated by incorporation into lipid rafts (Meyer zum Bueschenfelde et al., 2004) or tetraspannin-rich microdomains in intracellular compartments (Kropshofer et al., 2002) from where they can redistribute to the cell surface upon maturation and/or T cell contact (Boes and Ploegh, 2004; Boes et al., 2003). We observed that HLA-DR expression was moderately upregulated upon maturation on LPS-DCs (Fig.28 A-red line) and WTF-DCs (Fig.28 A-green line). Remarkably, the majority of WTF-DCs fail to support redistribution of FN1-reactive MHC-II from intracellular compartments (Fig.28 B-green line and Fig.29 C in green). This suggests that MV-infection

might interfere with trafficking of cellular proteins at an undefined level. In our system, it is however unclear, whether inefficient recruitment of this subset would contribute to the inability of WTF-DCs to promote T cell activation.

With B APCs, SA-stimulated T cell activation occurred independently of the presence of FN1-reactive clusters (Kropshofer et al., 2002). Also in mature DCs, it has been suggested that accumulation of clustered MHC-II at the pre-synaptic side (as relevant for T cell activation) was regulated mainly at the level of ubiquitin-dependent degradation rather than recruitment (Shin et al., 2006). Though, we have shown that MV can modify ubiquitin-dependent degradation in T cells by surface contact (Avota et al., 2004), its ability to do so in infected including DCs is unknown. Lastly, surface accumulation levels of FN1 reacted MHC-II was similar for WTF-DCs and MGV-DCs (Fig.28 B and Fig.33 B, respectively) which differed with regard to their ability to promote T cell activation (Fig.31E, F and Fig.34 respectively) and allogenic T cell expansion (Klagge et al., 2000; Schlender et al., 1996).

Actin cytoskeletal rearrangement driven accumulation of MHC-II clusters at the presynaptic site significantly enhances engagement of TCR, as required for successful T cell activation (Al-Alwan et al., 2003, 2001). Although, MHC-II clusters on WTF-DCs were generally smaller than those seen for LPS-DCs (Fig.30C and B respectively), the overall architecture of the interface, as determined by confocal microscopy, was similar for both DC species (Fig.24, Fig.25 and Fig.26). These analyses are, however, biased in the selection of stable conjugates. Thus, it cannot be excluded that T cells conjugating to WTF-DCs are compromised in their ability to efficiently redistribute CD3 into mature, functional synapses, as was observed previously in conjugates formed between MV preexposed T cells and LPS-DCs (Müller et al., 2006). Formation of spatially organised IS in T cells requires, prolonged contact durations. Therefore, aberrant distribution patterns of CD3 in these structures, if occurring, are not likely to contribute to the type of contacts

predominating for WTF-DC/T cell interactions (Fig.31 B and E-red line). During these, the ability of T cells to flux calcium is initially unaltered (Fig.31 F), and this is consistent with the observations made for CD3/CD28 activation of MV preexposed T cells (Avota et al., 2004). Altogether, our findings indicate that DC activities preceding successful activation of T cells such as tethering, integrin-dependent adhesion and translocation, as well as local concentration of MHC-II and costimulatory molecules to levels exceeding the threshold for signal initiation should be maintained in WTF-DCs. Subsequently, however, neither contacts nor calcium flux can be stabilised and sustained in approximately 60% of conjugates (Fig.31 F). Although this was not specifically addressed, it is also likely that transient interactions of less than 2 minutes may, if at all, not efficiently support viral transmission to T cells. Transient interactions are typically observed with immature DCs in the absence of antigen (Benvenuti et al., 2004a). However, this is not likely to be relevant in our allogenic system, which includes SA-loaded WTF-DCs. The requirements within the APC for conjugate stabilization and subsequent T cell activation is largely unidentified on molecular level. Yet there is evidence that signaling via MHC-II, activation of Rho GTPases, or redistribution of integrin-interacting proteins (Hofer et al., 2006; Shurin et al., 2005; Al-Alwan et al., 2003) are involved. These processes have not as yet been looked at in detail in MV-infected DCs. It is, however, highly probable that the viral gp complex expressed at the surface of the MV-infected DCs plays an important role in the formation of the aberrant synapse. This is supported by our finding that prolonged, activatory interactions occur at higher frequency with MGV-DCs (Fig.34) and clusters of H protein can be detected in the WTF-DC/Tcell interface (Fig.32.A). Pertaining to membrane association, there is no evidence that the F protein differs. This is true, because MV-infected DC cultures reveal extensive syncytia formation in the absence of the fusion inhibitory peptide (Grosjean et al., 1997). It remains to be determined whether the

presence of the complex acts to destabilise conjugates at the level of the DCs. This interaction could happen, for example, by insertion into activation clusters or disruption of the synaptic interface on these cells, or at the T cell level, by causing rapid collapse of T cell cytoskeletal structures (Müller et al., 2006; Faure et al., 2004).

# 6. Summary

Interaction with dendritic cells (DCs) is considered as central to immunosuppression induced by viruses, including measles virus (MV). Commonly, viral infection of DCs abrogates their ability to promote T cell expansion, yet underlying mechanisms at a cellular level are undefined. It appears that MV-WTF infection modulate DCs morphology and dynamic adhesion on extra cellular matrix proteins such as FN or ICAM-1. By morphological criteria, WTF-DCs resembled LPS-DCs, associated with their mature phenotype also adhered less efficiently to the FN or ICAM-1 support. Reduced adhesion could not be explained by a lack of β1-integrin expression or activation. Similarly, MV-DCs strongly resembled LPS-DCs in that levels of focal adhesion kinase phosphorylated at Y397 were high and not further enhanced upon FN ligation. Fascin, a downstream effector of integrin signaling was highly upregulated in LPS-DCs and moderately in WTF-DCs, and differences in its subcellular distribution were not observed between both cell cultures. Apparently, however, fascin associated less efficiently with PKCα in WTF-DCs then in LPS-DCs.–In line with findings for murine DCs, high motility of mature human DCs was found to require expression of Rac-GTPases. Human LPS-DCs and more so, DC transfected to express constitutively active Rac1 were the most motile DC-species analysed, confirming that migration of human DC also involved Rac activity. The velocity of WTF-DCs on FN is below that of LPS-DCs, indicating that maturation induced by WTF may be insufficient to completely promote integrin signaling which leads to Rac activation.

The organisation of MV-DC/T cell interfaces was consistent with that of functional immune synapses with regard to CD3 clustering, MHC class II surface recruitment and MTOC location. These analyses are based in the selection of stable conjugates. Subsequently, however, neither contacts nor calcium flux can be stabilised and sustained in the majority

of MV-DC/T cell conjugates and only promoted abortive T cell activation. Formation of spatially organised IS in T cells requites, prolonged contact durations. Therefore, aberrant distribution patterns of CD3 in these structures, if occurring, are not likely to contribute to the type of contacts predominating for WTF-DC/T cell interactions. It is also likely that transient interactions of less than 2 minutes may if at all, not efficiently support viral transmission to T cells. Transient interactions are typically observed with immature DCs in the absence of antigen, but this is not likely to be relevant in our allogenic system, which includes SA-loaded WTF-DCs. Thus, MV-infected DCs retain activities required for initiating, but not sustaining T cell conjugation and activation. This is partially rescued if surface expression of the MV glycoproteins on DCs is abolished by infection with a recombinant MV encoding VSV G protein instead, indicating that these contribute directly to synapse destabilisation and thereby act as effectors of T cell inhibition.

# 7. Zusammenfassung:

Die Interaktion mit Dentritischen Zellen (DCs) wird für die Immunsuppression, welche durch Viren einschließlich des Masernvirus (MV) hervorgerufen wird, als ein zentraler Mechanismus angesehen. Für gewöhnlich unterdrücken virale Infektionen von DCs deren Fähigkeit, die T-Zell Expansion zu vermitteln. Dies geschieht durch einen Mechanismus, welcher bisher nicht auf zellulärer Ebene definiert ist. Es scheint, dass eine MV-WTF Infektion die Morphologie der DCs und deren dynamische Adhäsion an extrazellulären Matrixproteinen wie FN oder ICAM-1 moduliert. Unter morphologischen Gesichtspunkten ähneln WTF-DCs den LPS-DCs. Entsprechend ihrem reifen Phänotyp adherieren erstgenannte ebenfalls weniger effektiv unter Einwirkung von FN und ICAM-1. Die reduzierte Adhäsion konnte nicht durch das Fehlen von ß1-Integrin Expression oder Aktivierung erklärt werden. Analog glichen MV-DCs den LPS-DCs in der Hinsicht sehr, dass deren Expressionslevel von Y397 phosphorylierter Fokaler-Adhäsions-Kinase hoch war und durch FN Ligation nicht weiter anstieg. Fascin, ein downstream Effektor des Integrin- Signalwegs, wurde in LPS-DCs stark und in WTF-DCs moderat hochreguliert. Differenzen in der subzellulären Verteilung des Fascin wurden zwischen den beiden Zellkulturen nicht beobachtet. Allerdings assoziierte Fascin in WTF-DCs weniger effizient mit PKCα, als in LPS-DCs. In Übereinstimmung mit Befunden bei murinen DCs wurde herausgefunden, dass eine hohe Motilität reifer humaner DCs die Expression von Rac-GTPasen voraussetzt. Humane LPS-DCs und mehr noch transfizierte DCs, welche konsitutiv aktive Rac1-GTPase exprimieren, waren die mobilsten unter den analysierten DC Typen. Dies bestätigt, dass die Migration humaner DCs unter Anderem von der Rac-Aktivität abhängt. Die Geschwindigkeit von WTF-DCs auf FN ist niedriger, als die von LPS-DCs, was darauf hinweist, dass die durch WTF induzierte Reifung unzureichend sein könnte, um die Integrin-Signalgebung auszulösen, welche zur Rac Aktivierung führt.

Die Ausbildung der MV-DC / T-Zell-Verbindungen stimmte mit der einer funktionalen immunologischen Synapse in Hinsicht auf die Formung von CD3 Clustern, die Oberflächenrekrutierung von MHC-II-Molekülen und der MTOC-Lokalisierung überein. Diese Befunde fußen allerdings auf der Selektion stabiler Konjugate. Dagegen konnten bei der Mehrzahl der MV-DC / T-Zell-Konjugate weder Kontakte noch Calcium-Influx stabilisiert und aufrechterhalten und nur eine unvollständige T-Zell-Aktivierung hervorrufen werden. Die Ausbildung räumlich organisierter Synapsen in T-Zellen setzt länger anhaltende Kontakte voraus. Das abweichende Verteilungsmuster von CD3 in diesen Strukturen steuert deshalb, soweit vorhanden, wohl nicht zu der Art von Kontakten bei, welche die WTF-DC / T-Zell-Interaktion dominieren. Es ist außerdem wahrscheinlich, dass transiente Interaktionen von weniger als zwei Minuten die virale Transmission zu T-Zellen, wenn überhaupt, nicht effizient unterstützen. Transiente Interaktionen werden typischer Weise bei unreifen DCs in der Abwesenheit von Antigen beobachtet, doch dies ist wahrscheinlich nicht relevant in dem hier verwendeten allogenen System, welches SA-geladene WTF-DCs verwendet. MV-infizierte DCs besitzen folglich die Eigenschaften, welche für die Initialisierung, aber nicht solche die für die Aufrechterhaltung der T-Zellkonjugation und Aktivierung der T-Zellen nötig sind. Dieses Unvermögen wird teilweise kompensiert, wenn die Oberflächenexpression von MV Glykoproteinen auf DCs durch die Infektion mit rekombinatem MV, welches das VSV G Protein kodiert, verhindert wird. Aus diesem Befund kann man schließen, dass die MV Glykoproteine direkt zur Destabilisierung der Synapse beitragen und deshalb als Effektoren der T-Zell Inhibition agieren.

# 8. Abbreviation

**Ab** antibody

**AIDA** software program

**AET** 2-aminoethylisothiouronium hydrobromide

**Ag** antigen

**APC** antigen-presenting cell

**APS** ammonium persulphat

**ATV** Adjusted trypsin-versene

**BCR** B-cell receptor

**BM** bone marrow

**BMMC** bone marrow mast cell

**BSA** bovine serum albumin CD-46

**cfu** colony-forming units

**(c) SMAC** central supramolecular activation cluster

**DIC** differential interference contrast

**3D** three-dimensional image analysis

**DMSO** dimethyl sulfoxide

**DTT** Dithiotheritol

**EB** ethidium bromide

**ECL** chemiluminescence substrate

**ED** vaccine straine Edmonston

**EDTA** ethylenediaminetetraacetic acid

**EGFP** enhanced green fluorescent protein

**ELISA** enzyme-linked immunosorbent assay

**ERK** extracellular signal-regulatory kinase

**EYFP** enhanced yellow fluorescent protein

**F(ab')2** antigen-binding fragment (of immunoglobulin)

**FACS** fluorescence-activated cell sorting

**FACE** -method by using FAK Kit

**FAK**–focal adhesion kinase

**FBS** fetal bovine serum

**Fc** complement-binding fragment Immunoglobulin

**FcεRI** high-affinity IgE receptor

**FITC** fluorescein isothiocyanate

**FIP** fusions-inhibitorisches peptid

**FN**- fibronectin

**FN1**-reactive MHCII

**GFP** green fluorescent protein

**GTP**-ases

**HBS** HEPES-buffered saline

**HBSS** Hanks' balanced salt solution

**HeNe** helium/neon (laser)

**HEPES** *N*-2-hydroxyethylpiperazine-*N*'-2-ethanesulfonic acid

**HRP** horseradish peroxidase

**ICAM-1** - intracellular adhesion molecule-1

**Ig** immunoglobulin

**IS** Immunological synapse

**LAT** linker for the activation of T cells

**LFA-1** leukocyte function-associated antigen-

**LB** Luria-Bertani (medium)

**LIBS** ligand-induced binding sites

**MAb** monoclonal antibody

**MAPK** mitogen-activated protein kinase

**MCF** mean channel fluorescence

**MCP** membrane cofactor protein, CD46

**MIBE** measles inclusion body encephalitis

**MFI** mean fluorescence intensity

**MGV** recombinant MV that contains the G protein of VSV insted of MV glycoproteins

**MHCII** major histocompatibility complex molecule

**moi** multiplicity of infection

**NK** natural killer (cells)

**NP-40** Nonidet P-40

**OD** optical density

**PAR1** protease-activated receptor 1

**PBS** phosphate-buffered saline

**PE** phycoerythrin *or* processing element

**PI** propidium iodide

**PIPES** piperazine-*N*,*N*'-bis(2-ethanesulfonicacid)

**PLL** plyL-Lysin

**PMA** phorbol 12-myristate 13-acetate

**PMSF** phenylmethylsulfonyl fluoride

**P**- phosphoprotein

**PRR** pattern recognition receptor

**pfu** plaque forming unit

**p.i.** *post infectionem*

**(p) SMAC** peripheral

**PTK** protein tyrosine kinase

**Rac1**-GFPase

**RBC** red blood cell

**RNA** ribonucleic acid

**SD** standard deviation

**SDS-PAGE** - SDS-Polyacrylamide gel electrophoresis

**SLAM** signaling lymphocyte activation molecule, CD150

**SRBCs** Sheep red blood cells

**SMACs** supramolecular activation clusters

**SSPE** subacute sclerosing panencephalitis

**TCR** T cell receptor

**TE** Tris/EDTA (buffer)

**TH1, TH2** T helper cell phenotypes (CD4+)

**TCID50** tissue culture infectious dose 50

**TCM** central memory T-cell

**TCR** T-cell receptor

**TEMED** Tetramethylethylenediamine

**TGF** tumor growth factor

**TLR** toll-like receptor

**TNF** tumor necrosis factor

**TRAIL** TNF-related apoptosis inducing ligand

**VSV** vesicular stomatitis virus

**WB** - Western immunoblotting

**WTF** Wildtyp Fleckenstein

# 9. Reference

Adams, J.C. (1995) Formation of stable microspikes containing actin and the 55kDa actin-bundling protein, fascin is a consequence of cell adhesion to thrombospondin-1: implications for the antiadhesive activities of thrombospondin-1. *Cell Sci.*,108, 1977-1990.

Adams, J.C. (1997 )Characterisation of cell-matrix adhesion requirements for the formation of fascin microspikes*. Mol Biol Cell,*8,2345-2363 108:1977-1990

Adams, J.C. (1997a). Thrombospondin-1. *Int. J. Biochem. Cell Biol.* 29:861-865

Adams, J.C. (1997b). Characterization of cell-matrix adhesion requirements for the formation of fascin microspikes. *Mol. Biol. Cell.* 8:2345-2363

Adams, J.C., and Schwartz, M.A. (2000) Stimulation of fascin spikes by thrombospondin-1 is mediated by the GTPases Rac and Cdc42. *J. Cell Biol.* 150:807-822

Al-Alwan, M.M., Rowden, G., Lee, T.D. and West, K.A. (2001) The dendritic cell cytoskeleton is critical for the formation of the immunological synapse. *J Immunol.* 166. 1452-1456.

Al-Alwan, M.M., Liwski, R.S., Haeryfar, S.M., Baldridge, W.H., Hoskin, D.W., Rowden, G. and West, K.A. (2003) Cutting edge: dendritic cell actin cytoskeletal polarization during immunological synapse formation is highly antigen-dependent . *J Immunol.* 171: 4479-4483.

Allenspach, E. J., P. Cullinan, J. Tong, Q. Tang, A. G.,Tesciuba, J. L. Cannon, S. M. Takahashi, R. Morgan, J.K. Burkhardt, and A. I. Sperling (2001). ERM-dependentmovement of CD43 defines a novel protein complex distalto the immunological synapse. Immunity 15:739-750.

Anilkumar N., Maddy Parsons, Raymond Monk, Tony Ng, and Josephine C. Adams Interaction of fascin and protein kinase Cα: a novel intersection in cell adhesion and motility (2003),The EMBO Journal Vol.22 No.20 pp.5390-5402

Aspenstrom, P. 1999. The Rho GTPases have multiple effects on the actin cytoskeleton.*Exp. Cell Res. 246:20*.

Avota, E., Harms, H. and Schneider-Schaulies, S. (2006) Measles virus induces expression of SIP110, a constitutively membrane clustered lipid phosphatase, which inhibits T cell proliferation. *Cell Microbiol.* 8: 1826-1839.

Avota, E., Müller, N., Klett, M. and Schneider-Schaulies, S. (2004) Measles virus interacts with and alters signal transduction in T-cell lipid rafts. *J Virol*. 78: 9552-9559

Avota, E., Avots, A., Niewiesk, S., Kane, L.P., Bommhardt, U., tel Meulen, V. and Schneider-Schaulies, S. (2001) Disruption of Akt kinase activation is important for immunosuppression induced by measles virus. *Nat Med.* 7:725-731.

Ballestrem C., Boris Hinz, Beat A. Imhof and Bernhard Wehrle-Haller Marching at the front and dragging behind: differential αVß3-integrin turnover regulates focal adhesion behaviour

Banchereau, J. and Steinman, R.M. (1998) Dendritic cells and the control of immunity. *Nature*. 392: 245-252

Bellini WJ, Rot JS, Rota.Virology of measles virus *J Infect Dis*. 1994 Nov;170 Suppl 1:S1523

Benvenuti, F., Lagaudriere-Gesbert, C., Grandjean, I., Jancic, C., Hivroz, C., Trautmann, A., et al (2004a) Dendritic cell maturation controls adhesion, synapse formation, and the duration of the interactions with naive T lymphocytes. *J Immunol.* 172: 292-301

Benvenuti, F., Hugues, S., Walmsley, M., Ruf, S., Fetler, L., Popoff, M., et al (2004b) Requirement of Rac1 and Rac2 expression by mature dendritic cells for T cell priming. *Science.* 305: 1150-1153

Bieback, K., Lien, E., Klagge, I.M., Avota, E., Schneider-Schaulies, J., Duprex, W.P., et al (2002) Hemagglutinin protein of wild-type measles virus activates toll-like receptor 2 signaling. *J.Virol*. 76: 8729-8736.

Binks M.,Joneas GE, Brikell PM, Kinnon C., Katz DR, Thrasher AJ. Integrins dendritic cell abnormalities in Wiskott-Aldrich syndrome.(1998)Eur J Immunol 1998 Oct; 28(10).3259-67

Boes, M. and Ploegh, H.L. (2004) Translating cell biology in vitro to immunity in vivo. *Nature.* 430: 264-271.

Boes, M., Bertho, N., Cerny, J., Op den Brouw, M., Kirchhausen, T. and Ploegh, H. (2003) T cells induce extended class II MHC compartments in dendritic cells in a Toll-like receptor-dependent manner. *J Immunol.* 171: 4081-4088.

Boes, M., Cerny, J., Massol, R., Op den Brouw, M., Kirchhausen, T., Chen, J. and Ploegh, H.L. (2002) T-cell engagement of dendritic cells rapidly rearranges MHC class II transport. *Nature*. 418: 983-988.

Borrow, P. and Oldstone, M.B. (1995) Measles virus-mononuclear cell interactions. *Curr Top Microbiol Immunol.* 191: 85-100.

Bromley SK, Iaboni A, Davis SJ, Whitty A., Green JM, Shaw AS, Weiss A,Dustin ML The immunological synapse and CD28-CD80 interactions.*Nat Immunol*. (2001) Dec;2(12):1159-66. PMID: 11713465

Brossard, C., Feuillet, V., Schmitt, A., Randriamampita, C., Romao, M., Rapso, G. and Trautmann, A. (2005) Multifocal structure of the T cell – dendritic cell synapse. Eur *J Immunol.* 35 : 1741-1753.

Burns, S., Hardy, S.J., Buddle, J., Yong, K.L., Jones, G.E. and Thrasher, A.J. (2004) Maturation of DC is associated with changes in motile characteristics and adherence. *Cell Motil Cytoskeleton*. 57: 118-132.

Burridge K. Petch LA.,Romer LH Signals from focal adhesions. *Curr Biol.*1992 Oct;2(10):537-9. Burridge K., Turner CE, Romer LH Tyrosine phosphorylation of paxillin and pp125FAK accompanies cell adhesion to extracellular matrix: a role in cytoskeletal assembly. *J Cell Biol.* 1992 Nov;119 (4):893-903

Campi, G., Varma, R., and Dustin, M.L. (2005) Actin and agonist MHC-peptide complex-dependent T cell receptor microclusters as scaffolds for signaling. *J Exp Med*. 202. 1031-1036.

Carlier MF,aurent V, Santolini J, Melki R, Didry D, Xia GX, Hong Y, Chua NH, Pantaloni D. Actin depolymerizing factor (ADF/cofilin) enhances the rate of filament turnover: implication in actin-based motility. *J Cell Biol.* 1997 Mar 24;136(6):1307-22. PMID: 9087445

Caux C, Dieu MC, Vanbervliet B, Vicari A, Bridon JM, Oldham E, Aït-Yahia S, Brière F, Zlotnik A, Lebecque S, Selective recruitment of immature and mature dendritic cells by distinct chemokines expressed in different anatomic sites. *J Exp Med.* 1998 Jul 20;188(2):373-86

Caux C. et al. Dendritic cell biology and regulation of dendritic cell trafficking by chemokines.Springer *Semin Immunopathol*. 2000;22(4):345-69. Review. PMID: 11155441

Cella M, Sallusto F, Lanzavecchia A.Origin, maturation and antigen presenting function of dendritic cells. *Curr Opin Immunol*. 1997 Feb;9(1):10-6. Review. PMID: 9039784

Chow, A., Toomre, D., Garrett, W. And Mellman, I. (2002) Dendritic cell maturation triggers retrograde MHC class II transport from lysosomes to the plasma membrane. *Nature*. 418: 988-994.

Chen E, Yang M, Tao P. Zhonghua Shi Yan He Lin Chuang Bing Du Xue Za Zhi Selective inhibition of HSV-1 DNA and protein synthesis by antiviral antibiotic 17997]. 2000Sep;14(3):247-9. PMID: 11498689

de la Fuente, H., Mittelbrunn, M., Sanchez-Martin, L., Vicente-Manzanares, M., Lamana, A., Pardi, R., et al (2005) Synaptic clusters of MHC class II molecules induced on DCs by adhesion molecule-mediated initial T-cell scanning. *Mol Biol Cell*.16. 3314-3322.

Delon J, Bercovici N, Raposo G, Liblau R, Trautmann A. Antigen-dependent and -independent Ca2+ responses triggered in T cells by dendritic cells compared with B cells.*J Exp Med*. 1998 Oct 19;188(8):1473-84. PMID: 9782124

Doher, K., Wolfstein, A., Prank, U., Echeverri, C., Dujardin, D., Vallee, R. and Sodeik, B. (2002) Function of dynein and dynactin in herpes simplex virus capsid transport. *Mol Biol Cell.* 13:2795-2809

Dhib-Jalbut S, Xia J, Rangaviggula H, Fang YY, Lee T. Failure of measles virus to activate nuclear factor-kappa B in neuronal cells: implications on the immune response to viral infections in the central nervous system. *J Immunol.* 1999 Apr 1;162(7):4024-9. PMID: 10201924

Drbal, K., Angelisova, P., Rasmussen, A.M., Hilgert, I., Funderud, S. and Horejsi, V. (19999 The nature of the subset of MHC class II molecules carrying the CDw78 epitopes. *Int Immunol*. 11: 491-498.

Dubois, B., Lamy, P.J., Chemin, K., Lachaux, A. and Kaiserlian, D. (2001) Measles virus exploits dendritic cells to suppress CD4+ T-cell proliferation via expression of surface virus glycoproteins independently of T-cell trans-infection. *Cell Immunol.* 214: 173-183.

Dustin ML, Golan DE, Zhu DM, Miller JM, Meier W, Davies EA, van der Merwe PA.Low affinity interaction of human or rat T cell adhesion molecule CD2 with its ligand aligns adhering membranes to achieve high physiological affinity. *J Biol Chem*. 1997 Dec5;272(49):30889-98. PMID: 9388235

Dustin, M.L., Tseng, S.Y., Varma, R. and Campi, G. (2006) T cell-dendritic cell immunological synapses. *Curr Opin Immunol*. 18: 512-516.

Erlenhoefer C, Wurzer WJ, Löffler S, Schneider-Schaulies S, ter Meulen V, Schneider-Schaulies J CD150 (SLAM) is a receptor for measles virus but is not involved in viral contact-mediated proliferation inhibition *J Virol.* 2001 May;75(10):4499-505.

Esolen LM, Ward BJ, Moench TR, Griffin DE.Infection of monocytes during measles.*J Infect Dis.* 1993 Jul;168(1):47-52. PMID: 8515132

Faure, S., salazer-fontana, L.I., Semichon, M., Tybulewicz, V.L., Bismuth, G., Trautmann, A., et al (2004) ERM proteins regulate cytoskeleton relaxation promoting

Fujinami et al.,T cell-APC conjugation. *Nat Immunol*. 5: 272-279, 1998

Friedel, P., den Boer, A.T. and Gunzer, M. (2005) Tuning immune responses: diversity and adaptation of the immunological synapse. *Nat Rev Immunol*. 5:532-545

Friedman RS, Jacobelli J, Krummel MF. Surface-bound chemokines capture and prime T cells for synapse formation.*Nat Immunol.* 2006 Oct;7(10):1101-8. Epub 2006 Sep 10. *Nat Immunol.* 2006 Nov;7(11):1234.

Fujinami RS, Sun X, Howell JM, Jenkin JC, Burns JB.Modulation of immune system function by measles virus infection: role of soluble factor and direct infection.*J Virol*. 1998 Dec;72(12):9421-7. PMID: 9811674

Fugier-Vivier, I., Servet-Delprat, C., Rivaller, P., Rissoan, M.C., Liu, Y.J. and Rabourdin-Combe, C. (1997) measles virus suppresses cell-mediated immunity by interfering with the survival and functions of dendritic and T cells. *J Exp Med.* 186: 813-823.

Garrett WS, Chen LM, Kroschewski R, Ebersold M, Turley S, Trombetta S, Galán JE, Mellman I.Developmental control of endocytosis in dendritic cells by Cdc42.*Cell.* 2000 Aug 4;102(3):325-34. PMID: 10975523

Gatti, E. and Pierre, P. (2003) Understanding the cell biology of antigen presentation: the dendritic cell contribution*. Curr Opin Cell Biol.* 15: 468-473.

Geyeregger R, Zeyda M, Bauer W, Kriehuber E, Säemann MD, Zlabinger GJ, Maurer D, Stulnig TM.Liver X receptors regulate dendritic cell phenotype and function through blocked induction of the actin-bundling protein fascin.*Blood*. 2007 May 15;109(10):4288-95. Epub2007 Jan 25. PMID: 17255360

Gombos, I., Detre, C., Vamosi, G. and Matko, J. (2004) Rafting MHC-II domains in the APC (presynaptic) plasma membrane and the thresholds for T-cell activation and immunological synapse formation. *Immunol Lett*. 92: 117-124.

Griffin GE, Leung K, Folks TM, Kunkel S, Nabel GJ.Activation of HIV gene expression during monocyte differentiation by induction of NF-kappa B. *Nature*. 1989 May 4;339(6219):70-3. PMID: 2654643

Griffin DE, Grose R, Hutter C, Bloch W, Thorey I, Watt FM, Fässler R, Brakebusch C, Werner S.Arboviruses and the central nervous system.Springer Semin Immunopathol. 1995;17(2-3):121-32. Review. PMID: 8571164

Grose R, Hutter C, Bloch W, Thorey I, Watt FM, Fässler R, Brakebusch C, Werner S.,A crucial role of beta 1 integrins for keratinocyte migration in vitro and during cutaneous wound repair.*Development*. 2002 May;129(9):2303-15. PMID: 11959837

Grosjean, I., Caux, C., Bella, C., Berger, I., Wild, F., Banchereau, J. and Kaiserlian, D. (1997) Mesles virus infects human dendritic cells and blocks ther allostimulatoty properties for CD4+ T cells. *J Exp Med.* 186: 801-812

Guan JQ, Vorobiev S, Almo SC, Chance MR.Mapping the G-actin binding surface of cofilin using synchrotron protein footprinting.*Biochemistry.* 2002 May 7;41(18):5765-75. PMID: 11980480

Gunzer, M., Weishaupt, C., Hillmer, A., Basoglu, Y., Friedl, P., Dittmar, K.E., et al (2004) A spectrum of biophysical interaction modes between T cells and different antigen-presenting cells during priming in 3-D collagen and in vivo. *Blood.* 104: 2801-2809.

Harizi H, Gualde N.The impact of eicosanoids on the crosstalk between innate and adaptive immunity: the key roles of dendritic cells.*Tissue Antigens*. 2005 Jun;65(6):507-14. Review. PMID: 15896197

Hart DN. Dendritic cells: unique leukocyte populations which control the primary immune response. *Blood*. 1997 Nov 1;90(9):3245-87. Review. PMID: 9345009

Hilbold, E.M., Poloso, N.J. and Roche, P.A. (2003) MHC class II-peptide complexes and APC lipid rafts accumulate at the immunological synapse. *J Immunol*. 170: 1329-1338.

Helin E, Vainionpää R, Hyypiä T, Julkunen I, Matikainen S.Measles virus activates NF-kappa B and STAT transcription factors and production of IFN-alpha/beta and IL-6 in the human lung epithelial cell line A549.*Virology*. 2001 Nov 10;290(1):1-10. PMID: 11882993

Hofer, S., Pfeil, K., Niederegger, H., Ebner, S., Nguyen, V.A., Kremmer, E., et al. (2006) Dendritic cells regulate T-cell deattachment though the integrin-interacting protein CYTIP. *Blood.* 107: 1003-1009.

Hughes PE, Pfaff M.Integrin affinity modulation.*Trends Cell Biol*. 1998 Sep;8(9):359-64.Review. PMID: 9728397

Hynes RO.Integrins: bidirectional, allosteric signaling machines.Cell. 2002 Sep20;110(6):673-87. Review. PMID: 12297042

Inaba K, Witmer-Pack M, Inaba M, Hathcock KS, Sakuta H, Azuma M, Yagita H, Okumura K, Linsley PS, Ikehara S, Muramatsu S, Hodes RJ, Steinman RM.The tissue distribution of the B7-2 costimulator in mice: abundant expression on dendritic cells in situ and during maturation in vitro. *J Exp Med*. 1994 Nov 1;180(5):1849-60. PMID: 7525841

Inaba K, Steinman RM, Pack MW, Aya H, Inaba M, Sudo T, Wolpe S, Schuler G. Identification of proliferating dendritic cell precursors in mouse blood.*J Exp Med*. 1992 May 1;175(5):1157-67. PMID: 1569392

Katz SL. A vaccine-preventable infectious disease kills half a million children annually *Infect Dis* 2005 Nov 15;192(10):1686-93

Kerdiles, Y.M., Sellin, C.I., Druelle, J. and Horvat, B. (2006) Immunosuppression caused by measles virus: role of viral proteins. *Rev Med Virol*. 16: 49-63.

Klagge, I.M., ter Meulen, V. and Schneider-Schaulies, S. (2000) Measles virus indiced promotion of dendritic cell maturation by soluble mediators does not overcome the immunosuppressive activity of viral glycoproteins on the cell surface. *Eur J Immunol*. 30 : 2741-2750.

Klagge, I.M., Abt, M., Fries, B. and Schneider-Schaulies, S. (2004) Impact of measles virus dendritic-cell infection on Th-cell polarization in vitro. *J Gen Virol*. 85 : 3239-3247.

Kropshofer, H., Spindeldreher, S., Rohn, T.A., Platania, N., Grygar, C., Daniel, N., et al. (2002) Tetraspan microdomains distinct from lipid rafts enrich select peptide-MHC class complexes. *Nat Immunol*. 3: 61-68

Kruse, M., Meinl, E., Henning, G., Kuhnt, C., Berchtold, S., Berger, T., et al (2001), Signalin lymphocytic activation molecule is expressed on mature CD83+ dendritic cells and is up-regulated by IL-1 beta. *J Immunol.* 167: 1989-1995.

Meyer zum Bueschenfelde, C.O., Unternaehrer, J., Mellman, I. and Bottomly, K. (2004) Regulated recruitment of MHC class II and costimulatory molecules to lipid rafts in dendritic cells. *J Immunol.* 173: 6119-6124.

Minagawa, H., Tanaka, K., Ono, N., Tatsuo, H. and Yanagi, Y. (2001) Induction of the measles virus receptor SLAM (CD150) on monocytes. *J Gen Virol*. 82 : 2913-2917.

Müller, N., Avota, E., Schneider-Schaulies, J., Harms, H., Krohne, G. and Schneider-Schaulies, S. (2006) Measles virus contact with T cells impedes cytoskeletal remodeling associated with spreading, polarization, and CD3 clustering. *Traffic. 7:* 849-858.

Nurmi, S.M., Autero, M., Raunio, A.K., Gahmberg, C.G. and Fagerholm, S.C. (2006) Phosphorylation of the LFA-1 integrin beta 2-chain on Thr-758 leads to adhesion, Rac-1/Cdc-42 activation and stimulation of CD69 expression in human T cells. *J Biol Chem.*

Ohgimoto, S., Ohgimoto, K., Niewies, S., Klagge, I.M., Preuffer, J., Johnston, I.C., et al (2001) The haemagglutinin protein is an important determinant of maesles virus tropism for dendritic cells in vitro. *J Gen Virol.* 82 : 1835-1844.

Pellinen, T. and Ivaska, J. (2006) Integrin traffic. *J Cell Sci*. 119: 3723-3731

Pollara, G., Kwan, A., Newton, P.J., Handley, M.E., Chain, B.M. and Katz, D.R. (2005) Dendritic cells in viral pathogenesis: protective or defective? *Int J Exp Pathol*. 86: 187-204

Pohl C, Shishkova Y, Schneider-Schaulies S.,Visuses and Dendritic cells: Enemy mine 2007, *J. Cellular Microbiology*

Reay, P.A., Matsui, K., Wulfing, C., Chien, Y.H. and Davis, M.M. (2000) Determination of the relationship between T cell responsiveness and the number of MHC-peptide complexes using specific monoclonal antibodies. *J Immunol.* 164:5626-5634.

Revy, P., Sospedra, M., Barbour, B. and Trautmann, A. (2001) Functional antigenindependent synapses formed between T cella and dendritic cells. *Nat Immunol*. 2:925-931.

Rinaldo, C.R., Jr. and Piazza, P. (2004) Virus infection of dendritic cells: portal for host invasion and host defense. *Trends Microbiol*. 12: 337-345

Roy S, Ruest PJ, Hanks SK.FAK regulates tyrosine phosphorylation of CAS, paxillin, and PYK2 in cells expressing v-Src, but is not a critical determinant of v-Src transformation.*J Cell Biochem*. 2002;84(2):377-88. PMID: 11787067

Sanchez-Madrid, F. and del Pozo, M.A. (1999) Leukocyte polarization in cell migration and immune interactions. *Embo J*. 18: 501-511.

Sancho, D., Vicente-Manzanares, M., Mittelbrunn, M., Montoya, M.C., Gordon-Alonso, M., Serrador, J.M. and Sanchez-Madrid, F. (2002) Regulation of microtubuleorganizing center orientation and actomyosin cytoskeleton rearrangement during immune interactions. *Immunol Rev*. 189: 84-97.

Schlender, J., Schnorr, J.J., Spielhoffer, P., Cathomen, T., Cattaneo, R., Billeter, M.A., et al (1996) Interaction of measles virus glycoproteins with the surface of uninfected peripheral blood lymphocytes induces immunosuppression in vitro. *Proc Natl Acad Sci* USA. 93: 13194-13199

Schneider-Schaulies, S. and tel Meulen, V. (2002a) Triggering of and interference with immune activation: interactions of measles of maesles virus with monocytes and dendritic cells. *Viral Immunol*. 15:4117-428.

Schneider-Schaulies, S. and tel Meulen, V. (2002b) Modulation of immune functions by measles virus. *Springer Semin Immunopathol*. 24: 127-148.

Schneider-Schaulies, S. and Dittmer, U. (2006) Silecing T cells or T-cell silecing: concepts in virus-induced immunosuppression. *J gen Virol*. 87: 1423-1438.

Schneider-Schaulies, S., Klagge, I.M. and ter Meulen, V. (2003) Dendritic cells and measles virus infection. *Curr Top Microbiol Immunol*. 276: 77-101.

Schnorr, J.J., Xanthakos, S., Keikavoussi, P., Kampgen, E., ter Meulen, V. and Schneider-Schaulies, S. (1997) Induction of maturation of human blood dendritic cell precursors by measles virus ins associated with immunosuppression. *Proc natl Acad Sci USA*. 94: 5326-5331.

Schnorr JJ, Cutts FT, Wheeler JG, Akramuzzaman SM, Alam MS, Azim T, Schneider-Schaulies S, ter-Meulen V.Immune modulation after measles vaccination of 6-9 months old Bangladeshi infants.Vaccine. 2001 Jan 8;19(11-12):1503-10. PMID: 11163674

Servet-Delprat, C., Vidalain, P.O., Valentin, H. and Rabourdin-Combe, C. (2003) Measles virus and dendritic cell functions: how specific response cohabits with immunosuppression. *Curr Top Microbiol Immunol*. 276: 103-123.

Servet-Delprat, C., Vidalain, P.O., Bausinger, H., Manie, S., Le Deist, F., Azocar, O., et al (2000) Measles virus induces abnormal differentiation of CD40 ligand-activatedhuman dendritic cells. *J Immunol*. 164: 1753-1760

Shimaoka M, Xiao T, Liu JH, Yang Y, Dong Y, Jun CD, McCormack A, Zhang R, Joachimiak A, Takagi J, Wang JH, Springer TA.Structures of the alpha L I domain and its complex with ICAM-1 reveal a shape-shifting pathway for integrin regulation.*Cell*. 2003 Jan 10;112(1):99-111. PMID: 12526797

Shin, J.S., Ebersold, M., Pypaert, M., Delamarre, L., Hartly, A. and Mellman, I. (2006) Surface expression of MHC class II in dendritic cells is controlled by regulated ubiquitination. *Nature*. 444: 115-118.

Shurin, G.V., Tourkova, I.L., Chatta, G.S., Schmidt, G., Wie, S., Djeu, J.Y. and shurin, M.R. (2005) Small rho GTPases regulate antigen presentation in dendritic cells. *J Immunol*. 174: 3394-3400.

Shutt, D.C., Daniels, K.J., Carolan, E.J., Hill, A.C. and Soll, D.R. (2000) Changes in the motility, morphology and F-actin architecture of human dendritic cells in an in vitro model of dendritic cell development. *Cell Motil Cytoskeleton*. 46: 200-221.

Spielhofer, P., Bachi, T., Fehr, T., Christiansen, G., Cattaneo, R., Kaelin, K., et al (1998) Chimeric measles viruses with a foreign envelope. *J Virol*. 72: 2150-2159.

Steineur, M.P., Grosjean, I., Bella, C. and Kaiserlian, D. (1998) Langerhans cells are susceptible to measles virus infection and actively suppress T cell proliferation. *Eur J Dermatol.* 8: 413-420.

Steinman, R.M. (2003) The control of immunity and tolerance by dendritic cell. *Pathol Biol* (Paris). 51: 59-60.

Swetman Andersen, C.A., Handley, M., Pollara, G., Ridley, A.J., Katz, D.R. and Chain, B.M. (2006) β1-Integrins determine the dendritic morphology which enhances DC-SIGN-mediated particle by dendritic cells. *Int Immunol*. 18: 1295-1303.

Szabolcs P, Moore MA, Young JW.Expansion of immunostimulatory dendritic cells among the myeloid progeny of human CD34+ bone marrow precursors cultured with c-kit ligand, granulocyte-macrophage colony-stimulating factor, and TNF-alpha.*J Immunol*. 1995 Jun 1;154(11):5851-61. PMID: 7538534

Tatsuo H, Ono N, Tanaka K, Yanagi Y. [The cellular receptor for measles virus: SLAM (CDw 150)]Uirusu. 2000 Dec;50(2):289-96. Review. Japanese. PMID: 11276818

van der Merwe PA.Modeling costimulation.*Nat Immunol*. 2000 Sep;1(3):194-5. No abstract available. PMID: 10973274

Verma, R., Campi, G., Yokosuka, T., Saito, T. and Dustin, M.L. (2006) T cell receptor-proximal signals are sustained in peripheral microclusters and terminated in the central supramolecular activation cluster. *Immunity*. 25: 117-127.

Vicente-Manzanares, M., Sancho, D., Yanze-Mo, M. and Sanchez-Madrid, F. (2002) The leukocyte cytoskeleton in cell migration and immune interactions. *Int Rev Cytol*. 216: 233-289

Vidalain PO, Azocar O, Rabourdin-Combe C, Servet-Delprat C.Measle virus-infected dendritic cells develop immunosuppressive and cytotoxic activities.*Immunobiology*. 2001 Dec;204(5):629-38. Review. PMID: 11846228

Vogt, A.B., Spindeldreher, S. and Kropshofer, H. (2002) Clustering of MHC-peptide complexes prior to their engagement in the immunological synapse: lipid raft and tetraspan microdomains. *Immunol Rev*. 189: 136-151.

Vuori K, Ruoslahti E.Activation of protein kinase C precedes alpha 5 beta 1 integrin-mediated cell spreading on fibronectin.*J Biol Chem*. 1993 Oct 15;268(29):21459-62. PMID: 7691809

Ward DG, Walton TJ, Cavieres JD.Irreversible effects of calcium ions on the plasma membrane calcium pump.*J Membr Biol.* 1993 Dec;136(3):313-26. PMID: 8114081

Wulfing, C., Sjaastad, M.D. and Davis, M.M. (1998) Visualizing the dynamics of T cell activation: intracellular adhesion molecule 1 migrates rapidly to the T cell/B cell interface and acts to sustain calcium levels. *Proc Natl Acad Sci* USA. 95: 6302-6307.

Wulfing, C., Rabinowitz, J.D., Beeson, C., Sjaastad, M.D., McConnell, H.M. and Davis, M.M. (1997) Kinetics and extent of T cell activation as measured with the calcium signal*. J Exp Med.* 185: 1815-1825.

Yanagi Y, Tishon A, Lewicki H, Cubitt BA, Oldstone MB.Diversity of T-cell receptors in virus-specific cytotoxic T lymphocytes recognizing three distinct viral epitopes restricted by a single major histocompatibility complex molecule.*J Virol*. 1992 Apr;66(4):2527-31. PMID: 1372370

Miyamoto S, Teramoto H, Coso OA, Gutkind JS, Burbelo PD, Akiyama SK, Yamada KM.Integrin function: molecular hierarchies of cytoskeletal and signaling molecules.*J Cell Biol*. 1995 Nov;131(3):791-805. PMID: 7593197

Zamir E, Geiger B, Kam Z.Quantitative multicolor compositional imaging resolves molecular domains in cell-matrix adhesions.PLoS ONE. 2008 Apr 2;3(4):e1901. PMID: 18382676

Zigmond SH, Joyce M, Yang C, Brown K, Huang M, Pring M.Mechanism of Cdc42-induced actin polymerization in neutrophil extracts.*J Cell Biol.* 1998 Aug 24;142(4):1001-12. PMID: 9722612

Zilliox, M.J., Parmigiani, G. and Griffin, D.E. (2006) Gene expression patterns in dendritic cells infected with measles virus compared with other pathogens.Proc Natl Acad Sci USA. 103: 3363-3368.

# 10. Publication

**4/2007** Immune synapses formed with measles virus-infected dendritic cells are unstable and fail to sustain T cell activation

Autor: Shishkova Y. et al., 2007

Journal: Cellular Microbiology


**8/2007** Viruses and Dendritic cells: Enemy mine

Autor: Pohl C., Shishkova Y., Schneider-Schaulies S.
Journal: Cellular Microbiology

**POSTERS**

**Tübingen Marz17-20, 2004**

KG-1 Cell line as in vitro model to studing the interaction of Measles virus with Dendritic cells

Y. Shishkova, S.Schneider-Schaulies

Annual Meeting of the " Geselschaft für Virologie", Joint meeting with "Societa Italiana di Virologia"

**Münich, March 15-18, 2006**

Measles virus infection of Dendritic cells alters their adhesion properties and their ability to correctly organise an immunological synapse.

Y. Shishkova, S.Schneider-Schaulies

Annual Meeting of the " Geselschaft für Virologie"

# 11. Curriculum Vitae

**Name:** Yoana Shishkova

**Birth date:** 25/04/1969

**Nationality**: Bulgarian

**Contact:** Tel: 49-911-9375616 (home); 49-015118357882 (mobile)

**E-mail:** joana.shishkova@online.de

**Address**: Pirckheimer Street 11, 90408, Nürnberg, Germany

**Education Background:**

**2003 – 2007** **PhD of Biology**

Institute of Virology and Immunology

University of Würzburg, Germany

**Dissertation Project:** Investigations of Measles virus regulation on activation and function of antigen presenting cells

**4/2002-9/2002** **Professional development:**

Molecular biology in vocational education and training centre IFW GmbH, Jena, Germany

**6/2002** **Internship** in the firm JenaBioScience, Jena, Germany

**1989 – 1993** **Master of Biology and Ecology**

University of Plovdiv, Bulgaria

**Thesis:** Clinical investigations in toxically environments – investigations of accumulation of heavy metals such as mercury and lead at the bodily fluids and organs.

Grade: “very good”

**Working Experience:**

**2002 – 2003** **Scientist** at the Group “Molecular cell biology” (Prof. Dr. Wetzker) University Clinic Jena, Germany